2017

VIRTUALIZATION OF FUELBEDS: BUILDING THE NEXT GENERATION OF FUELS DATA FOR MULTIPLE –SCALE FIRE MODELING AND ECOLOGICAL ANALYSIS

Eric Martin Rowell

VIRTUALIZATION OF FUELBEDS: BUILDING THE NEXT GENERATION OF FUELS DATA FOR MULTIPLE –SCALE FIRE MODELING AND ECOLOGICAL ANALYSIS

By

Eric Martin Rowell

M.S. Atmospheric Sciences, South Dakota School of Mines and Technology, Rapid City, South Dakota, 2005

B.S. Landscape Architecture, University of California, Davis, California, 1996

Dissertation

presented in partial fulfilment of the requirements
for the degree of

Doctor of Philosophy
In Forestry

The University of Montana
Missoula, MT

December 2017

Approved by:

Scott Whittenburg, Dean of The Graduate School

Carl A. Seielstad, Chair
Department of Forest Management

David Affleck
Department of Forest Management

Andrew Larson
Department of Forest Management

LLoyd P. Queen
Department of Forest Management

Richmond Clow
Department of Native American Studies

Virtualization of Fuelbeds: Building the next generation of fuels data for multiple-scale fire modeling and ecological analysis
Chairperson: Carl A. Seielstad

The primary goal of this research is to advance methods for deriving fine-grained, scalable, wildland fuels attributes in 3-dimensions using terrestrial and airborne laser scanning technology. It is fundamentally a remote sensing research endeavor applied to the problem of fuels characterization. Advancements in laser scanning are beginning to have significant impacts on a range of modeling frameworks in fire research, especially those utilizing 3-dimensional data and benefiting from efficient data scaling. The pairing of laser scanning and fire modeling is enabling advances in understanding how fuels variability modulates fire behavior and effects.

This dissertation details the development of methods and techniques to characterize and quantify surface fuelbeds using both terrestrial and airborne laser scanning. The primary study site is Eglin Airforce Base, Florida, USA, which provides a range of fuel types and conditions in a fire-adapted landscape along with the multi-disciplinary expertise, logistical support, and prescribed fire necessary for detailed characterization of fire as a physical process. Chapter 1 provides a research overview and discusses the state of fuels science and the related needs for highly resolved fuels data in the southeastern United States. Chapter 2, describes the use of terrestrial laser scanning for sampling fuels at multiple scales and provides analysis of the spatial accuracy of fuelbed models in 3-D. Chapter 3 describes the development of a voxel-based occupied volume method for predicting fuel mass. Results are used to inform prediction of landscape-scale fuel load using airborne laser scanning metrics as well as to predict post-fire fuel consumption. Chapter 4 introduces a novel fuel simulation approach which produces spatially explicit, statistically-defensible estimates of fuel properties and demonstrates a pathway for resampling observed data. This method also can be directly compared to terrestrial laser scanning data to assess how energy interception of the laser pulse affects characterization of the fuelbed. Chapter 5 discusses the contribution of this work to fire science and describes ongoing and future research derived from this work. Chapters 2 and 4 have been published in International Journal of Wildland Fire and Canadian Journal of Remote Sensing, respectively, and Chapter 3 is in preparation for publication.

Acknowledgements

This dissertation represents significant time, effort, and ideas of many people. I would like to personally thank my advisor Carl Seielstad for the mentorship, encouragement, and continual pushing for a product worthy of what he felt my abilities offer. I am grateful to Dr. LLoyd Queen, Dr. Andrew Larson, Dr. David Affleck, and Dr. Richmond Clow for their patience and willingness to participate in this endeavor. I would also like to acknowledge my sincere gratitude to Dr. Louise Loudermilk, Dr. Joseph O'Brien, and Dr. Scott Goodrick at the USFS Southern Research Station for support both through funding and collaboration for the fuel simulation study. I also acknowledge the contributions of Dr. Andrew Hudak and Benjamin Bright at the USFS Rocky Mountain Research Station with regards to the aggregation from TLS to ALS. Specifically, I thank Dr. Roger Ottmar at the USFS Pacific Northwest Research Station for his vision and diligence in facilitating the RxCADRE. I also would like to acknowledge Kevin Hiers for his enthusiasm in regards to 3D fuels and the potential for these data in future research.

Finally, I wish to thank my family (Rachel, Mason, Finn, and Esme) who have been unwavering in supporting the completion of this dissertation. You all have been my rock through this process.

Table of Contents

List of Figures

List of Tables

Chapter 1– Introduction

1.1 Overview

This dissertation examines methods to characterize and quantify pre- and post-fire surface fuels using terrestrial laser scanning in combination with field measurements, airborne laser scanning, and fuelbed simulations. The research focuses on the Southeastern United States, where there is growing consensus amongst researchers that many ecological processes in the region's fire adapted ecosystems are driven by fine scale variations in fuel type, amount, and arrangement. As a result of this understanding, there is growing demand for richer fuels data to capture observed variability at fine grains. Advances in fire behavior modeling have also introduced the need for new fuels data to represent variability in 3-dimensions, to be used in tandem with optical and thermal remote sensing data to validate outputs from new fire models. Deriving high-resolution surface fuels data to meet these needs is the focus of this dissertation, which is presented in the following five related chapters.

Chapter one provides background information, terminology, and research context. Chapter two describes the methods for collecting, integrating, and quantifying error in terrestrial laser scan data for the purposes of describing fuelbeds in non-forested ecosystems of the Southeast. Chapter three examines multi-scale approaches for characterizing and quantifying fuelbed mass across non-forested and longleaf pine dominated stands, quantifying fuel consumption, and deriving relationships with coincident fuels data imputed from airborne laser scanners. Chapter four introduces a novel approach to simulate fuelbeds as a bridge between laser scanned and field-based data. Simulated fuelbeds provide scalability and a framework to distribute highly resolved and robust fuels data across landscapes. Chapter five summarizes overall findings of this research and provides a framework for integration of the analyses into a cohesive fuels characterization to meet

the needs of next generation fire behavior models and advance the understanding of ecological effects of fire at fine-scales.

1.2 Research Context

The impetus for this research can be traced to discussions within the Core Fire Science Caucus (referred to from here on as the CFSC) regarding a lack of integrated, co-located, multi-scale measurements of pre-fire fuels, active fire, and post-fire effects for studying fundamental fire processes and integrating them into the myriad of fire behavior, smoke, and fire effects models (Ottmar *et al.* 2016a). The CFSC is an ad hoc group of ~30 scientists whom meet periodically to discuss fire research state of knowledge and to identify research gaps. This self-directed fire science team is open to all fire scientists and managers, with a stated mission of improving core fire science for the benefit of managers (Sandberg *et al.* 2003).

In 2005, the CFSC identified two primary research threads requiring further elucidation that are expected to influence fire research for the next 20 years. These two threads included enhancing the capabilities of fire behavior modeling and addressing the knowledge gaps that inhibit the ability to model all types of fire in all types of fuelbeds under all fire environments (Sandberg *et al.* 2003). The underpinnings of the CFSC's perspective were later expressed institutionally in the United States Forest Service (USFS) Wildland Fire and Fuels Research and Development Strategic Plan (USDA Forest Service 2006), which calls for research focusing on the physical fire processes, fire characteristics at multiple scales, and fire danger assessment. Specifically, under the physical fire processes (Element A1) there is a call for improved understanding of the fundamental, multi-scale, physical processes that govern fire behavior; sorted into four primary concentrations including fire transitions, heat transfer, fire emissions, and

complex fuels (USDA Forest Service 2006). A natural integrator to fill these gaps in understanding are physics-based fire behavior models (Linn *et al.* 2002; Mell *et al.* 2009).

My research investigates the role of three-dimensional imaging in initiating high resolution and accurate accounting of fuels to inform these physics-based fire behavior models. Specifically, my work seeks to enumerate spatial datasets regarding surface fuel loading in grasslands, shrublands, and longleaf pine forests. Characterization and quantification of fuelbeds is a fundamental pre-requisite for understanding the primary processes governing fire behavior.

To date, three-dimensional data collection such as Light Detection and Ranging (lidar) have been applied mostly at shrub scale- for example to individual palmetto, sagebrush and arctic willow shrubs (Loudermilk *et al.* 2009; Olsoy *et al.* 2014; Greeves *et al.* 2015, 2017). However, fuels are seldom homogenous in spatial distribution and producing robust estimates of fuel mass for mixed heterogeneous fuelbeds has until recently been virtually intractable. The primary focus of my research, then, is to develop and validate methods to generate laser-based fuel metrics and to develop virtual fuelbeds in mixed fuels for utilization in emerging fire behavior and smoke models. The specific objectives of this research are:

1. To evaluate the ability to collect and integrate multi-scale terrestrial laser scanning data over large areas (circa 2ha) and local scales (circa 400 m^2) for the purpose of producing a cohesive fuels height model to serve as the foundation for understanding additional fuels products (Chapter 2);
2. To produce scientifically defensible estimates of fuel mass and consumption resulting from prescribed fire at multiple scales and compare these data against independent airborne laser scanning data for the same area (Chapter 3); and,

3. To develop alternative methods to bridge field and laser data through fuelbed simulation, to improve understanding of spatial distributions of fuel type and mass and increase efficacy of laser scanning for fuels characterization.

It is important to acknowledge that these objectives are part of a larger, longer-term evolution of fuels science and fire modeling. Thus, this dissertation can be thought of as the beginning of a new line of inquiry with 5-10 years of investigation ahead. Ongoing and future work is discussed in Chapter 5.

1.3 Background

Relationships between spatial disturbances and their temporal frequencies are fundamental to ecosystem processes and resultant landscape patterns. Specifically, the role of fire is a common fixture in many/most terrestrial ecosystems (McKenzie *et al.* 2011). Fire is a complex spatio-temporal process on a landscape, driven and regulated by abiotic and biotic features (Johnson 1992; Johnson and Miyanishi 2001; van Wagtendonk 2006). Of the three primary contributors to fire behavior, regime, and effects as outlined by Falk *et al.* (2007), vegetation\fuels is the most difficult to quantify spatially due to limits on intensive ground sampling and traditional remote sensing technology and techniques (Brown and Bevins 1986). Temporally, fire, and by association vegetation \fuels are distributed in five broad categories (McKenzie *et al.* 2011). These categories include frequency\fire interval, duration, seasonality, spatial distribution, pattern, and severity\intensity.

Within the domain of fuels and vegetation, each temporal category has key elements defining how fuels are arranged, spatially interact, and ultimately combust to produce an array of feedbacks and outcomes (Falk *et al.*2007). Furthermore, vegetation\fuels are elements of the fire triangle, tied with weather\climate and topographic drivers, which control and are controlled by

energy sources and energy conversion regulators. Solar inputs are converted to potential energy via photosynthesis and stored in pools until specific fire conditions arise for conversion to kinetic energy (McKenzie *et al.* 2011). Primary factors contributing to how and when fuels burn are abundance, arrangement, and compactness of fuels. These factors, along with moisture and attendant weather, ultimately drive how ignition is transformed into heat, heat-transfer and fire spread.

A primary regulator of fire spread is the overstory plant community (tree density and canopy cover), where solar insolation and wind are regulated by interception within the canopy, controlling variables as soil and fuel moisture, and light competition, and affecting mid-story regeneration type and function (Battaglia *et al.* 2003; Mitchell *et al.* 2009a). In Southeastern long-leaf pine forests Battaglia *et al.*(2003) showed that open canopy conifer forests allowed for light levels ranging from 30-90% of incoming radiation and produced conditions allowing for a diverse and vigorous understory with sufficient fine needle cast from the canopy to maintain frequent fire intervals (Kirkman *et al.* 2001). Similarly, soil moisture, temperature, and water storage were found to be more regulated in unburned (high canopy density) sites in Northern Arizona as compared to a high severity burn site that had shifted to a grass type resulting from fire in a Ponderosa pine forest (Montes-Helu *et al.* 2009). In areas where portions of overstory canopy is retained following fire, a diverse mosaic of surface fuels is expected due to preferential gains or losses in solar insolation along with the effective redistribution of biomass resulting from competition (Pecot 2005; Mitchell *et al.* 2006; O'Brien *et al.* 2008).

In pine forests of the southeastern United States, frequent and low intensity fires are critical components to successful regeneration of longleaf pine (Wahlenburg 1946). The primary carrier of fires in these systems is fine fuels (grasses, shrubs, pine needles); specifically, longleaf needle

cast is the integral pyrogenic fuel due to its resin content and physical traits that allow for combustion across a broad range of fuel moistures (Hendricks *et al.* 2002; Ottmar *et al.* 2003; Bartlette *et al.* 2005). Perturbations in fire return intervals and fire intensity in these systems can lead to rapid changes in hardwood species allowing woody mid-stories to develop that alter the ability for the system to maintain conditions that support continued frequent fire (Glitzenstein *et al.* 1995). Additionally, previous studies have shown the dependence of high understory plant on fine scale variations in fire behavior, which ultimately is controlled by fire-maintained variations in canopy cover and surface fuels (Walker and Peet 1984; Kirkman *et al.* 2004). Hiers *et al.* (2009) suggested that fire effects in frequently burned longleaf forests are governed by fine-grained (~0.5 m spatial scale) fuels variability (the so-called Fuel Cell Concept). This finding, although not yet fully validated, identifies a need for improved spatial characterization of fuels corresponding with high resolution thermal and multi-spectral imagery, in order to quantify fuel and fire heterogeneity simultaneously at fine grains.

1.3.1 Application to broader fire research and fire behavior modelling

Organization and distribution of fuels also plays an important role in determining the growth and behavior of fires on a landscape (Finney 2001a, 2002). Similar effects occur at a range of scales where changes in fuel type, arrangement, and/or ignition pattern (e.g., strip or spot) influence the interactions of flaming fronts (Maynard *et al.* 2016). Convergence of flaming fronts can result in increases in flame height, propagation, heat release rate, and flame angle as two fronts merge (Martin and Dell 1978). Fuel patterns can also impact the way fire interacts across a landscape. For example, where fuels are fire inhibitors, fuel moistures are high, or there is a lack of combustible fuels (e.g. bare ground, sparse vegetation) fire is forced to burn around features creating heterogeneous patterns of fire behavior and effects (Loudermilk *et al.* 2009; Dell *et al.*

2017). Beer and Enting (1990) describe three possible regimes of fire spread- uninhibited spread where there is a generally uniform front of combustion that burns all available fuels; no spread due to conditions not supporting propagation; and geometrically constrained propagation where random variations in combustion are dependent on regional spatial patterns. Wind flow dynamics over fuelbeds also play an integral role in the propagation of fire by generating turbulence within and above the fuelbed (Pimont *et al.* 2009). Sudden heterogeneities in canopy induce additive canopy-based turbulences that accelerate surface winds (Dupont and Brunet 2006). These interactions between large coherent structures and fire interactions are difficult to quantify and require additional investigation (Pimont *et al.* 2009).

To examine the integration of wind-flow dynamics at local scales and the effects of fuels and fire propagation numerous investigations using computational fluid dynamics based fire behavior models (CFD) has occurred (Pimont *et al.* 2009). Experiments have been developed to duplicate observed wind characteristics that occur over vegetation using CFD models, specifically with heterogeneous fuels (e.g. Mueller *et al*. 2014) and along forested edges (Dupont and Brunet 2008). These studies observe windspeed and canopy roughness thresholds above which canopy winds are laminar and below which there are vertical accelerations of wind-flow that induce turbulence and influence fire propagation. There are numerous additional inputs affecting how fire propagates involving fuel arrangement, flaming front interaction, and wind-flow dynamics and these inputs have generally been evaluated at large-scales (e.g., 30-1000m) to understand how tree canopies influence fire behavior. There are also important but as yet unquantified relationships between the aforementioned inputs and the complex responses of vegetation to fire (Loudermilk *et al*. 2012). The Ecology of Fuels (Mitchel *et al.* 2009) and the wildland fuel cell concept (Hiers *et al.* 2009) both attempt to integrate fuel heterogeneity, fire behavior, and fire effects and to

identify spatial limits on these processes (Loudermilk *et al.* 2012). Ultimately, the unifying element that will allow these ideas to be tested is robust, scalable fuels characterizations that are compatible with CFD models. Improvements in fine-scale fuels measurements will allow for enhancements in fine-scale CFD modeling that can be more easily compared to *in situ* high resolution thermal infrared measurements.

Testing the wildland fuel cell concept requires alternative fuel sampling methods, as quantifying fire and fuel heterogeneity at fine scales has met with limited success to date (Mitchell *et al.* 2006). Fuels have typically been characterized at stand-scale (Ottmar *et al.* 2003) and fine scale sampling is usually averaged over the larger unit and generally represents mass and vertical variability, but lacks information on horizontal fuel continuity (Fernandes *et al.* 2000; Ottmar *et al.* 2007). Rationale for using stand level averages is partly based on fire behavior models currently in use for management (e.g. BEHAVE PLUS (Andrews *et al.* 2005), FARSITE (Finney 2004)), which incorporate assumptions of fuels homogeneity that derive from Rothermel's fire spread model (1972).

Typical fuels measurements include transects (Brown 1974) and point intercept data (Mueller-Dombois and Ellenburg 1974) to determine mass of coarse woody debris, along with fuel depth, and cover. These methods are used to estimate fuels across the landscape for the purpose of coarse-grained fire behavior and effects modeling, but they do not encompass the full range of heterogeneity across the landscape (Hardy *et al.* 2008). In fact, the inability to characterize spatial non-uniformity of fuels and fire behavior is one of the primary drivers for development of CFD fire behavior models for wildland fire. These models attempt to integrate atmospheric and fire fluid dynamics using physical principles to propagate fire across the landscape (as opposed to empiricism). They have the potential to improve understanding of fire processes that cannot be

seen because they occur at scales difficult to observe or at the extreme limits of fire behavior. The Wildland Fire Dynamic Simulator (Mell *et al.* 2009) and FIRETEC/higrad (Linn *et al.* 2005) are the two primary models in use. The desire to validate these models with field measurements has become a driving force behind comprehensive multi-disciplinary experiments such as the Prescribed Fire Combustion and Atmospheric Dynamics Research Experiment (RxCADRE).

One avenue to improve fuelbed characterization has been through application of airborne and terrestrial laser scanning. Commonly referred to as Light Detection and Ranging (LiDAR), these systems employ laser emissions ranging from 10 kHz to 300 kHz that can register multiple returns per pulse. The laser returns are used to construct three-dimensional point clouds or digitized waveforms that represent 3-D models of aboveground and surface features. The utilization of airborne laser scanning (ALS) to derive fuel metrics has been applied to canopy bulk density (Riaño *et al.* 2003; Andersen *et al.* 2005), surface fuel model classification, by fusing multi-spectral data with ALS (Riaño *et al.* 2003; Mutlu *et al.* 2008), surface fuel loading (Hudak et al. 2016), and canopy base height (Andersen *et al.* 2005; Rowell 2005). These metrics have been derived for inclusion in current standard fire models (FARSITE, Finney 2003), as well as to produce landscape estimates of critical fuel patterns.

As ALS datasets have become increasingly rich in resolution (~9-13 returns per meter^2) there have been improvements in the ability to estimate important forestry metrics. Jakubowski *et al.* (2013) report reductions in root mean square error (RMSE) for models of eleven key forest metrics as ALS pulse density increases. This in part due to higher probability of laser pulses being intercepted by features representing the full range of heights occurring on the landscape. The primary source of uncertainty, however, is how the laser pulse interacts with an object. It is known that ALS data are collected when sufficient energy is returned to the sensor to trigger a return. The

value returned represents a weighted average of the energy intercepted by the energy footprint. Hopkinson *et al.* (2005) noted systematic underestimation of vegetation heights when field measured and ALS height metrics were compared. Inversely, the same study demonstrated that ground height measurements between GPS and ALS showed a slight over estimation of height by ALS instruments. These findings are significant for characterizing surface fuels, as many of these fuel types are typically less than 0.5m in height and the findings from Hopkinson *et al.* (2005) denote underestimates of heights ranging from 22-63 percent. The level of error for surface fuel features is significant enough to impact estimates of height, mass, and cover that are used to characterize the landscape.

Because Terrestrial Laser Scanners (TLS) provide more highly resolved data, their employment in surface fuels characterization is expected to improve derivation of fuelbed metrics and perhaps to improve estimations from ALS-derived metrics as well. TLS collect local and highly resolved three-dimensional data (0.001 to 0.5m point spacing). Related to fuels characterization, TLS has been used to estimate biomass of individual shrubs (Hosoi and Omasa 2006; Loudermilk *et al.* 2009; Olsoy *et al.* 2014; Greeves *et al.* 2014). Loudermilk *et al.* (2009) quantified heterogeneous fuelbeds in the southeastern United States by deriving krigged surface volumes from high resolution TLS scans and comparing with point intercept estimates of volume. Ultimately, a primary limitation in characterizing heterogeneous fuelbeds results from the ubiquitious mixture of fuel elements that are difficult to segment from one another in laser scans (Rowell *et al.* 2016a). These fuels generally have different mass\density partitioned throughout the fuelbed (e.g shrubs, woody debris, grass, etc.), which have different combustion characteristics (Fonda 2001). The general limitation of TLS data stems from the oblique scan orientation that causes occlusion of the laser pulses. Penetration of laser pulses into dense features (e.g. palmetto

shrubs) is highly limited as the energy passes through gaps and is intercepted by objects. The assumptions developed by Hosoi and Omasa (2006) and supported by Loudermilk *et al.* (2009) suggest that "over sampling "by scanning from multiple angles overcomes some of the problem of canopy interception of energy and shadowing effects. Ultimately the amount of biomass within a hull of a vegetation clump remain uncharacterized by the TLS, and its presence and amount is known only by relying on assumptions that the surface area of a hull is a well-correlated proxy for leaf area.

Despite these limitations, there is significant potential to improve characterization of all fuel types using TLS, from the framework of biomass quantity, arrangement, type, and vertical\horizontal connectivity. Furthermore, TLS fuel derivatives will allow for improved comparisons with ALS derived fuels data, as they both are capable of describing local and larger landscapes in ways that traditional fuels inventories have been unable to perform. A key limitation from the standpoint of ALS data to date has been the inability of the laser to characterize fine fuels (Seielstad and Queen 2003). This assertion is substantiated from fuel mapping studies conducted in the New Jersey pine barrens (Skowronski *et al.* 2007; Clark et al.2009), where ladder and hazardous fuels were primary features characterized using lidar transects. Fine fuels in this study were generally characterized only when there was an absence of overstory vegetation.

1.3.2 Integrated Fuels Characterization

Given the different limitations of ALS and TLS data, I have developed a framework describing how these two data sources can be leveraged together to produce cohesive, integrated landscape-scale fuel characterizations. As described previously, ALS data have known underestimations of height that lead to error associated with surface fuel metrics. However, TLS is an advantageous method to improve characterization of local metrics that can be used to inform

ALS-derived metrics across the landscape. The concept depicted in figure 1, utilizes ALS-derived metrics as a unifying element for estimating fuel properties for the landscape and TLS metrics, field measurements, and fuelbed simulations to relate back to ALS-based measurements, where cross-validation occurs when all three types of data exist for the same area. Then, additional TLS, field, and simulated fuelbed data are collected to densify the training data needed to impute the ALS-based fuels metrics. The proposed model also allows for investigation of fuels and subsequent fire behavior across multiple scales as well as cumulative effects as a function of grainsize. When integrated with existing methods and results regarding canopy metrics, this approach is expected to provide context for asking and answering questions about the impacts of scale and spatial variability on fire behavior, fire behavior, wind-flow dynamics, and smoke production from fire.

Figure 1. The Integrated Fuels Concept: In this model, ALS and TLS coupled with simulated fuelbeds provide the basis for scalable fuels data for both surface and canopy layers. Using this approach, fuels data can be ported for high resolution fuels assessment and modeling ($0.25m^2$) typical of the southeastern US or scaled up to scales of $10\text{-}20m^2$ that are most useable for western fire science. The key benefit is that all scales start at the highest resolution and are aggregated to coarser scales which produce more robust datasets.

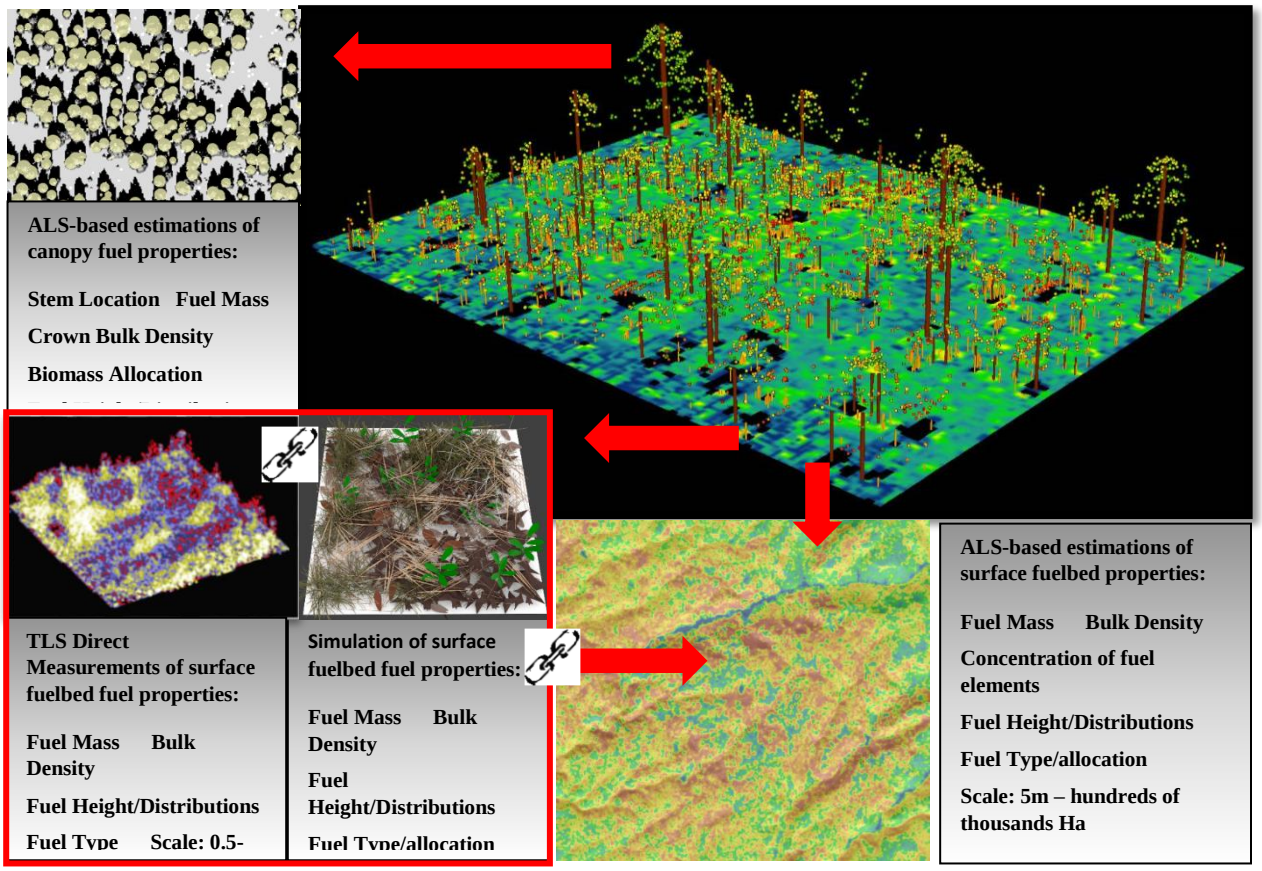

Chapter 2 – Initial Research

Development and validation of fuel height models for terrestrial lidar — RxCADRE 2012

2.1 Abstract

Terrestrial laser scanning (TLS) was used to collect spatially continuous measurements of fuelbed characteristics across the plots and burn blocks of the 2012 RxCADRE experiments in Florida. Fuelbeds were scanned obliquely from plot/block edges at a height of 20 m above ground. Highly instrumented plots (HIPs) were scanned at ~8 mm spot spacing from a single viewing position pre- and post-fire while blocks were scanned from six perspectives pre- and four post-fire at ~2 cm spot spacing. After processing, fuel height models were developed at 1 m^2 spatial resolution in burn blocks and 0.25 m^2 resolution in plots and compared with field measurements of height. Spatial bias was also examined. The resultant fuel height data correspond closely with field measurements of height and exhibit low spatial bias. They show that field measurements of fuel height from field plots are not representative of the burn blocks as a whole. A translation of fuel height distributions to specific fuel attributes will be necessary to maximize the utility of the data for fire modeling.

2.2 Introduction

Fire science and management typically utilize statistical inference and generalization to produce fuels data for fire behavior prediction (Anderson 1982; Burgan and Rothermel 1984; Keane 2013). The emergence of next-generation wildland fire behavior models that simulate fire propagation through three dimensional lattices at fine grain has placed new demands on fuels data (Linn *et al.*2002; Morvan and Dupuy 2004; Mell *et al.* 2007; Pickett *et al.* 2009; Prince *et al.* 2010). However, distributing fuel realistically across landscapes is difficult, and measuring three-dimensional locations of fuels in the field accurately is time consuming and hard to replicate. Consequently, most fuels data are collected within small areas (transects or plots) and must be abstracted to represent fuels on larger domains. Given the very high spatial variability observed in

even fairly simple fuelbeds (Keane *et al.* 2012), the need to describe the actual arrangement of materials as an alternative to abstraction has increased irrespective of domain size. Further, because fuelbeds used in validation of fire behavior prediction cannot be disturbed by field sampling before burning, a remote sensing approach is required.

Recent advances in laser scanning are producing more replicable and accurate renderings of fuels in regards to the spatial distribution of plant elements. Experiments in the southeastern United States have integrated terrestrial laser scanning (TLS) to extract volumes of shrub fuels in laboratory experiments (Loudermilk *et al.* 2009), as well as to fuse TLS data with thermal images of fire behavior in long-leaf pine forests (Hiers *et al.* 2009). Outside of the realm of fuels, experiments to detail plant area density as a function of voxel-based canopy volume in wheat, shrubs and trees (Hosoi and Omasa 2006; Van der Zande *et al.* 2006; Hosoi and Omasa 2008) have yielded strong correlations with dry biomass.

In each of these instances there is a requirement for high spatial resolution data and measurements from multiple perspectives to reduce occlusion from foreground objects and to maximize penetration into vegetation (Hosoi and Omasa 2008). These previous approaches show promise for characterizing individual plant elements in controlled environments, but the characterization of fuels matrices over larger domains in natural environments using TLS data has not been widely investigated. Given considerable uncertainties in estimating specific fuels attributes such as mass by size-class or surface area to volume ratio, the potential near-term advantage of TLS for providing improved fuels data is in mapping characteristics of the fuelbed in terms of the height, shape, and arrangement of vegetation across landscapes up to a few hectares in size with the purpose of explicitly characterizing some of the spatial variability in fuels that may affect fire behavior and effects.

This paper describes methods for acquiring and processing high resolution TLS data across 2-ha blocks of mixed grass and shrub fuels in the southeastern United States as developed through the Prescribed Fire Combustion and Atmospheric Dynamics Research Experiment (RxCADRE) conducted at Eglin Air Force Base, Florida. The objectives of the study are to produce a single large dataset suitable for validation of fire behavior models. To meet this objective, data accuracy and bias are quantified in the 2-ha blocks where scans were collected from 10 perspectives per block (40 individual scans). We report accuracies associated with the spatial fidelity (easting, northing, and height accuracies) of the complex acquisition modes of TLS data and hypothesize that the majority the error within the point clouds is introduced as a function of how the laser samples objects at the farthest ranges from scan origin. We also speculate that variability between height metrics from TLS and field measurement are the result of characterization modes and not spatial incongruities that cascade from the processing stream. This research shows how integration of large TLS point clouds can be used to produce spatially explicit and continuous measurements of fuelbed height over 2-ha areas at ~2 cm resolution, in conjunction with the other measurements of RxCADRE described in this issue. We provide a simple analysis of height comparisons from field validation and TLS-based estimations to quantify errors and bias that will allow for further types of analysis as biomass, percent cover, and fuel type and arrangement.

2.3 Methods

2.3.1 Study area

Terrestrial laser scanning (TLS) data were acquired at Eglin Air Force Base, Florida, in October 2012. Eglin AFB is located in the panhandle of northwestern Florida, USA, which was originally a unit of the former Choctawhatchee National Forest; Eglin is an important resource in the

management of longleaf pine ecosystems with 180,000 ha of longleaf pine sandhills and flatwoods (for site map and details see Ottmar *et al.* 2016b). Landscapes with dimensions of 100 m x 200 m (S blocks) were established in two fuel types, grass-dominated and shrub-dominated, and were subsequently burned with strip head fires.

2.3.2 Field data

One meter square clip plots were measured adjacent to each TLS sampling area (Ottmar *et al.* 2016b). For the six S-blocks, one square meter pre-burn plots (n=25 per block) were established around the perimeter of each 2 ha area at 20-m intervals. Each field plot was monumented with a metal pole on its southeast corner. Plots on the eastern edge of each block were offset eastward by one meter so they did not fall within the burn block itself. Metal poles were wrapped with retro-reflective tape for easy identification within the TLS point cloud. Field measurements for all small field plots included maximum height, average "center of mass" height, canopy cover, and dry biomass weight by lifeform (grass, forb, and shrub). Plots were also photographed obliquely from the north to document pre-fire spatial organization of fuel elements. Blocks S3, S4, and S5 were mowed the previous spring and are generally grass dominated with low shrubs and forbs that are primarily at the same height as the grass clumps. Blocks S7 and S8 have a significant oak and palmetto component and have not been treated mechanically or chemically.

2.3.3 TLS data collection and processing

Laser scans were completed pre-and post-burn using an Optech ILRIS^{TM} 3_6D-HD instrument scanning at 10 kHz. Two modes of data were captured for the RxCADRE project: first, the six S-blocks representing relatively homogeneous and continuous grass fuels interspersed with shrubs

over 100 m x 200 m extents (block S9 is not included in these analyses as there were issues related to acquisition of the data including too small of a view window that ultimately excluded the reflective poles used to tie scans together. Details of the RxCadre sample design are reported by Ottmar *et al.* (2016b). In the S-blocks, the TLS instrument was also positioned in the mobile boom lift at a height of 20 m above the fuelbed. Laser scans were collected at six positions around each burn block (Figure 2) at 20-m horizontal distance from the edge of the block. Post-fire scans were collected from the east and west positions only for a total of four per block.

In each scan, the laser was pointed downward at an angle of 23°. The scanner was operated from the ground using a tablet computer with a wireless connection. Scanner settings were optimized to achieve consistent point density across the block with the caveat that point density necessarily declines as range increases. The ILRIS laser allows point density to be set as a function of focal distance; all S-block scans were set to collect 2-cm spot spacing at 90 m, ranging from 8 mm at 20-m range to 56 mm at 300-m range. The 2 cm sampling resolution is based on constraints for sampling in the field. Due to the data collection occurring on an active bombing range at Eglin AFB, we had limited access to the range between missions. Data collections were limited to 45 min. per scan location for an average scan time of 8 hours per S-block including moving the boom lift between each scan location.

Figure 2. (*a*) An example of the fuelbed for block S3 from the boom lift, (*b*) TLS data clipped to the block boundary with scan locations, and (*c*) a three-dimensional graph demonstrating height variability for a 10 m x 10 m subset of the TLS data.

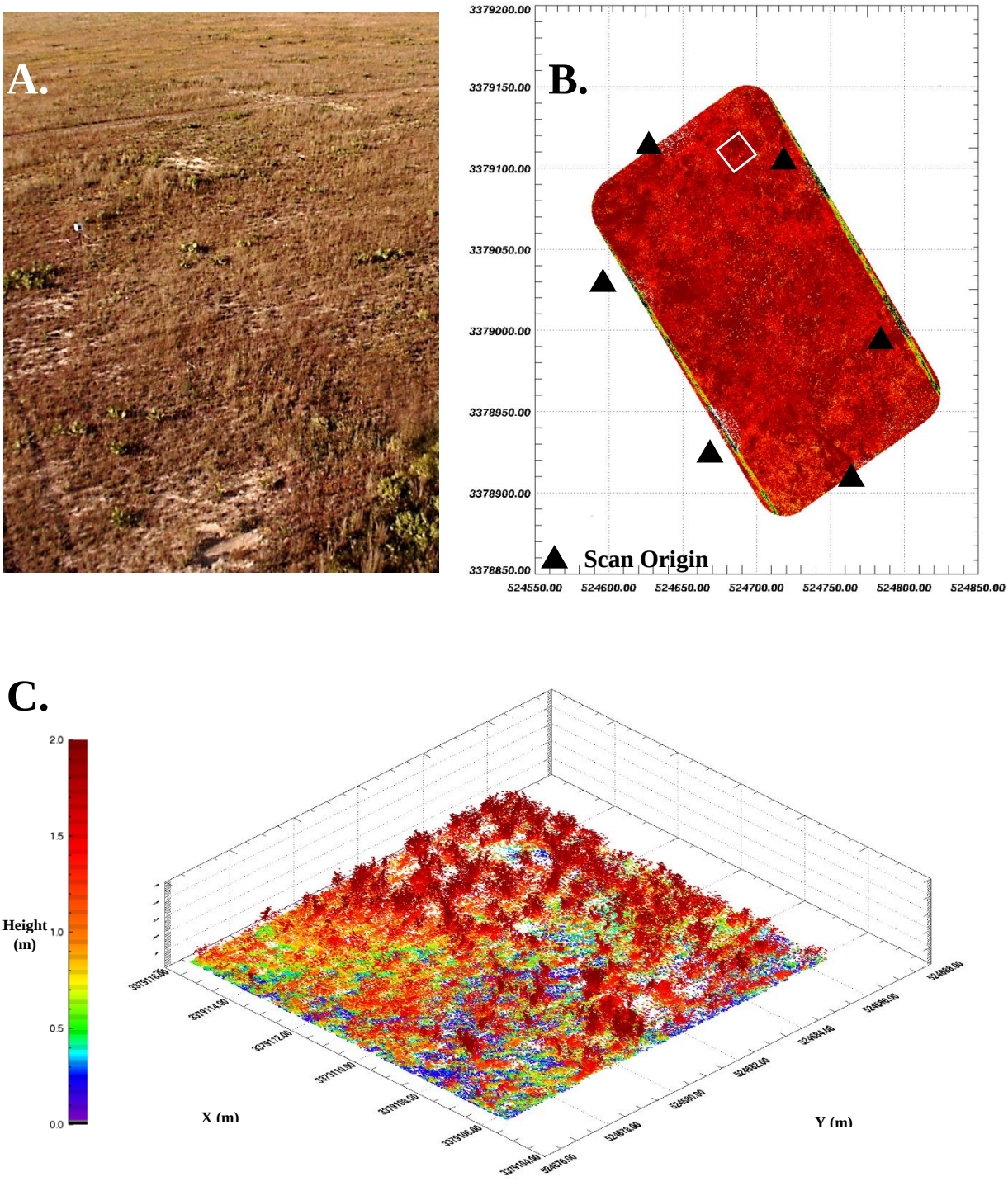

The 2cm resolution at 90 meters range allowed for relatively dense data resolution within the block in a time frame that allowed for completion of the data collection prior to the execution of the prescribed fire**.** Time-of-flight scanners collect richer datasets near the point of origin of the scan with less dense point spacing as range increases. As the laser pulse moves away from the ILRIS instrument, the point spacing increases linearly with range at a rate of 16.8 mm per 100 m of range. Additionally, the illuminated footprint of the scanner increases linearly with range, becoming less sensitive to canopy gaps as spot size increases (Seielstad *et al.* 2011). Spot size in the foreground of each S-block was 16 mm, expanding to 29 mm at 100 m range. Though we acknowledge that there is higher point densities on the edges

2.3.4 TLS processing

Each scan was initially corrected to a GPS control data set (as collected in the RxCADRE experiment) around each block using the Polyworks software suite (Innovmetric: Quebec, Canada) by replacing corner post locations in the raw point clouds with GPS locations. The ILRIS laser scanner collects data in individual 40° x 40° windows which then need to be aligned with one another. Scan-to-scan corrections were completed by selecting identifiable points within the control data (usually monument posts) and then further refining the scan correction using the automated align algorithm within Polyworks. The corner reference points were more easily identified in post-burn scans; therefore these points were used to tie adjacent scan scenes together to create a reference for the pre-burn scans. Because all laser scans were collected from the same locations, pre- and post-burn, pre-burn scans were aligned by using the locations of the post-burn scan head as the initial control points.

Matching of scans was highly dependent on the auto-align algorithm in Polyworks. The absence of hard targets in the pre-fire scans made matching of scenes difficult. Polyworks uses a proprietary meshing algorithm in the auto-align procedure. In dispersed fuelbeds, the meshing algorithm struggles to manifest identifiable objects such as the corner posts in enough detail to accurately merge scans. Therefore, an open-source point alignment software package was employed to refine alignment (Cloud Compare 2014) using individual points rather than meshes. All scans from each scanhead location were merged together using code developed in the lead author's lab and written in IDL, and adjacent scan groups were aligned to the group showing the least variability in alignment quality and encompassing the greatest number of visible metal posts. Scan groups were aligned and merged by selecting coincident points and applying an alignment matrix to orient each group into a common projected space. All scan groups were then merged into a single dataset for each burn block and clipped to a 20-m buffer around each burn block. These block datasets were then converted into lidar-specific .las format files and an initial surface and ground separation was performed within LASTools (rapidlasso GmbH, Gilching, Germany) using the LASGround algorithm.

Initial assessment of the ground surface classification suggested differential occlusion of ground points within the center of the burn blocks compared to edges (e.g. 'ground' returns within the fuel height model [FHM] appear lifted in block centers compared with areas at the edges where ground is clearly identified and separate from the FHM). We suggest that occlusion was a function of oblique viewing angles that preferentially samples upper reaches of the fuels canopy with less representation of lower fuel objects and the ground. To correct for this condition, airborne scanning laser (ALS) data (for methods see Hudak *et al.* 2016) collected at the same time as the TLS data were used to adjust the TLS data for geoid and normalized height using the TLS Processor DTM

Correct routine written in IDL. This routine imports .las format laser data and interpolates the ALS ground points into a bare earth digital terrain model (DTM), in this case, at 0.25 m^2 resolution. The bare earth TLS data points were compared to the coincident ALS ground points and differences between elevations were used to adjust the TLS data to the proper geoid height for both ground and FHM strata. Corrected geoid heights for the FHM were then differenced from the digital elevation model (DEM) to produce the normalized heights above ground.

2.3.5 TLS data accuracy assessment

Vertical and horizontal accuracy of TLS data were assessed on three criteria. To assess accuracy, point clouds from each of the small field plots were extracted by importing feature datasets of the TLS point clouds into the ArcGIS environment and identifying highly reflective lidar points (intensity values >8000). These reflective data points generally represent low gain returns from the highly reflective retro-tape encasing the 1-m tall aluminum poles at each field plot corner. The points representing monumented plot corners were isolated by selecting 1 m x 1 m buffers around clusters of highly reflective points. At each corner post, 1 m^2 plot boundaries representing the field plots were digitized using the plot corner as the southeast corner of the field plot. Points from monumented plot corners were cleaned to remove reflective artifacts such as ghosting (Seielstad *et al*. 2011) and remaining points were spatially joined with the field plot locations identified above. The result was a cleaned FHM for each small field plot.

The first level of assessment regards the horizontal accuracy of scan-to-scan representations of the corner posts. Plot corner points from each scan station were compared to all coincident corner points for each 2 ha block, with associated errors reported as root mean square error (RMSE). Each plot corner was assessed in the horizontal and vertical domain. The second

level of assessment regards vertical error from scan station to scan station. For all combinations of scan stations for each 2 ha block, 0.5 m^2 resolution bare earth DEMs were extracted using the BLAST2DEM routine in LASTools lidar processing suite. These DEMs were imported into the ArcGIS environment, where raster calculations were conducted and zonal statistics based on the clip plots extracted. Multiple DEMS were generated for each scan station to assess whether there was significant differences between scans. Even by normalizing heights to the ALS DEM if a scan swath is pitched at a 30 degree angle for instance, there will be artifacts or the surface might be lifted if there are erroneous low points. So we compared every single scan swath from the TLS to insure that there were no incongruities. The third level of assessment regards spatial bias between plot corners as determined by the comparison of TLS derived post locations with surveyed GPS points.

2.3.6 Spatial bias

To assess variability of height metrics as a function of distance from scan station, height-normalized laser data were clipped to block boundaries and examined as a function of distance from block centroids. We hypothesized that as scan distance increases towards the center of the block, the increasingly oblique nature of the scan could result in differential occlusion of ground, thus skewing the fuel height model higher in the center of the plot. In effect, viewing vertically-oriented grass fuels from above may reduce the probability of detecting foliage, particularly at top of canopy, compared with viewing them obliquely. A smaller laser spot size may produce a similar effect. To test this hypothesis we examined height metrics in 10-m wide concentric rings centered on block centroids out to 50 m distance (block edges on east and west sides). There were two centroids per block that represent the center of all scan groups. As we are unable to measure the

interior of the block due to altering the fuelbed that may influence fire behavior during the prescribed burn, we sought to assess point density and potential bias within the block compared to the validation plots that occur closest to the scan station and have the highest point densities.

2.3.7 TLS-based height metrics

Height metrics were extracted from the height distribution of each 1 m^2 field plot including mean height, standard deviation height, inflection height, and the first and second peak of the distribution (figure 3). The first peak of the height distribution is the highest frequency height bin (from bottom) greater 1 cm in height. The second peak is the second highest frequency after the first peak. Two mean height metrics were calculated; the first mean height uses all points in the plot subset and the second mean excludes all points that are ≤1 cm to reduce the influence of the ground points on the average. The inflection point is calculated by using a derivative function on the frequency values of the histogram. The function outputs signed values of the slope of the histogram and looks for a sign change to positive for heights 5 cm greater than the height of the first peak.

This inflection point is hypothesized to represent the transition from grass clumps, low forbs, and shrubs to grass seed heads and taller shrubs. In previous work, the inflection height of grass fuel matrices was systematically lower than inflection heights associated with shrub fuels (Rowell and Seielstad 2012). Aside from vector based height metrics, raster based height metrics were generated across each S-block using LASCanopy in the LASTools suite. These products included maximum, mean, minimum, standard deviation, first, fifth, tenth, twenty fifth, fiftieth, seventy fifth, ninetieth, ninety fifth, and ninety ninth percentile heights at one meter spatial resolution.

2.4 Results

2.4.1 Horizontal and vertical accuracy

For these results, accuracies are derived through comparison of highly reflective points around plot corners. The horizontal accuracy assessment (Table 1) produces average between-scan easting and northing errors for all posts of 10.75 mm and 9.94 mm, respectively. For individual blocks, S5 contained that largest northing error of 13.97 mm and S4 had the largest easting error (11.43 mm). The vertical accuracy assessment results in between-scan errors ranging from 40 to 120 mm. Assessment of the vertical accuracy of the segmented plot corners indicated better alignment between adjacent scans in blocks S3, S4, and S5. Blocks S7 and S8 exhibited larger error indicating less certainty regarding alignment of some adjacent scan stations. The latter blocks exhibited larger magnitude vertical error suggesting less certainty in definition of ground between some scan stations, effectively resulting from the more heterogeneous fuelbed that might occlude tops of the poles from being accurately sampled from all directions due to tall shrubs.

These results summarize the vertical accuracies in regards to scan-to-scan comparisons of bare earth interpolated surfaces. The vertical offsets derived from scan-to-scan comparison of bare earth interpolated surfaces (Table 1) produced average error of 8.83 mm across all S-blocks. The lowest vertical errors were associated with block S3 (5.41 mm) and highest vertical errors were associated with block S8 (15.84 mm). Given the between-scan consistency of bare earth surfaces, the differences in vertical accuracy obtained from bare earth points versus plot corner posts (from above) are likely attributable to the difficulty in characterizing post heights consistently at long scan distances.

2.4.2 Comparison with GPS control points

Comparison of 35 GPS surveyed points (6 to 8 per block) with the predicted points from the TLS data showed offsets for all blocks (Table 2) ranging from 75 to 185 cm. Errors were

similar and minor in S3 and S4 (easting RMSE = 1mm, northing RMSE = 1mm, height RMSE=5.3 and 5.9 respectively). Co-location errors were evident in 1 to 2 individual scan stations in each block for S4–S8, specifically the vertical offset. After a second-order polynomial transformation, RMSE was reduced to less than a millimeter for S3 and S4, and to 14 to 19 cm for S5–S8. The internal

Figure 3 (*a*) An example of a normalized histogram of the TLS fuel height distribution with the peak frequency, mean height, inflection point, and second peak frequency for plot 18 in block S4, and (*b*) the plot photo of the same area.

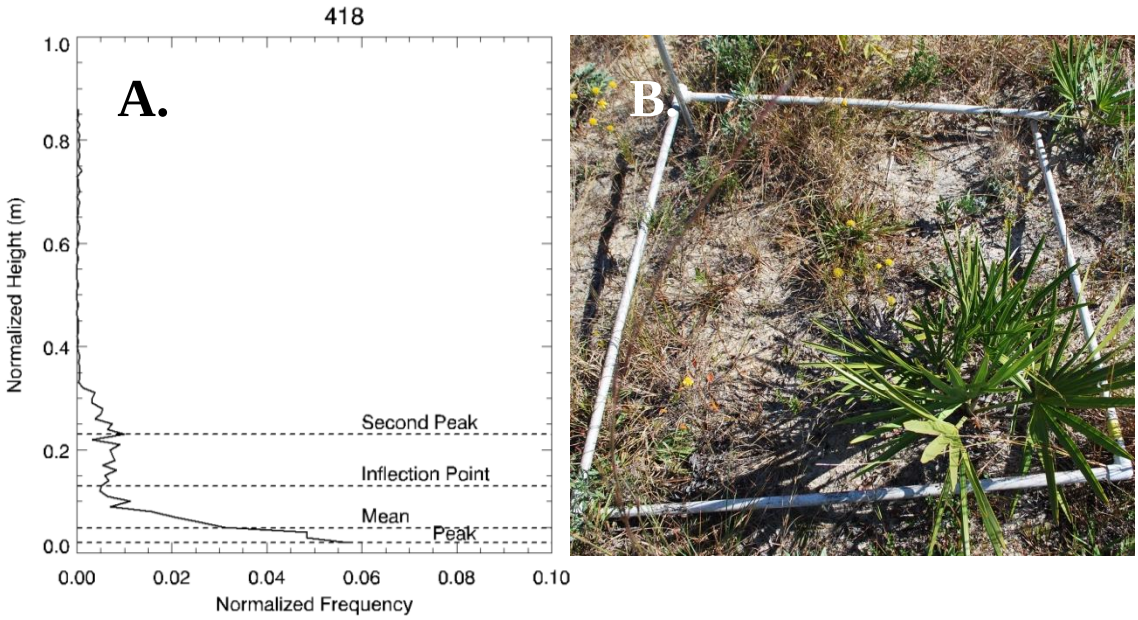

Table 1. Scan to scan errors associated with the merging of opposing scans into a single dataset

Errors are reported as root mean square error (RMSE) for horizontal and vertical domains representing identified plot corners in the point cloud. The vertical RMSE for the bare earth is the RMSE of the difference for each scan direction compared to all other scans in a block.

Block ID	Plot posts error (cm)			Bare earth vertical error (mm)
	X	**Y**	**Z**	
S3	0.1	0.1	5.9	5.4
S4	0.1	0.1	5.3	6.8
S5	0.1	0.9	3.9	6.8
S7	3.0	2.0	11.0	6.1
S8	3.0	4.0	12.1	15.0

Table 2. Differences between TLS post locations and GPS survey points before and after 2nd-order polynomial transformation

Root mean square error for TLS and GPS data pre- and post- second-order polynomial transformation

Block ID	Root mean square error	
	Pre-transform (cm)	Post-transform (cm)
S3	74.9	<0.01
S4	97.8	<0.01
S5	147.0	14.5
S7	74.0	18.5
S8	185.0	19.3

consistency of the untransformed point clouds was high as evidenced by coincidence of posts in the aligned scans. The observed offsets from the GPS survey points shows that the internal alignments of the point clouds did not perfectly align with the surveyed geometry. It is probably not coincidental that the largest error occurs in shrub-dominated plots where identification of posts in the point clouds is more difficult.

2.4.3 Height of vegetation

Maximum heights of field-collected and TLS derived data were compared to assess the ability to predict heights of fuel elements. These results show a reasonable relationship between maximum heights of both datasets ($r^2 = 0.70$, adjusted $r^2 = 0.70$, $p<0.0001$) (figure. 4). The scatter plot of maximum heights reveals general agreement between the dependent and independent observations at heights of ≥50 cm. Below this threshold, there was more variability in the estimated maximum height and the laser tends to overpredict (bias of 9.6 cm). For instances of over prediction, these results appear to be caused by contamination of the plot point clouds due to ghosting from the reflective corner posts and subtle misalignment of plot boundaries due to uncertainty of the corner point used to anchor each 1-m^2 plot polygon. Ghosting occurs when areas of high reflectance are averaged with a background of lower reflectance objects creating a trailing cloud from the highly reflective surface towards the background. Where TLS derived maximum height is underestimating the maximum height substantially (4 cases), plot misalignment is the primary culprit.

Very weak relationships were observed between TLS mean height and field-estimated center of mass height (not shown) and it is not evident that relationships should exist given how

Figure 4. Scatter plot of observed and TLS-based maximum height for clip plots in the S-blocks demonstrating the overestimation of height from the TLS estimate.

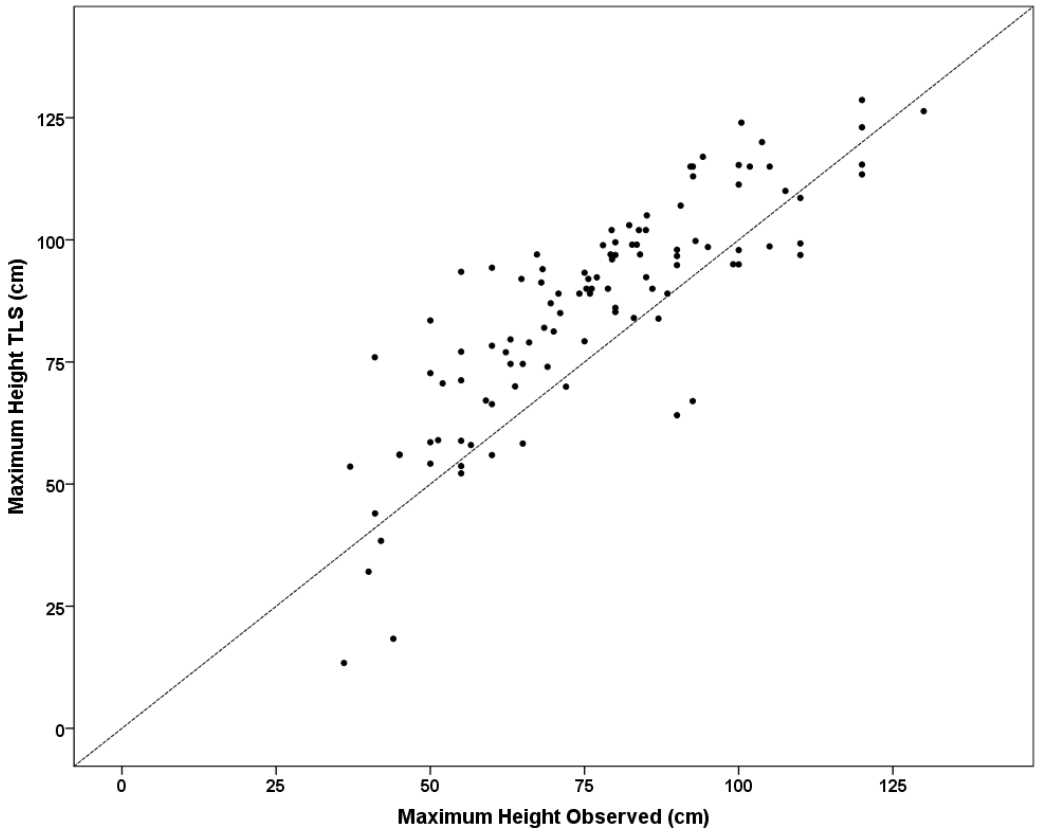

field estimation was executed (a measurement based on the ocular assessment of the mean height of each life form). However, variability in scan angle might be expected to produce variations in characterizations of central tendency particularly in vertically-oriented fuels such as grasses. However, no consistent spatial bias is evident for maximum or mean heights (Table 3) as characterized by trends in means from center of blocks to edges. In grass-dominated S4 and S5, heights declined by 4 cm on average from centroid to edge, but this effect is not apparent in grass-dominated S3. In shrub-dominated S7 and S8, small changes between distance rings from centroid are random. Overall, the average absolute difference in maximum heights between rings is 4.8 cm with negative and positive values equally represented. Variability as characterized by standard deviation of heights is very consistent across all blocks.

While these data don't absolutely resolve the question of spatial bias, they suggest that bias, if present, is small. Additional evidence supporting the conclusion of no bias can be found in comparison of maximum height data from coincident field and TLS measurements and from all maximum height data from each block (Table 4).

As noted above, TLS and field heights track consistently for the small field plots with overestimation by TLS. Comparison of these results with TLS-derived maximum heights for entire blocks suggests that fuels are consistently taller on average across the blocks than indicated by either field or TLS measurements from the small field plots. Though there was significant trampling of the fuelbeds outside of the clip plots, care was given to not disturb the clip plots before TLS scanning. To further examine whether proximity of the small plots to scan stations (overhead perspectives, small spot sizes) contributed to these differences, block boundaries were buffered by 10 m inward and then maximum height metrics were recomputed for these areas. Maximum heights were no different along block edges than across entire blocks, suggesting consistent height

Table 3. Reported maximum, mean, and standard deviation height for concentric rings of TLS normalized height data at 10-m increments from the centroid of each S-block

Block ID	Height	Distance from plot centroid				
	(cm)	0–10 m	10–20 m	20–30 m	30–40 m	40–50 m
S3	max	0.89 ± 0.17	0.91 ± 0.17	0.96 ± 0.17	0.96 ± 0.18	0.94 ± 0.19
	mean	0.39 ± 0.07	0.40 ± 0.08	0.42 ± 0.08	0.43 ± 0.08	0.41 ± 0.10
	stddev	0.17 ± 0.04	0.18 ± 0.04	0.20 ± 0.04	0.20 ± 0.04	0.20 ± 0.04
S4	max	0.89 ± 0.21	0.99 ± 0.20	0.95 ± 0.21	0.92 ± 0.23	0.89 ± 0.23
	mean	0.36 ± 0.11	0.40 ± 0.13	0.38 ± 0.12	0.35 ± 0.13	0.29 ± 0.12
	stddev	0.21 ± 0.05	0.22 ± 0.04	0.22 ± 0.05	0.22 ± 0.06	0.22 ± 0.07
S5	max	0.96 ± 0.18	0.98 ± 0.21	0.98 ± 0.20	0.95 ± 0.20	0.87 ± 0.20
	mean	0.38 ± 0.09	0.41 ± 0.12	0.41 ± 0.13	0.38 ± 0.11	0.31 ± 0.10
	stddev	0.21 ± 0.04	0.22 ± 0.05	0.22 ± 0.05	0.22 ± 0.05	0.20 ± 0.05
S7	max	1.20 ± 0.23	1.12 ± 0.26	1.04 ± 0.26	1.06 ± 0.27	1.09 ± 0.25
	mean	0.53 ± 0.15	0.48 ± 0.16	0.43 ± 0.15	0.43 ± 0.16	0.43 ± 0.16
	stddev	0.28 ± 0.07	0.26 ± 0.07	0.24 ± 0.07	0.25 ± 0.08	0.26 ± 0.08
S8	max	0.95 ± 0.23	0.92 ± 0.25	0.96 ± 0.23	0.96 ± 0.26	0.97 ± 0.25
	mean	0.33 ± 0.11	0.30 ± 0.12	0.31 ± 0.11	0.30 ± 0.13	0.30 ± 0.12
	stddev	0.22 ± 0.06	0.22 ± 0.07	0.23 ± 0.07	0.23 ± 0.07	0.24 ± 0.07

Table 4. Reported mean maximum, and standard deviation height for clip plots collected around the block for TLS normalized height data and the mean maximum height for each block

Block	Field plot height (cm)		TLS plot height (cm)		Block total TLS height (cm)	
	Max	Stdev	Max	Stdev	Max	Stdev
S3	74.72	21.63	80.24	24.10	93.0	20.0
S4	76.32	24.97	77.84	24.64	91.0	22.0
S5	68.36	25.89	72.48	20.80	92.0	21.0
S7	79.40	26.50	89.00	18.52	1.07	26.0
S8	86.64	30.01	96.01	18.13	97.0	28.0

Figure 5. A sample of three 1-m wide transects from the origin of a scan across to the origin of the opposing scan with the running maximum height (dashed line) and the running mean height (solid line). (*a*) The top two transects are from S3, the bottom transect is from S7. (*b*) Graphs depicting the number of TLS points as a function of range, where the highest density is on either end of the graph near the origin of the scans.

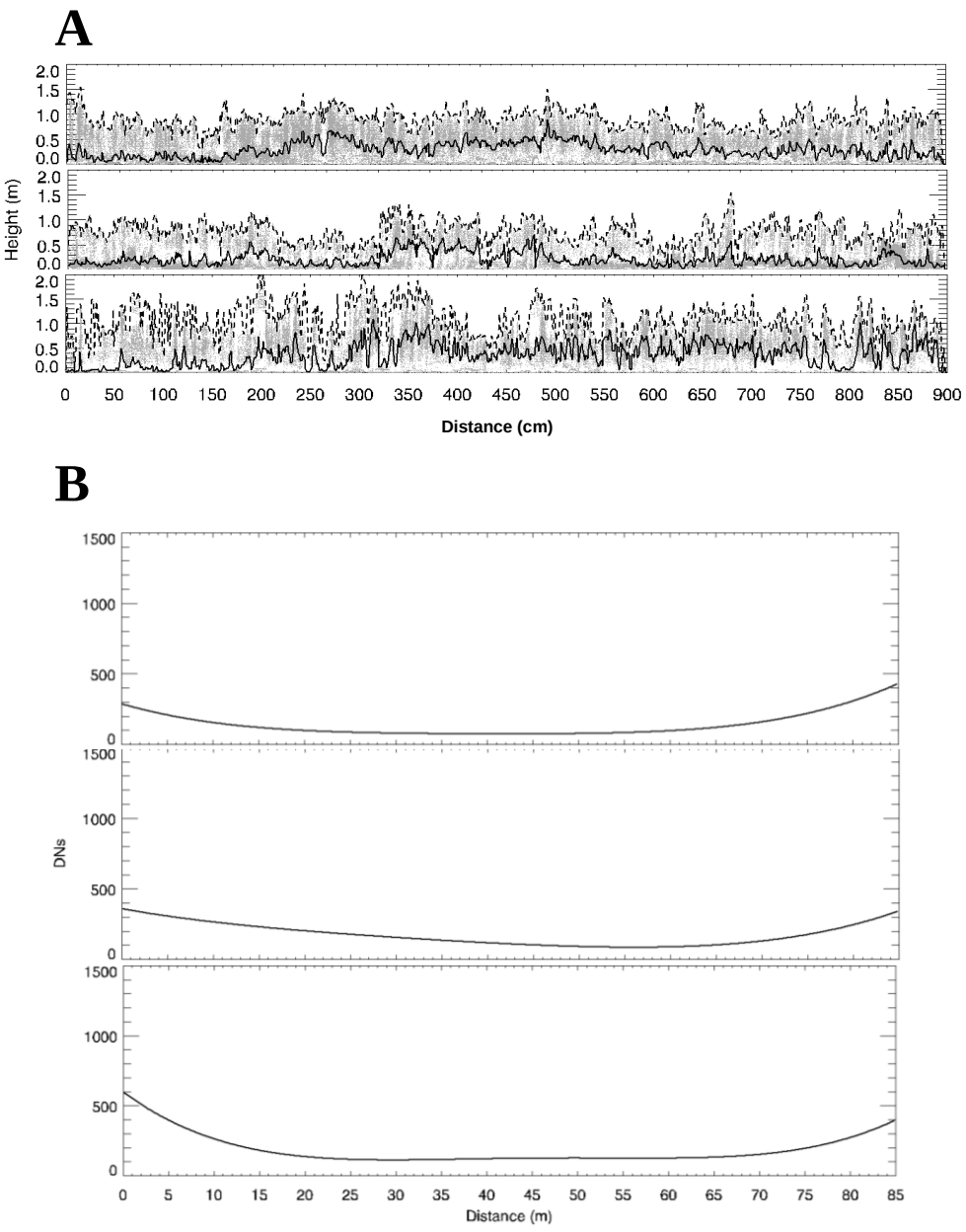

characterization across the blocks and supporting the conclusion that the field plots are not representative of the blocks with respect to canopy top.

Further assessment of the fuel height model for 1-m wide transects at the 100 m or halfway north-south mark on 2 ha blocks (S4, S5, S7) shows mean height trending lower for the grass dominated blocks (S4 and S5) and higher for the shrub dominated blocks (S7) (Figs. 5*a*, 5*b*). Data suggest a more rapid reduction in sampling frequency for shrub- and oak-dominated blocks (S7) with point counts dropping over 50% within 15m of the scan origin. The latter effect is almost certainly attributable to occlusion.

2.5 Discussion

Before this study, it was not evident that consistent measurements of fuel heights across domains >1 ha were practical from TLS. Potential error associated with stitching together many scenes of diffuse vegetation combined with instability of the scanning platform was unknown. Further, the inherent variability in scan angle, spot size, and density across the blocks raised questions of data consistency. Intuitively, one might anticipate that as scan angle becomes more oblique, the laser may tend to sample higher in the fuelbed especially in vertically oriented fuels such as grasses and taller shrubs. As spot size increases, the ability of the laser pulse to penetrate through gaps in the canopy was decreased as the larger footprint has a higher probability of being intercepted by objects effectively reducing the potential for the laser to characterize lower strata of the fuelbed. It is more difficult to speculate on the impacts of variations in data density because data density varied by a factor of five across the S-blocks.

Despite these uncertainties, the geometric consistency of scans from the S-blocks appears high and there is little evidence for spatial bias, perhaps because scan angles and spot sizes are

effectively mixed at any point on the landscape. Canopy top (maximum height) is measured consistently as evidenced by comparisons with field data and by examining heights as a function of distance from block centers. The TLS does over predict height in the small field plots, but the measurements also suggest that the fuelbeds are consistently taller across the blocks than the field measurements. Vierling *et al.* (2013) were successful in capturing accurate shrub heights in sage-brush steppe using TLS data at moderate distances (40m) and also found an underestimation of height by approximately 10%. In short, the TLS data appears to provide an improved spatially explicit representation of fuel height within the blocks, which is difficult to obtain using field data collection. Additionally, given the mode of data collection and the understanding of bias we can adjust across the block to improve characterizations of fuel height used for fire behavior modeling.

The validity of other TLS height metrics such as mean and standard deviation is unknown due to the absence of similar field measurements, although each of the TLS metrics appears spatially consistent across the blocks. The inability to directly match laser height distributions with similar field measurements is a chronic problem in lidar remote sensing (Popescu *et al.* 2002; Hopkinson *et al.* 2005; Riaño *et al.* 2007; Streuker and Glenn 2006; Glenn *et al.* 2010). In this study, 99th percentile height is the only viable field validation metric obtained. Developing models to translate lidar height metrics to specific fuels metrics will be necessary. A useful target starting point for modeling is biomass prediction because field plot measurements of biomass are more objective compared to the height measurements collected in this study. Others have utilized both convex hulls and voxel volumes to tease out biomass in sage steppe systems (Olsoy *et al.* 2014) and Arctic shrubs (Greaves *et al.* 2014) from relatively short ranges of ± 5m with generally good success. However, given the typical importance of a canopy cover metric in lidar biomass prediction combined with the difficulty in producing consistent cover metrics from oblique TLS

scans, there remains considerable uncertainty for using TLS to predict attributes such as fuel load over larger areas. Initial investigation with scan data from the more richly-sampled HIPs plots showed that the surface area of meshed point clouds correlated well with pre-fire fuel mass, although the approach did not work well in the S-blocks. In the latter areas, reduced data density produced mesh volumes with artificially inflated surface areas due to excessively large triangulated facets. The application of convex hulls (after Olsoy *et al.* 2014) and mesh surface areas to fuel load estimation is the subject of ongoing research.

Perhaps the most promising area of future work is developing fuel type classifications from laser height metrics (e.g. shrub, grass, and bare). Preliminary application of unsupervised classification techniques (ISODATA; Principal Components) reveals coherent spatial pattern that is difficult to interpret with available field data due to the mixture of vegetation types within validation plots. It may be that comparisons of pre- and post-fire laser height metrics with spatially explicit fire energy measurements from airborne and ground-based thermal radiometers (Hiers *et al.* 2009) will aid in understanding some of the observed variations in TLS height metrics in mixed fuels.

With respect to field sampling and processing techniques, this research identified useful protocols as well as shortcomings. Extensive monumenting with retro-reflective tape (used on highway signs) was critical for establishing geometry and for closely identifying locations of field plots. Conversely, the 50 cm aluminum boxes used to monument block corners were not useful for stitching scans together because they were not resolved in enough detail from the farthest scan stations to provide consistent tie points. A consideration when using the reflective tape was the contamination of plots with ghost points as described in Seielstad *et al.* (2011), which contributes strongly to the TLS height bias observed in the field plots. These erroneous data were mostly

removed from the validation datasets by thresholding intensity although residual points remained which artificially inflated maximum height estimated from the TLS data, specifically in sites dominated by taller grasses. The prevalence of mixed fuelbeds combined with imperfect field plot identification in the scans also resulted in sloppy height comparisons where tall fuels occurred along field plot edges. Scanning from the boom lift provided a stable platform except when winds exceeded ~6 m sec^{-1}, but controlling the scanner remotely was also very important in maximizing stability. For processing TLS data from natural landscapes, software that renders individual points rather than meshes is important for identifying specific targets such as monument poles. For validation purposes, future projects would benefit from field plots distributed within the burn units, at least some plots established in homogenous fuels, and direct field measurements of monumented pole heights. Potentially laboratory based experiments with synthetic or truly homogenous fuel beds (Hosoi and Omasa, 2008) would also enable better understanding of the potential use of TLS for fuelbed characterization.

Without the DEM corrections derived from the airborne laser altimeter, vegetation in the center of the blocks would be biased downward in height because the ground surface is not as well characterized when all scan angles are highly oblique and data density is relatively low. Further, the availability of high-quality GPS ground control allowed precise spatial reconciliation of the lidar data with other data collected. These caveats highlight the uniqueness of the multidisciplinary approach afforded by RxCADRE, and point to the difficulties (and cost) in obtaining quality datasets. All of the TLS scans for RxCADRE were completed in four full-time weeks of effort by a field crew of three, and processing of data to the point reported in this paper was completed in about six months of full-time work and much trial-and-error by two analysts. Although efficiencies

have been gained that can be applied to future acquisitions, it should be acknowledged that TLS is not necessarily an alternative to field measurements of fuels in terms of time savings.

Finally, although the height data produced in this study are not yet widely applicable to fire modeling, it is worth considering how they might be used for that purpose. The canopy top metric (99^{th} percentile height) defines the volume occupied by fuel at one meter spatial resolution. Canopy top alone does not address how much fuel resides in the volume, where it is concentrated, or what its characteristics are. However, we anticipate that height of maximum amplitude, inflection points, or central tendency metrics will address where biomass is concentrated in the vertical domain. The big unknown is how much fuel exists in a given cell. Fuel loading will need to be modeled from the height distributions or fuel types will have to be classified so that fuel characteristics can be inferred from field measurements. In the meantime, it would be worth investigating model sensitivity to fuels variability to determine how accurate the fuels data need to be.

2.6 Conclusion

This study marks an approach in which surface fuels heights are characterized across 2-ha burn blocks that are relatively big by TLS standards. The resultant fuel height data correspond with field measurements of height and are spatially accurate. They represent a first step toward spatially explicit and continuous fuels data for fire modeling. They can be represented at multiple scales and resolutions and are potentially useable for many types of modeling. The translation of height data to fuel attributes is the subject of current and future research.

Chapter 3 – Fuel Estimation

Predicting mass of mixed surface fuel beds across scales using terrestrial and airborne laser scanning

3.1 Abstract

Quantifying spatially-explicit surface fuel mass is an important step in development of scalable datasets of mixed fuels that are expected to allow fine-scale fire behavior and effects to be assessed more realistically. Leveraging terrestrial and airborne laser scanning data (TLS and ALS) collected at Eglin Airforce Base, Florida, USA, we use voxel counting methods to quantify pre- and post-fire occupied volume of fuelbeds from terrestrial laser scanning data, predict fuel mass at 0.25 m^2 resolution from volume using LOOCV linear regression models, quantify consumption, and utilize outputs to inform a multiple linear model of ALS height metrics to predict fuel mass at 5 m resolution across larger landscapes. Results show strong relationships between TLS voxel-based occupied volume and observed fuel mass (*Adjusted* R^2 0.62 – 0.87; SE (19-35%)) in forest, shrub, and grass fuels. Using TLS fuel mass as an independent variable with ALS-derived dependent variables allowed prediction of landscape-scale total surface fuel load (*Adjusted* R^2 0.71 ; SE (26%)). Post-fire fuel mass was strongly related to TLS occupied volume (*Adjusted* R^2 0.84-0.85; SE (11-16%)), which allowed for estimates of consumption at plot scale (*Adjusted* R^2 0.91; SE 20%). Realistic consumption estimates at fine grain (0.5m) were produced but not validated due to the necessary absence of pre-fire mass data from the areas where consumption was measured. Collectively, the ALS-TLS combination produced accurate fuel mass estimates for a range of spatial scales and grain sizes useful to a variety of emerging fire models.

3.2 Introduction

Spatially explicit surface fuel loading is a critical input for emerging physics-based fire models (Linn *et al.* 2002; Mell *et al.* 2007) and for prediction of fine-scale ecological fire effects (Hiers *et al.* 2009; Loudermilk *et al.* 2009). However, characterization of surface fuels in three dimensions is not readily achievable through conventional fuels inventory methods (Keane *et al.*

2001). Traditional fuel measurements are generally abstractions used to represent fuelbeds at coarse grains (10-30 m) rather than spatially explicit representations of all the fuel elements that make up fuelbeds. (Hardy *et al.* 2008). Laser scanning, both terrestrial (TLS) and airborne (ALS), is providing gains in 3-D characterization of biomass. Here, we combine TLS and ALS to predict fuel loads before and after fire at resolutions of 0.5 – 5.0 m and on landscapes ranging in size from 0.04 ha to 1000 ha. Our research focuses on longleaf pine systems in the southeastern United States where the spatial scale and arrangement of surface fuels is hypothesized to drive major ecological processes (Mitchell *et al.* 2006; Hiers *et al.* 2009; Loudermilk *et al.* 2012).

In the frequently burned pine systems of the southeastern United States, prescribed fires are used to maintain forest health through management of surface fuels comprised largely of pine litter (Varner *et al.* 2015). In these fire dependent ecosystems, a fire return interval of 2-5 years is imperative for maintaining the pine overstories that deposit needles and ensure the spread of periodic low intensity fire (Mitchell *et al.* 2009; O'Brien *et al*. 2016). Frequent fire also consumes litter and duff to expose mineral soil, enhances recruitment of longleaf pine seedlings, and in xeric environments, helps maintain the oak midstories that increase hydraulic lift and shading beneficial to seedling survivability (Loudermilk *et al.* 2016). Similarly, in the western United States, low intensity surface fires are a key restoration and long-term management tool for maintaining ponderosa pine savannas (Swetnam and Baisan 1996). Characterizing surface fuels from litter, coarse woody debris, and regeneration patches is also important for understanding transitions of surface fire into crown fires (Scott and Reinhardt 2001).

Specific to the southeastern United States, the ecology of fuels refers to linkages between pine stocking density, needle litter deposition, and distribution of coarse woody debris that allow fire to persist and to move across the landscape at varying intensities and produce fine-grained

patterns in understory plant species composition (Mitchell *et al.* 2009; Dell *et al.* 2017). Hiers *et al.*'s (2009) wildland fuel cell concept theorizes that in forest systems dominated by frequent surface fires, fine-scale heterogeneity (< 0.25m^2) drives fire behavior, with direct linkages to ecological response. These authors examined spatial autocorrelation in coincident *in situ* digital infrared thermography and terrestrial laser scanning data (TLS) to show that fuel composition, characteristics, and architecture were spatially independent at scales >0.25m^2 (Hiers *et al.* 2009).

Recent approaches to characterize fuel have increasingly moved toward high resolution laser scanning and simulations and focused primarily on canopy fuels (Riano *et al.* 2003; Andersen *et al.* 2003; Garcia *et al.* 2011; Pimont *et al.* 2016). Several studies have used airborne and terrestrial laser scanners to estimate crown bulk density, crown base height, crown diameter, and crown length for the purposes of fire behavior modeling (Riano *et al.* 2003; Andersen *et al.* 2003; Pimont *et al.* 2016). Typically, these attributes are characterized as discrete objects such as individuals or clusters of trees with generally well characterized statistical distributions of mass based on allometries and direct measurement.

More confounding are surface fuel beds representing assemblages of smaller, more discrete fuel elements that are grouped or not well characterized individually (Pimont *et al.* 2016). Surface fuels are the primary carrier of fires in the southeastern United States (Mitchell *et al*. 2009) and the link between surface fires and crown fires is important for predicting potential fire intensity and severity (Scott and Reinhardt 2001). Independent of fire, several studies have used terrestrial laser scanning (TLS) data to estimate above ground biomass (AGB) of individual plants, for example in sagebrush steppe (Olsoy *et al.* 2014) arctic shrub plant communities (Greaves *et al.* 2015), and in shrubs of the southeastern United States (Loudermilk *et al.* 2009).

Outside of shrub systems, TLS point clouds have been used to estimate AGB of grasslands (Umphries 2013; Cooper *et al.* 2017) and winter wheat over multiple growing seasons (Eitel et al. 2014). Ultimately, the latter studies have examined homogeneous fuel beds or discrete components of fuel beds such as shrubs. Seielstad and Queen (2003) employed a surface roughness technique to determine fuel class from ALS data in lodgepole pine forests of the northern Rocky Mountains. Mutlu *et al.* (2008) integrated ALS and multispectral data to produce traditional fuel model classifications for input into the FARSITE model (Finney 2009). Hudak *et al.* (2016) predicted *in situ* AGB from selected airborne laser scanning (ALS) metrics using a multiple linear regression model in the same mixed fuel beds considered in our study. However, only a few studies have attempted to use higher resolution TLS data in mixed herbaceous, shrub, and litter fuel beds. Rowell *et al.* (2016b) utilized simulated fuel beds to examine arrangement of AGB in longleaf pine systems and compared results against TLS measurements of fuels. Their study found a significant underrepresentation of point data in the lowest strata of the fuel bed (<10cm), where the bulk of available AGB exists in the form of litter. Attempts at characterizing mixed type fuel beds using TLS have consistently demonstrated the difficulty in identifying metrics within point clouds to enable accurate predictions or un-mixing of individual fuel types (Loudermilk *et al.* 2009; Rowell and Seielstad 2012).

One approach to improve characterization of the 3-D arrangement of fuel mass and type is to segment fuel beds into volumes (voxels) with dimensions that match the size of discrete fuel objects. An alternative approach is to identify the objects and their dimensions. Both approaches are possible using TLS point clouds to define spatial domains and to produce volumetric objects that can be summed to represent occupied volume (Popescu and Zhao 2008; Kim *et al.* 2016). An alternative association between TLS data and biomass measurements is the use of convex hulls or

interpolated surfaces from the point clouds (Olsoy *et al.* 2014; Greaves *et al.* 2015; Li *et al.* 2015). Typically, with highly resolved TLS data very small (≤ 1cm) voxel volume domains are specified, dependent on the resolution and range of the TLS data (Hosoi and Omasa 2006; Kim *et al.* 2015). Surface areas of convex hulls have shown strong correlations with field biomass in western sage (Olsoy *et al.* 2014; Kim *et al.* 2015) and arctic shrub (Greaves *et al.* 2015) systems. Studies that include both voxel counting and convex hull estimates of surface area and/or volume have yielded strong relationships (Greaves *et al.* 2015; Kim *et al*. 2015), although the uncertainty introduced by obscuration of laser energy in complex vegetation along with the variability in the range of the laser to the target affects optimal voxel size (Hosoi and Omasa 2007; Greaves *et al.* 2015).

In this study, we employ voxel counting methods of TLS data to predict AGB in mixed fuel beds. We use a relatively coarse dimension (10cm) to roughly match the size of discrete elements in the fuel beds. Specific objectives are to: 1) predict AGB from TLS data in heterogeneous herbaceous/shrub and forest litter fuel matrices at fine grain (≤1m^2); 2) extrapolate total fuel mass (AGB, kg / m^2) over a range of scales (400m^2 to 2ha); 3) predict fuel consumption from TLS change detection at plot scale; and 4) integrate TLS and ALS to estimate fuel mass at landscape scale. Our data were collected as part of the 2012 RxCADRE experiment using both research and operational prescribed fires at Eglin AFB.

3.3 Methods

3.3.1 Study area

Field, TLS, and ALS data were acquired at Eglin Air Force Base, FL, in October 2012 as part of the RxCadre Experiments (Ottmar *et al.* 2016a). Eglin AFB is located in the panhandle of Florida, USA, originally a unit of the former Choctawhatchee National Forest. Eglin is an important resource in the management of longleaf pine ecosystems with 180,000 ha of longleaf

pine sandhills and flatwoods (for site map and details see Ottmar *et al.* 2016b). Data were derived from two general vegetation types (non-forest and longleaf pine forest) and from two unit types (S-Blocks and HIPS). The S-Blocks were six 100 x 200 m units located in grass and shrub fuels. The HIPS (Highly Instrumented Plots) were nine 20 x 20 m plots located in grass/shrub (n=6) and longleaf pine (n=3) litter fuels. One of the forested HIPS (HIPS 1) was not included in this study due to the lack of coincident thermal imagery (n=2 in longleaf pine litter fuels). The S-Blocks were burned individually in prescribed fires as part the RxCADRE experiments to generate validation data for fire behavior modeling. The HIPS were located within three large units; L1G, L2G, and L2F, that were 454, 127, and 151 ha. Three HIPS each were located in two large grass/shrub units and three HIPS were located in one large longleaf pine forest unit.

The forested burn units were characterized by a longleaf pine overstory, with a mixed oak midstory. Oak species included turkey oak (*Quercus laevis*), sand post oak (*Q. margaretta Ashe*), laurel oak (*Q. laurifolia*), and blue jack oak (*Q. incana Bartram*) among others (Hiers *et al.* 2007; Ottmar *et al.* 2016b) (Figure 6A &B). Understory fuels were comprised of a variety of herbaceous (grass and forb) fuels with pine and oak litter dominant. The non-forest burn units were characterized by various proportions of grasses, forbs, and shrubs. Grass species included little bluestem (*Schizachyrium scoparium*) and big bluestem (*Andropogon gerardii)* and shrub\forb species included woody golden rod (*Chrysoma pauciflosculosa*), gopher apple (*Licania michauxii*), saw palmetto (*Serenoa repens*), and persimmon (*Diospyros virginiana*) (Ottmar et al. 2016b) (Figure 6C). For prescribed fire protocols and prescription information for each unit refer to Ottmar et al. (2016a).

3.3.2 Field Data

Biomass was destructively sampled from small field plots surrounding each S-Block and HIPs (Ottmar *et al.* 2016b). Pre-fire destructive sampling included separation of mass by fuel type (grass, forb, shrub, litter, coarse wood). Post-fire destructive sampling was conducted at separate plots coupled with the pre-fire plots and sampling included separation of mass by residual fuel type. For the six S-Blocks, pre- and post-burn plots (n=25 per block at $1m^2$) were established around the perimeter of each 2 ha area at 20 m intervals and marked with metal poles wrapped in retro-reflective tape. The nine HIPs were sampled identically to the S-Blocks except that the fuel plots were $0.25m^2$ in size (n=9 per grass HIPs and n=12 for forested HIPs) and pre-fire plots were equally spaced by five meters on three sides of the HIPs. The anticipated upwind side of each non-forest HIPs was left unsampled to allow for fire to enter unimpeded by disturbances to the fuel beds. All plots were also photographed obliquely from the north. Post-fire consumption plots were established in equal intervals between pre-fire fuel plots. Post-fire plots were collected to capture residual dry weight biomass for herb (grass and forb), shrub, woody (1, 10, 100 hour fuels), and litter. Details of fuel data collection can be found in Ottmar *et al.* (2016b).

Figure 6. Examples of typical fuels encountered at Eglin AFB from oblique overhead perspective, including: A) A natural longleaf pine site indicative of broad tree spacing, substantial oak mid-story, and herbaceous ground cover. B) A managed longleaf pine site indicative of closely spaced longleaf pine, a saw palmetto understory, and substantial needle cast. C) A grass and shrub matrix indicative of the fuels typically encountered on the L1G, L2G, and S-Blocks comprising a variety of oaks, forbs, and herbaceous fuel type.

Figure 7. TLS point cloud for L2FH3 shows the relatively low density of longleaf pine overstory and significant oak midstory that is evident in natural unmanaged longleaf pine stands at Eglin AFB.Units are meters.

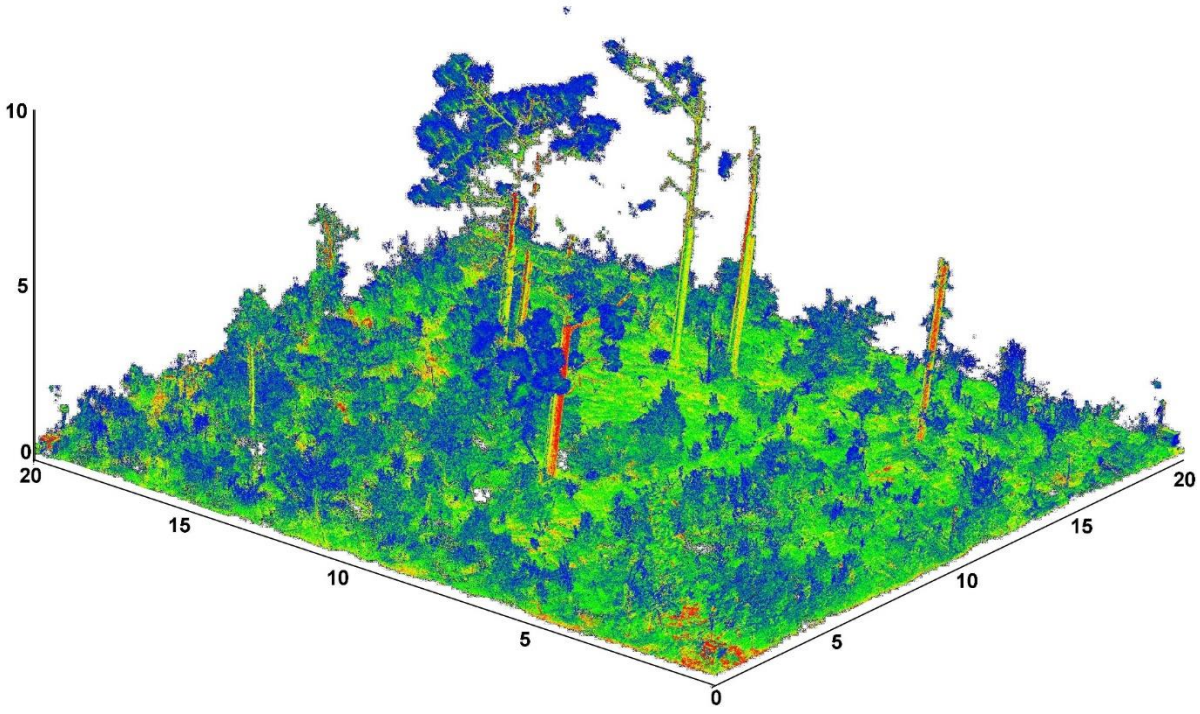

3.3.3 TLS Data Collection and Processing

Terrestrial laser scans were completed pre-and post-burn using an Optech ILRIS^{TM} 3_6D-HD instrument scanning at 10 kHz. For the S-blocks, the TLS instrument was positioned in an articulated boom lift at a height of 20 m above the fuelbed. Laser scans were collected at six positions around each burn block at 20-m horizontal distance from the edge of each block (Figure 7). Post-fire scans were collected from the east and west positions only for a total of four per block. In each scan, the laser was pointed downward at an angle of 23°. All S-block scans were set to produce 2-cm spot spacing at 90 m, resulting in 8 mm spacing at 20-m range to 56 mm at 300-m range. TLS sampling protocols for the HIPs plots were similar. The laser was raised to a height of 20m above ground with a downward pointing angle of 45° and the scan head was positioned nine meters from the plot edge. A single scan captured the entire plot producing ~8mm spot spacing. For instances in forested HIPs, data were collected from 3-7 perspectives at variable heights to minimize occlusion of the fuel bed by tree boles and canopies (Figure 8). Post-fire scans duplicated the pre-fire scans. Details of laser acquisitions can be found in Rowell *et al.* (2016a). Scanner settings were optimized to achieve consistent point density across each acquisition. Scan to scan correction, multiple scan integration, spatial alignment, and height normalization to ground methods are outlined in Rowell *et al.* (2016a).

To assess fuel load as AGB and calculate consumption, we merged the pre- and post-fire TLS acquisitions of only the HIPS into single datasets. S-Blocks were not compared for post-fire consumption due to irregular point density due to long range scanning described in Rowell *et al.* (2016a), therefore only pre-fire scans were used to estimate pre-fire fuel load. We use this method to account for objects missed in the pre-fire acquisition due to occlusion (figure 8). This method allows for capturing occupied space within the fuelbed that is missed by the laser in the pre-fire

scan (because it is occluded). Hereafter, pre-fire HIPS data means pre-fire and post-fire combined while post-fire data is only post-fire.

3.3.4 Airborne Laser Scanner Data

Discrete-return lidar data were collected on 3 November 2012 by Kucera International employing a Leica ALS60 instrument. ALS data were collected at 1200 m above ground level, at a pulse rate of 178.6 kHz, a field of view of 20 °, and a sidelap of 50%. A nominal point density of 6.8 points m^2 was achieved using these parameters (Hudak *et al.* 2016). Sub-meter vertical uncertainty (RMSE = 0.082 m) was achieved using 20 survey grade ground control points (Hudak *et al.* (2016). A 1-m digital terrain model (DTM) of the ground surface was interpolated using the GridSurfaceCreate function of FUSION (McGaughey 2014) using the minimum Z value instead of the mean Z, as is the default; this was done to preserve the heights of near-ground returns as positive values upon height normalization. The GridMetrics function of FUSION was used to calculate a suite of height and density metrics from all returns in the 0-2m height range, within 5m x 5m resolution bins. Nine of these metrics were selected as significant predictors of total surface fuel load in a multiple linear regression model that included both non-forest and forest plots (Hudak et al.2016). These same nine metrics were considered for upscaling TLS-based fuel mass predictions to the landscape level in our study.

3.3.5 Voxel Volume Estimation

We used 1000cm^3 voxels in this study (10 x 10 x10 cm) and counted occupied voxels within raster cells to produce gridded volumetric proxies for fuel mass. Voxels are three dimensional pixels that allow for volumetric representation of discontinuous surfaces using a regularly spaced three-dimensional grid (Stoker, 2009) (Figure 9). Voxelization and voxel counting scripts were written in the Interactive Data Language (IDL) software package (ver. 8.4, Harris Geospatial Solutions). Voxel domains were selected to produce voxel counts for 0.25m^2 cells (0.5 x 0.5 m rasters),

allowing for one processing stream for all TLS data sets. Voxelization was executed across the 2ha S-Blocks and 400m^2 HIPs so that models developed from the comparisons of plot data with TLS occupied volume could be applied across all of the TLS data sets.

Figure 8. Histograms representing height distributions for pre-burn biomass for hardwoods, palmetto, and grass fuels (a.) and post-burn fuels (b.). Occlusion of the laser data captures an outer hull of the fuelbeds that are apparent after fire has moved through a unit. Anecdotally, hardwoods remain relatively unchanged in terms of woody mass, internal elements of the palmetto are revealed, and grasses are almost totally consumed. The residual fuels exemplified in the palmetto instance are the basis for integrating the pre- and post-fire scans for the voxel occupancy calculation.

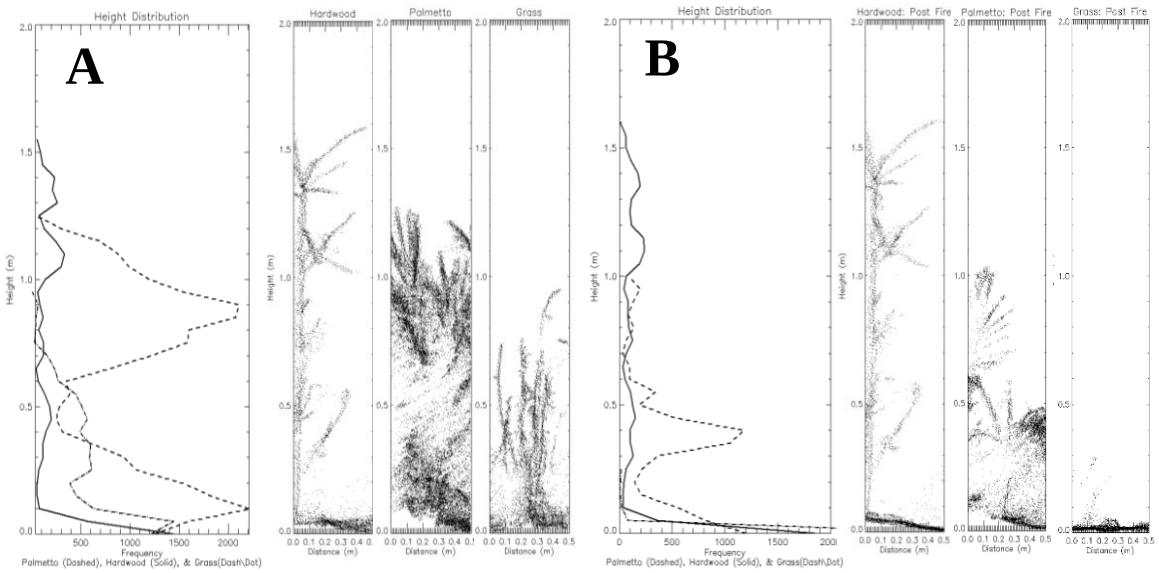

A 'filled' voxel was required to meet a threshold point density of 5 returns per cubic decimeter. Additionally, each counted return was required to have an intensity of 200-15000 DN. Logic for these criteria is a follows. Selection of the 10cm^3 voxel cell was determined based on a sensitivity analysis over a range of voxel scales (1, 8, 1000, 3375, and 4000 cm^3). Optimal voxel dimensions were selected for computational efficiency, common scale between S-Blocks and HIPS, and to maintain discrete features within the point cloud (e.g., individual plant parts and types). Others have noted that a limitation of voxel analysis using TLS data is data voids that are created when

the laser does not fully penetrate canopies of trees and shrubs (Hosoi and Omasa 2006; Greaves *et al.* 2015; Cooper *et al.* 2017). The use of relatively coarse voxels in our analysis moderates the occurrence of holes within plant crowns by bridging gaps created by occlusion and produces estimates of occupancy similar to the filled hull estimates used by Olsoy *et al.*(2014) and Greaves *et al.*(2015).

With respect to the intensity thresholds, values <200 DN generally result from halos around objects that represent partial interception of matter due to the high sensitivity and relatively large footprint of the ILRIS instrument (Seielstad *et al.* 2011). Values >15000 DN are associated primarily with reflections from atmospheric aerosols. For these reasons, returns that did not meet our intensity criteria were removed, similar to Greaves *et al*. (2015) and Pfennigbauer (2010).

Total occupied volume was calculated as the sum of all voxel domain centroids that fell within a 0.25m^2 cells (rasters). For the S-Blocks, which used 1m^2 field plots, occupied volume was gridded to 1m^2 by summing the voxel volumes of four connected 0.25m^2 cells. Occupied volume is represented in Eq (1),

$$\boldsymbol{OV_{Total}} = \sum \boldsymbol{OV_{i_0 \ldots i_i}} \quad [1]$$

where total occupied volume (OV_{total}) is the sum of occupied volume (OV) for height strata ranging from 10cm to 80cm above the ground surface. Importantly, the lowest 10cm is excluded due to uncertainty in precise definition of ground at the scale of analysis, and all voxels above 80 cm are excluded to reduce the risk of inflating volume estimates from individual leaves and stems protruding above the dominant fuel layer. Occupied volume is calculated at cubic decimeters and expressed in cubic meters.

Figure 9. Typical fuels characteristic of the S-Blocks and examples of stacked voxel density for 1cm^3 voxel cells for A) Sparse, low grass, and exposed bare ground, B) Grass and shrub matrices (saw palmetto, and C) Tall and dense grass bunches.

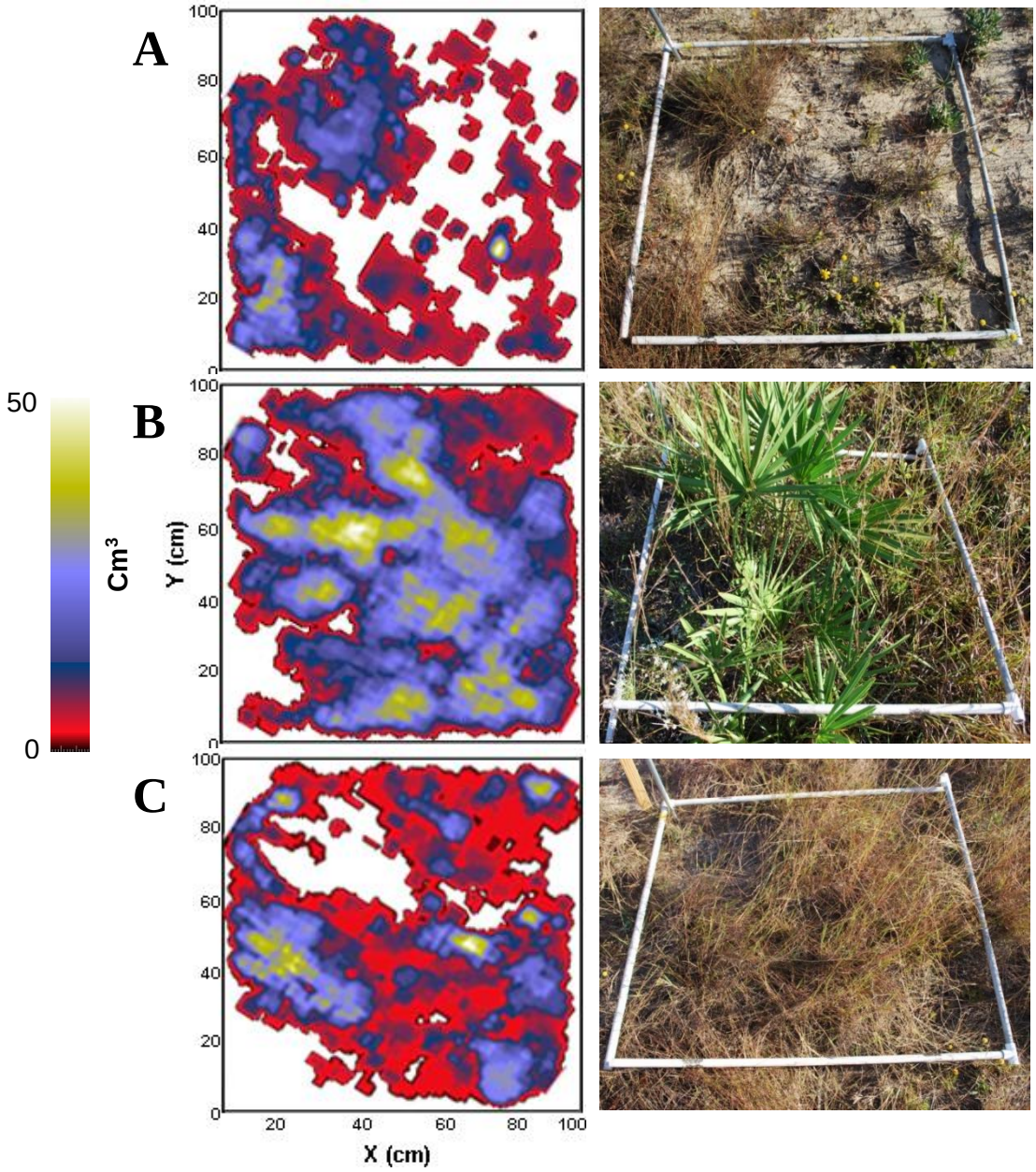

3.3.6 Pre-Fire Biomass Prediction using TLS and Field Data

To estimate pre-fire AGB using TLS-derived occupied volume for the S-Blocks and HIPs, Leave-One-Out-Cross-validation (LOOCV) linear models were developed using the train function in the caret package (Kuhn 2017) through a script in R version 3.2.5 (R Core Team 2017). The regression model is of the form Eq. [2]:

$$AGB = b_0 + b_1(OV_{Pre,+PostTls}) \quad [2]$$

where AGB is the predicted aboveground biomass in the surface fuelbed OV is occupied volume from the combined pre- and post- fire point clouds. Regression intercept and slope parameters are represented as b_0 and b_1, respectively. Separate regression models were developed for the non-forested and forested HIPs as well as for each of the six pre-fire S-Blocks, resulting in eight separate models. Additionally, two combined models were produced, one for all of the pre-fire HIPs and one for all of the pre-fire S-Blocks. The models were used to predict fuel mass density in kg m^{-2} across the HIPs at 0.5m x 0.5m resolution and the S-Blocks at 1m x 1m resolution, respectively.

3.3.7 Biomass Prediction using TLS and ALS

ALS metrics considered in the predictive modeling included mean height, kurtosis, the return proportion from 0.0 to 0.05 m, mode of returns from 0.0 to 0.5 m, the return proportion from 0.0 to 0.05 m, standard deviation of height for elevations between 0.05 to 0.15 m, standard deviation of height for elevations between 0.15 to 0.50 m, the coefficient of variation for heights between 0.15 to 0.50 m, standard deviation of height for elevations between 0.50 to 1 m, and standard deviation of height for elevations between 1 to 2 m. These ALS metrics were calculated using the CloudMetrics function of FUSION software (McGaughey 2014). AGB from the models

described above were summed to 25m^2 resolution to facilitate model development using the ALS data. This resolution matches the resolution used by Hudak *et al.* (2016) with the same ALS dataset. We employed a multiple linear model using the 'lm' function in R. Candidate ALS metrics were thinned to represent "best" regressions using the 'regsubsets' function in the 'leaps' package of R. The Akaike Information Criterion (AIC) statistic was used as the basis for choosing the best subset model. We tested normality of the response variable and the model residuals using the Shapiro-Wilk W statistic. We also tested for dissimilarity between predictions and observed values using a bootstrap test for equivalence (Robinson *et al.* 2005). Coefficient of determination (*adjusted* R^2) values were used to evaluate the robustness of the relative predictive power of the regressions. Prediction error was assessed by calculating the Root Mean Square Error (RMSE).

3.3.8 Post-fire Biomass Prediction and Consumption using TLS and Field Data

Post-fire TLS-derived occupied volume for the HIPs was used to estimate post-fire AGB with a Leave-One-Out-Cross-validation (LOOCV) linear model. The regression model for plot-scale estimation is presented as Eq. [2]:

$$AGB_{post} = b_0 + b_1(OV_{post\text{-}tls}) \quad [3]$$

where post-fire AGB is the predicted aboveground biomass (kg) of mixed type fuelbeds for grass/shrub and forested sites as a function of TLS-based occupied volume (OV_{tls}). Regression intercept and slope parameters are represented as b_0 and b_1, respectively. Separate regression models were developed for aggregated non-forest HIPs and aggregated forested HIPs, resulting in two separate models. To estimate consumption, we differenced the pre- and post-fire combined AGB from the post-fire estimated AGB. HIPs average consumption is reported per unit (20mx20m plot) and compared to the average consumption reported in Ottmar et al.(2016b). We

also present fuel consumption at the native 0.5 m resolution to depict the fine-grained spatial variability but note that these predictions are not validated.

3.4 Results

3.4.1 Pre-fire Estimates of Aboveground Biomass from Occupied Volume

Pre-fire occupied volume from the voxel analysis was linearly correlated with dry-weight AGB and model predictions center on the 1:1 line when compared to observed biomass (Figure 10a and b). For the HIPS, the forested and non-forest models explained 84% (Adj. $R^2 = 0.84$) and 71% (Adj. $R^2 = 0.71$) of the variability respectively. Models of total fuel load per $0.25m^2$ in forested fuel beds produced a 19.5% error (RMSE = 0.049 kg) and non-forest modeled estimates produced a 29.7% error (RMSE = 0.077 kg). Mapped spatial distributions of predicted AGB were produced from the models (Figure 11). They show high spatial variability at 0.5 m grain, reflecting diverse patches of vegetation types and open areas. Residuals of the linear model for the forested model were not significantly non-normal by the Shapiro-Wilk test (W=0.92834, P= 0.11), but the grass model residuals did indicate significant non-normality (W=0.92856, P<0.005). Bootstrap tests of equivalence rejected the null hypothesis of dissimilarity (P = 0.025) for both the forested and non-forest data, suggesting that predictions and observations were similar with no bias or disproportionality (Robinson *et al.*2005).

A combined model for the HIPs using both the forested and non-forest data explained 67% of the variability (Adj. $R^2 = 0.67$, RMSE 0.076 kg, Table 5). Residuals of the combined model were not non-normal when one extreme outlier residual was removed (W=0.96219, P=0.086) at alpha 0.05 levels, although this result was non-significant. Bootstrap tests of equivalence rejected

the null hypothesis of dissimilarity *(P* = 0.025). Linear model parameters indicate a steep slope of the linear model (Table 1), suggesting a general constricted estimate of occupied volume produced from the TLS instrument. Pre-fire AGB and occupied volume were also closely related in the S-Blocks. Individually, the S-Block models explained 66-76% of AGB variability (Table 5). Associated error ranged from an RMSE of 0.056 - 0.103 kg m^{-2} (19.2-35.1%) across grass and shrub burn units (Figure 12). Residuals for each S-Block indicated no significant non-normality. Bootstrap tests of equivalence rejected the null hypothesis of dissimilarity *(P* = 0.025) for all individual S-Blocks. Inter-comparison of boxplots for each block show broader ranges of voxel-derived occupied volume values compared to dry-weight biomass (Figure 13).

Figure 10. Linear regression models predicting A) forested pre-fire HIPS B) grass\shrub pre-fire HIPS C) forested post-fire HIPS D) grass\shrub post-fire HIPS. Separate models are used in each case.

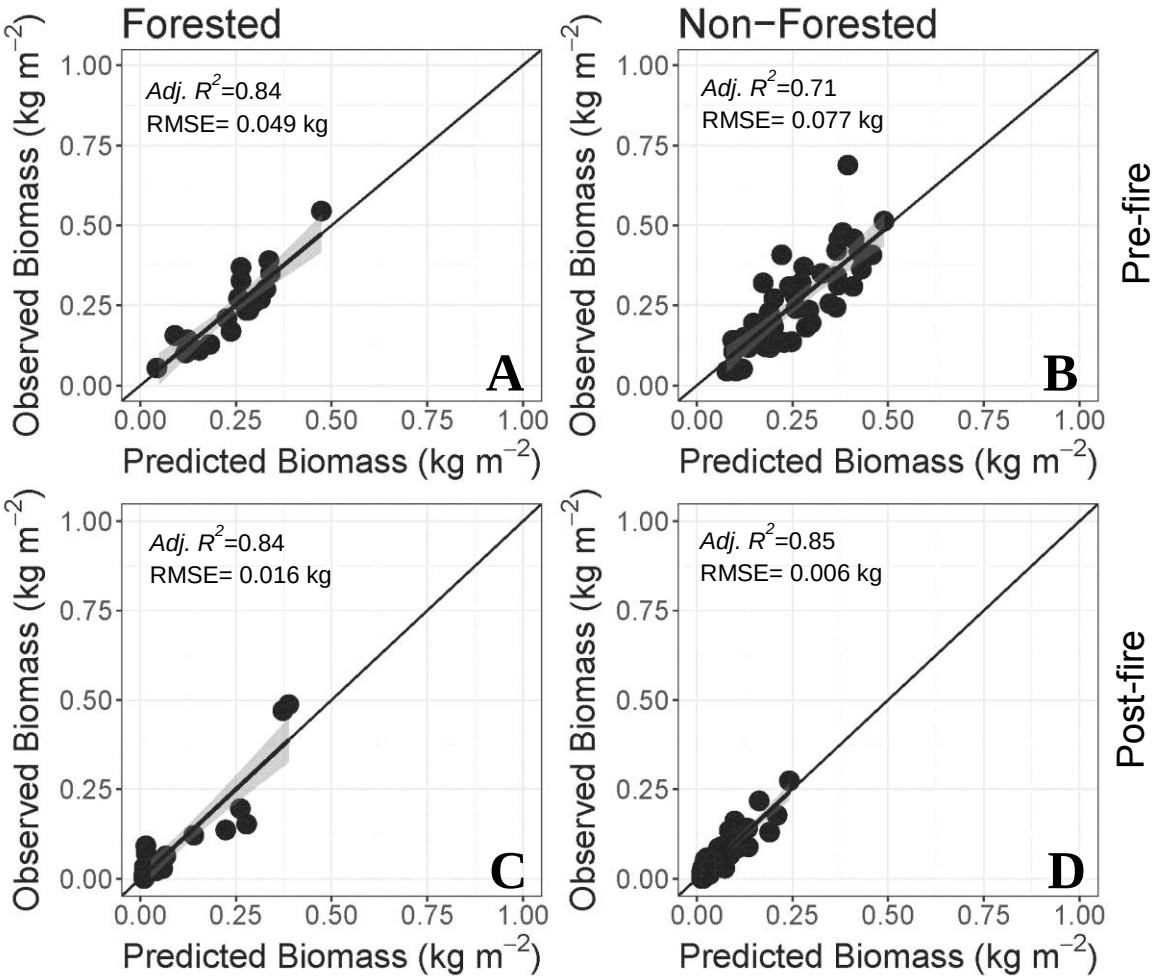

Figure 11. Pre-fire AGB is mapped for each of the HIPs demonstrating the variability and distribution of mass across the HIPs from the forested and grass\shrub predictive models presented in in Figures 10A and 10B.

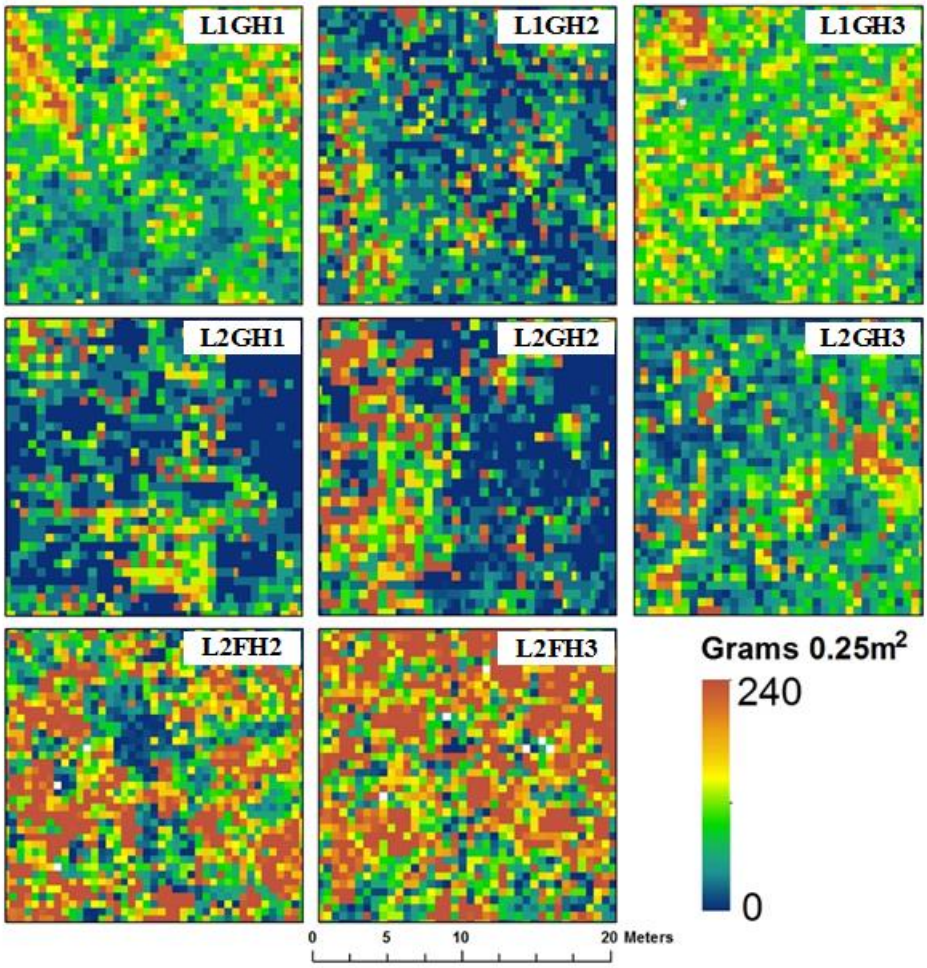

Table 5. Linear regression model coefficients predicting pre-fire AGB from occupied volume for HIPs and S-Block sites.

Predictor	Estimate	Std. Error	*t*-value	Pr(>|t|)	Significance
HIPs Grass/Shrub					
(Intercept)	60.90	20.39	2.99	0.0044	**
Voxel OV	2.53	0.23	11.06	4.94e-15	***
HIPs Forested					
(Intercept)	26.41	23.07	1.15	0.266	
Voxel OV	2.14	0.21	10.26	2.07e-09	***
HIPs Combined					
(Intercept)	62.03	17.66	3.51	0.000773	***
Voxel OV	2.26	0.184	12.25	<2e-16	***
S-Blocks Grass/Shrub					
Grass					
(Intercept)	112.82	17.87	6.329	1.11e-07	***
Voxel OV	0.542	0.057	9.406	4.26e-12	***
Shrub					
(Intercept)	18.82	33.05	0.569	0.572	
Voxel OV	1.002	0.081	12.36	2.0e-07	***
All					
(Intercept)	44.91	23.52	2.19	0.0311	*
Voxel OV	0.872	0.056	15.48	2.0e-16	***

Signif. codes: 0 '***' 0.001 '**' 0.01 '*' 0.05 '.' 0.1 ' ' 1

Figure 12. Linear regression models predicting pre-fire AGB from voxel estimated occupied volume for S-Block by grass, shrub, and all combined.

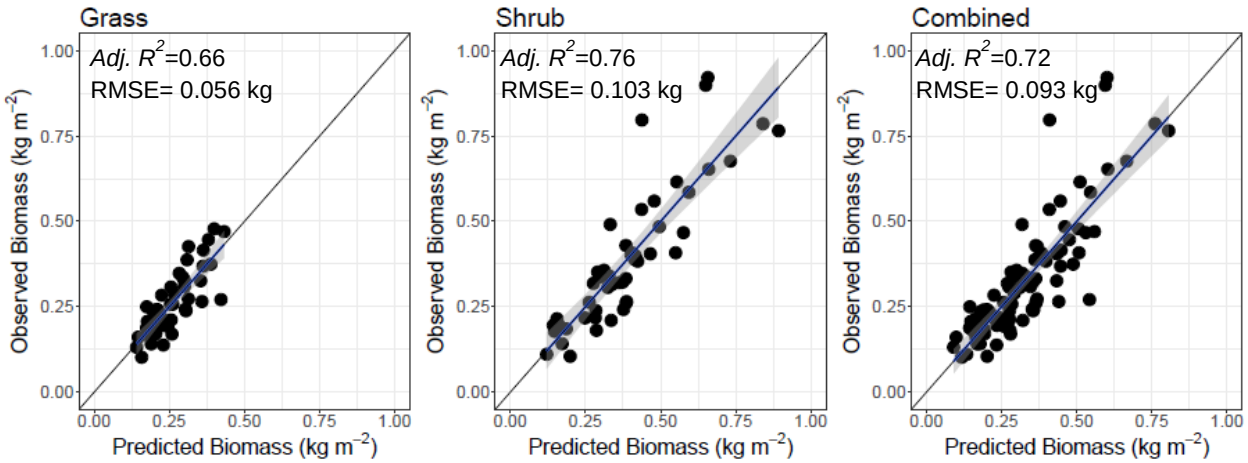

Figure 13. Boxplots depict the distribution of dry weight biomass (DWB) in grams per meter squared and voxel occupancy (OV) in cubic decimeters for the S-Blocks. These distributions show similar ranges between S-Blocks, Mann-Whitney-Wilcoxon non-parametric tests show that the DWB and OV distributions are equivalent across S-Blocks, with the exception of S5.

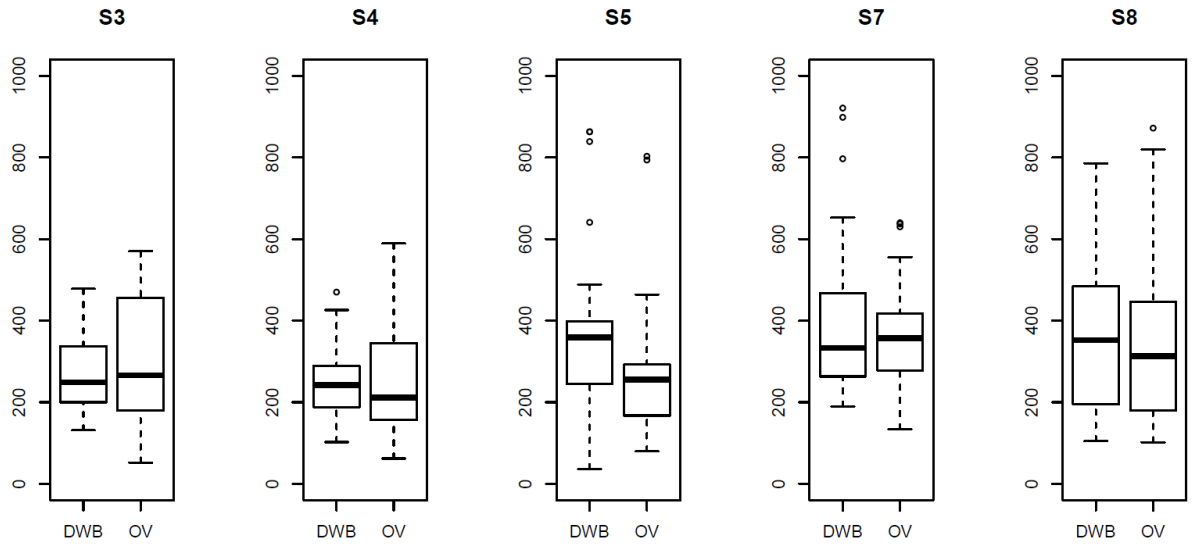

We assume that dry weighed biomass and voxel-based occupied volume are identical populations (P>0.5), except for burn unit S5 (W=195, P=0.023). Integration of the S-Blocks in a single model explained 52.6% of the variability (Adj. R^2=0.52; RMSE= 0.1224 kg). As previously noted, S5 occupied volume was statistically from a different population distribution then the dry weight biomass. Dropping S5 from the integrated model improved the relationship between OV and AGB, explaining 72% of the variability and reducing the error (Adj. R^2=0.72; RMSE= 0.09325 kg). In both cases, the residuals were non-normal and the null hypothesis was rejected (W =0.89135, P<0.0001 and W =0.91856, P<0.0001 respectively). Removal of outliers did not improve the results, with p values remaining below 0.05 levels. The S-Blocks were also modeled collectively using a multiple linear model with burn block ID as a factor. Sixty-three percent of fuels variability was explained by this model (Adj. R^2 = 0.63; RMSE = 0.1117kg; Figure 12).

3.4.2 ALS-based Surface Fuel Loading

A useful model was derived from the five selected using the best subsets ALS height metrics (following Hudak et al. 2016) and the TLS (Table 6) estimates of fuel load at 1m^2 spatial resolution (Adj. R^2 = 0.71; RMSE = 0.032 kg, Figure 14). Observed versus predicted fuel load again centered on the 1:1 line. Fuel load estimates were non-normal by the Shapiro-Wilk test (W=0.9264, P<0.0001) and did not achieve normality using alternative transformations. Residuals from the model were normally distributed (W=0.9939, P=0.91). The range of ALS fuel predictions encompassed ranges similar to those observed in the TLS-based fuels predictions. Bootstrap tests of equivalence rejected the null hypothesis of dissimilarity (P = 0.025), which suggests that predictions and observations were similar with no bias or disproportionality. Mapping model results depicts patterns of variability that were observed in the field, with higher concentrations of AGB in the forested (L2F) and shrub (L2G, S7-S9) dominated units of the site and lowest

concentrations in the chemically treated grass (L1G) units (Figure 14). Distributions of ALS-derived fuel mass track similarly to Hudak *et al*. (2016) spatially. Spatially explicit estimates of occupied volume explain more of the variability than observed dry weight biomass plots alone.

Table 6. Multiple linear regression model coefficients predicting pre-fire AGB from TLS estimates of fuel mass and five selected ALS metrics.

ALS Predictor	Estimate	Std. Error	*t*-value	Pr(>|t|)	Significance
(Intercept)	7.941e-02	2.342e-02	3.391	0.001001	**
Kurtosis (0-2 m)	1.503e-04	7.434e-05	2.022	0.045877	*
Mode (0–0.05 m)	-2.691e-01	7.784e-02	-3.458	0.000805	***
Proportion (0–0.05 m)	-8.653e-02	2.333e-02	-3.709	0.000343	***
Proportion (0.05–0.15 m)	-6.974e-02	1.956e-02	-3.566	0.000560	***
s.d. (0.05–0.15 m)	1.121e+00	2.816e-01	3.979	0.000132	***

Signif. codes: 0 '***' 0.001 '**' 0.01 '*' 0.05 '.' 0.1 ' ' 1

Figure 14. Multiple linear regression models predicting pre-fire AGB from five ALS metrics.

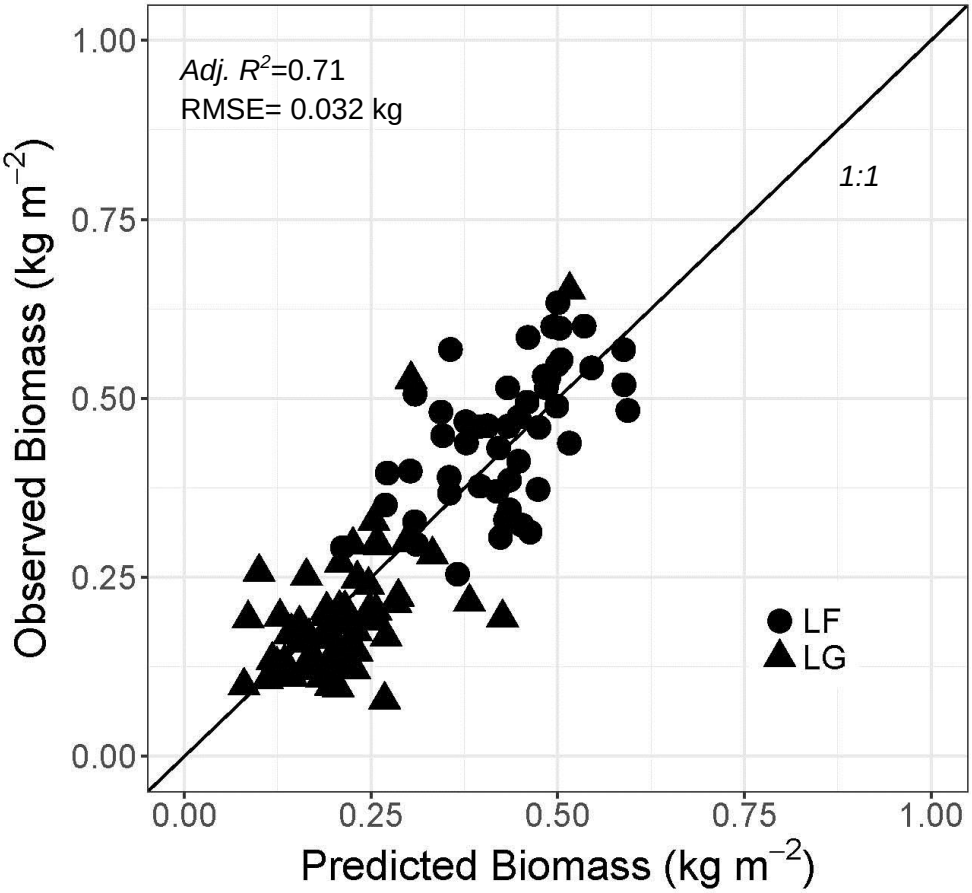

Figure 15. Pre-fire fuel mass from the ALS-derived model for the study area. Forest (L2F) and shrub (S7-S9) areas show high concentrations of fuels relative to chemically treated grass areas (L1G).

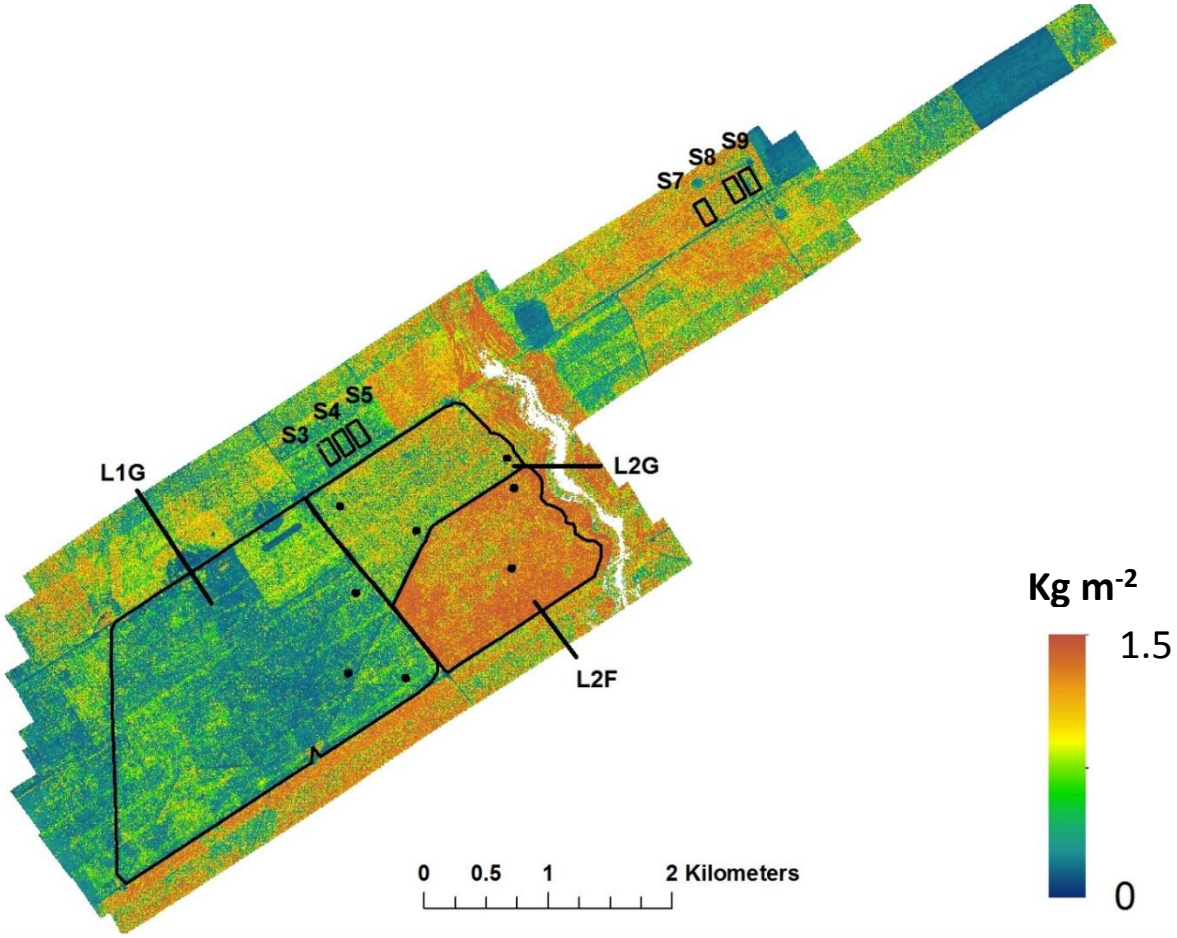

3.4.3 Post-fire Estimates of Above Ground Biomass and Consumption

Similar to the pre-fire models, post-fire occupied volumes from the voxel analysis were highly correlated with post-fire dry-weight AGB (Figure 10c and d). For the HIPS, the forested and non-forest models explained 84% (Adj. $R^2 = 0.84$) and 85% (Adj. $R^2 = 0.85$) of the variability respectively. Models of total post-fire fuel load (Table 7) in forested fuel beds produced a 69.6% error (RMSE = 0.016 kg) and non-forest modeled estimates produced a 46.4% error (RMSE = 0.061 kg). Residuals of the forested and non-forest linear models were not significantly non-normal by the Shapiro-Wilk test (W=0.92576, P= 0.089; W=0.95452, P<0.0393). Bootstrap tests of equivalence rejected the null hypothesis of dissimilarity (P = 0.025) suggesting that predictions and observations were similar, with no bias or disproportionality.

Differencing the pre- and post-fire estimates of AGB for the HIPS produced estimates of consumption (Figure 16). Consumption at the HIPs plot-scale (20x20m) compared favorably with field measurements, producing a 17% (RMSE= 0.066 kg m^{-2}) error in prediction. Predicted consumption at 0.25m^2 spatial resolution is shown in Figure 17. The patterns depicted are rational based on observations of fire behavior and pre-fire fuels but cannot be validated for reasons described previously.

Table 7. Linear regression model coefficients predicting post-fire AGB from occupied volume for HIPs sites.

Predictor	Estimate	Std. Error	*t*-value	Pr(>|t|)	Significance
Post-Fire HIPs Grass/Shrub					
(Intercept)	12.81	3.90	3.292	0.00179	**
Voxel OV	0.72	0.042	17.49	<2e-16	***
Post-Fire HIPs Forested					
(Intercept)	9.30	13.35	0.696	0.494	
Voxel OV	1.03	0.095	10.85	4.55e-10	***
Post-Fire HIPs Combined					
(Intercept)	8.80	5.22	1.684	0.963	
Voxel OV	0.88	0.047	18.68	<2e-16	***

Signif. codes: 0 '***' 0.001 '**' 0.01 '*' 0.05 '.' 0.1 ' ' 1

Figure 16. Post-fire consumption comparisons between HIPs from pre-fire predictions (Table 1) minus post-fire AGB predictions vs observed consumption at a plot level

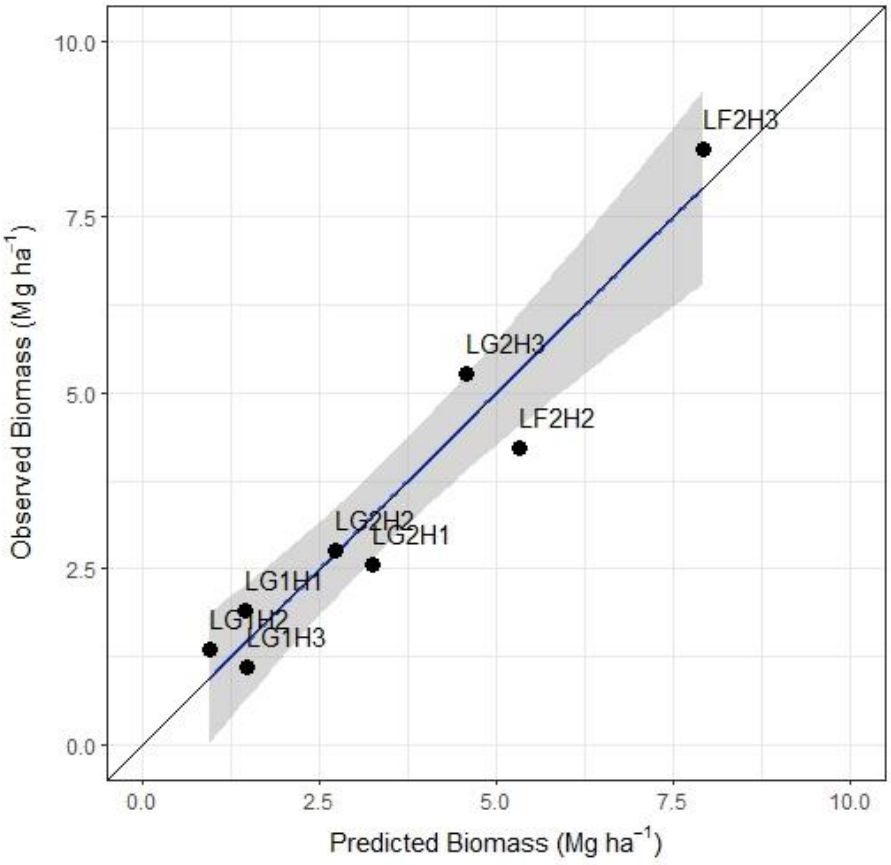

Figure 17. Fuel consumption for each of the HIPs at 0.25m^2 resolution showing variations in consumption patterns from plot to plot. The models used to produce these outputs are depicted in Figure 10. The bottom two tiles are forested, the top six tiles are grass/shrub.

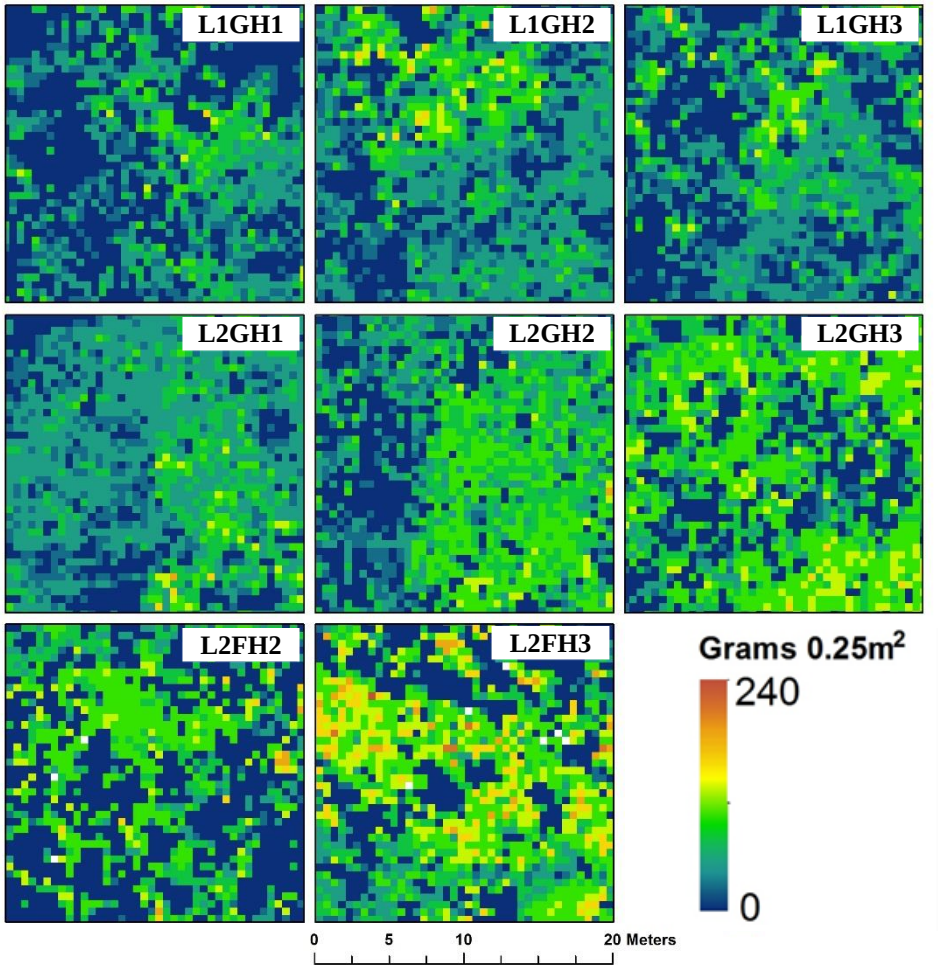

3.5 Discussion

We demonstrate that AGB can be directly predicted with reasonable efficacy using relatively simple TLS-based occupied volume estimates. To our knowledge, this represents the first successful fuel load prediction from TLS in fuel beds with mixtures of grasses, forbs, shrubs, and litter. We also utilized TLS-predicted AGB as a surrogate for *in situ* field measurements to predict landscape-scale surface fuel loads using ALS, adding considerably to the methods and findings reported by Hudak *et al.* (2016). Finally, we quantified post-fire fuels and consumption across the HIPs plots, although there remains uncertainty regarding how TLS-based methods of fuel load estimation perform due to limited samples and as a result of field methods that make direct comparisons of consumption intractable.

We acknowledge that this study is not producing a three dimensional fuels data product directly. The compression of voxel data into 2-D voxel densities is necessary as the field data were collected to represent total fuel load and fuel mass as a function of fuel type, which we do not address in this paper. Our voxel analysis does export occupied volume per height strata that could be used to estimate three-dimensional metrics if similar data were collected in the field. We also note that the range of predicted fuels is not as broad as the observations as a result of regression modeling, which compress predictions towards the mean (Hudak *et al.* 2016).

3.5.1 Estimate of Aboveground Biomass from Occupied Volume

Overall, we report error rates that are similar to other biomass estimates from TLS data (Greaves *et al.* 2015, Cooper *et al.* 2017), and our approach to estimating AGB stands as an improvement on previous efforts in mixed southern fuel types (e.g., Loudermilk *et al.* 2009). In the HIPs, the forested areas produced the tightest predictions of AGB (19% error) compared to the non-forested areas (30% error). We speculate that there is generally less fuel type variability in the

forested. Additionally, the forested HIPs biomass was dominated by longleaf pine litter representing 37% of biomass in forest HIPs 2 and 81% of biomass in forest HIPs 3. Although the TLS does not sample the litter layer at the bottom of the fuel bed as occupied volume using our methods, it is clear that the variability in aboveground features such as shrubs, grass, and perched litter are playing a large role in overall fuels variability. The larger error observed in the grass and shrub dominated HIPs may be in part a result of using voxels to estimate biomass by occupied volume. Volume is not a proxy that considers the specific fuel density of the fuel type (grass, forb, or shrub) and therefore may underestimate mass as fuel density increases. Additionally, sparse objects such as grass blades consistently trigger reflections with the ILRIS, perhaps inflating occupied volume estimates and creating noise in the models. We note that there was a saturation point around 550 grams where fuel density increases at a faster rate than occupied volume. Ultimately, a separate model is likely needed for fuels that were dense (e.g. oak shrubs), but share similar occupied space with less dense fuels (e,g. tall forbs).

Others researchers have used the gridded surface areas of convex hulls instead of voxels to predict the total mass of sage brush (*A. tridentata* subsp. *Wyomingensis*; Olsoy *et al.* 2014) and low stature Arctic shrubs (*Betula nana* and *Salix pulchra*; Greaves *et al.* 2015). In these studies it is not clear if TLS metrics for surface area performed well due to only sampling shrubs with relatively consistent fuel densities such that larger shrubs have predictably more biomass than smaller shrubs. In the grass and shrub sites at Eglin, there was a broad spectrum of shrub species with different forms and dimensions that potentially differed significantly in fuel density from one and other. Robertson and Ostertag (2009) developed allometries from basal stem diameter to predict biomass of fourteen hardwood species common in the southeastern US and found significant variability in biomass in shrubs with small diameter stems. We speculate that part of

the variability in prediction of AGB in the grass\shrub HIPs is derived from time since last burn (1 year for one of the grass/shrub units and 3 years for the other). Variability in aboveground biomass for the hardwood species found in the units is known to decline as stem diameter increases (Robertson and Ostertag 2009), suggesting that over time we might expect convergence of fuel density in hardwood species as a function of time since fire. The unit that burned one year previously averaged 193.94 grams of dry weight biomass with one standard deviation representing 54% of the mean. In contrast, the unit burned three years previously averaged 318.86 grams of biomass with standard deviation accounting for 45% of the mean. The greater time since fire may account for some of the reduced variability in fuel mass observed in the latter unit as there are more relatively large hardwood shrubs. Further, the more recently burned unit was also treated with an herbicide (hexazinone) to inhibit hardwood recruitment (Ottmar *et al.* 2016b), increasing grass/forb dominance and reducing complexity to fuel variations.

The S-Blocks produced models with similar efficacy as the HIPs despite lower scan resolution and more oblique viewing angles. The variability of predictions of occupied volume and reciprocal measurements of dry weight biomass between S-Blocks is an important consideration. For example, occupied volume estimates in S5 were consistently lower than in the other S-Blocks despite containing similar biomass, suggesting a difference in the TLS dataset for this unit. It should be noted that occupied volume in S5 by itself was strongly correlated to observed dry weight biomass and performed similarly to other sites that contained strong shrub signatures, but when combined with the other S-Blocks, AGB was significantly and consistently under estimated.

Although spatially explicit, high resolution predictions of AGB across fuel types were produced in this study, we acknowledge that fire behavior depends on more than fuel load. Fuel

type, in particular, is critical as different fuels combust differentially depending on variations in fuel structure, density, moisture, and ambient temperature. Numerous studies have identified ranges of intensity, residence time, and consumption of primary litter components of longleaf pine dominated southern litter (Fonda 2001; Fonda and Varner 2004; Kane *et al.* 2008; Varner *et al.* 2015). Rowell et al. (2016b) integrated fuel bed simulations (synthetic fuel beds) with TLS-based height distributions to address distributions of fuel mass as a function of type and arrangement. Further development of this approach may prove useful for predicting fuel type probabilistically based on TLS height distributions and voxel arrangement. In our study, it is clear from comparisons of model outputs and photographs of field plots that occupied volume is sensitive to at least some aspects of fuel type (e.g., shrub versus grass).

3.5.2 Estimates of Aboveground Biomass from ALS and TLS

Greaves *et al.* (2017) showed that ALS-derived canopy volume can be calibrated using TLS canopy volume to produce robust estimates of tree biomass. Similarly, we found that TLS-derived occupied volume corresponds with fuel bed AGB and relates nicely to ALS canopy metrics via multiple linear modeling. We observe marked improvement in prediction of AGB using our method over the previous example outlined in Hudak *et al*. (2016), using the same ALS variables. We also report total fuel load per $25m^2$ which differs to reporting units used by others (Hudak *et al.* 2016; Ottmar *et al*. 2016b). Though this approach may be an improvement over conventional approaches, these estimates may not be suitable for current fire behavior models that are parameterized to use unit averages. However, unit averages could easily be derived from our data. By linking TLS and ALS data we have produced a framework to scale TLS-based AGB to landscape scales, provide assessments of spatial variability of AGB, and mechanisms to downscale relatively coarse estimates of AGB from ALS data. These findings are particularly encouraging

because they represent a mixed fuel beds including grass, shrub, and forest understory fuels with results that are similar to those found in calibrations for exclusively shrub fuels (Greaves et al. 2017). This study also marks a step forward for using TLS-based as a surrogate "truth" that in tandem with field data allows for improvements of landscape-scale estimates of AGB using other remotely sensed data. The primary limitation for the estimation of fuels using combined TLS and ALS data is the inability to identify specific fuel types to go along with the estimates of AGB. Classification of surface fuel beds into fuel types has been successful in other systems using ALS data alone or in combination with multi-spectral data (Seielstad and Queen 2003; Mutlu *et al.* 2008; Hiers *et al.* 2009; Garcia *et al.* 2011; Jakubowski *et al.* 2013). Some combination of these methods combined with our AGB estimates could significantly improve inputs to CFD fire behavior models. Research is continuing in terms of the uncertainty assessment because the two-stage model currently does not integrate error from the model stages that represent different spatial scales and model error propogation.

3.5.3 Estimates of Consumption from TLS-based Aboveground Biomass

Our findings demonstrate that post-fire AGB can be predicted using occupied volume. To our knowledge, these results are the first successful application using independent TLS-estimates of pre- and post-fire fuel mass together to calculate consumption of fuels. Though we produce a spatially explicit map of consumption that is rational, we are unable to validate these findings yet. Use of these mapping products could be beneficial for assessing fire energy release (Hudak *et al.* 2016) and when tied to fuel type, variability in emissions (Strand *et al.* 2016). Our method demonstrates an improvement in spatial estimates of consumption as compared to the CONSUME model and the First Order Fire Effects Model (FOFEM) (Ottmar *et al.* 2016b). A first attempt to employ the pre-fire model to estimate post-fire fuel mass over-estimated residual fuelload thus

using post-fire observed data was critical to producing the model used. Estimates of consumption across the HIPs were favorable, but direct comparison at plot-scales is intractable as pre-fire observations cannot be conducted at post-fire observation sites. Though the relationship between occupied volume and observed dry weight biomass was strong, the errors associated represented 69% of the mean observed for the forested unit and 46% of the mean observed for the grass\shrub unit. Error is introduced in plots that appeared to experience near total consumption from the TLS perspective, but most likely had residual fuels on the ground that were not fully consumed in the form of ash or black carbon. These fuels would not be distinct from the ground plane. One limitation to our approach in forested systems was possibly due to adjacent shrubs and tree branches introducing occupancy in the voxel arrays that is not represented in the field data. Our estimates of fuel consumption can also be tied to research assessing change detection using TLS data (Liang *et al.* 2009; Gupta *et al.* 2015). Though the aforementioned studies only address changes in height, merging these findings with spatially explicit consumption from our approach may yield improvements for consumption estimates in other systems.

3.6 Conclusions

The niche for the research presented here is in development of fine-grained, spatially-explicit fuels data for validating fire models, understanding how heterogeneity in fuels and fire behavior link to ecosystem processes, and testing theories such as the wildland fuel cell concept (Hiers et al. 2009). By combining fuel mass estimates like those developed here with fuel type classification methods, and coincident digital thermography may allow researchers the ability to conduct and validate high resolution CFD model runs to assess fine-scale fire dynamics and effects. Additionally, the integration of stem detection algorithms (Popescu and Wynne 2004; Rowell *et al.* 2006; Silva *et al.* 2017) and derivative crown fuel metrics allow for the spatial

distribution of canopy fuels to go along with surface fuels data (Andersen *et al.* 2004; Rowell *et al.* 2009), providing a comprehensive framework to understand the ecology of fuels. The ability to ascertain relationships between stocking density, litter distribution, and expected fire behavior over large landscapes using combinations of TLS and ALS fuels metrics could substantially aid managers across the southeastern United States by improving understanding of how fuels variability modulates fire behavior and produces fire effects

Chapter 4 - Simulation

Using simulated 3D surface fuelbeds and terrestrial laser scan data to develop inputs to fire behavior models

4.1 Abstract

Understanding fine-scale variability in understory fuels is increasingly important as physics-based fire behavior models are driving needs for higher resolution data. Describing fuelbeds three dimensionally is critical in determining vertical and horizontal distributions of fuel elements and the mass, especially in frequently burned pine ecosystems, where fine-scale fuels arrangement drives fire intensity and resulting fire effects. Here we describe research involving the use of highly resolved three-dimensional models. We create fuelbeds using individual grass, litter, and pine cone models designed from field measurements. These fuel models are distributed throughout the fuelbed to replicate fuel distribution in rectified nadir photography taken for each plot. The simulated fuelbeds are converted into voxel arrays and biomass is estimated from calculated surface area between mesh vertices for each voxel. We compare field-based fuel depth and biomass with simulated estimates to demonstrate similarities and differences. Biomass distributions between simulated fuel beds and terrestrial laser scan data correlated well using Weibull shape parameters ($r = 0.86$). Our findings indicate that integration of field, simulated, and terrestrial laser scanner data will improve characterization of fuel mass, type, and spatial allocations that are important inputs to physics-based fire behavior models.

4.2 Introduction

The ability to spatially describe wildland fuels across an array of scales is critical for decision making in operational wildfire and prescribed fire management (Mutch *et al.* 1993; Keane *et al.* 2001). Spatial fuels data have historically been used in fuels planning, fire behavior and effects modeling, and hazard assessment. With recent advances in fire behavior modeling, the need for these types of data has expanded to include higher-resolution three dimensional characteristics. New computational fluid dynamics (CFD) models provide opportunities to

examine the fine spatial scale (<1m) fire behavior, that potentially drives larger scale fire behavior and may spatially organize ecosystems (Hiers *et al. 2009*). These models rely on appropriately dimensioned fuels data which are not readily available from conventional sampling techniques. The basis for fuels measurements has been to provide a generalized fuels description considering that collecting all physical attributes of a fuel bed is usually intractable (Keane *et al.* 2001). In 2001, the Core Fire Science Caucus, a self-directed group of fire scientists, elucidated the need for a new context to describe fuels that coupled with advances in fire behavior and smoke modeling (Sandberg *et al.* 2003;Hardy *et al.* 2008). Fuel measurement methods were developed to support coarse-grained fire behavior or fire effects modeling that do not encompass the full range of heterogeneity or spatial non-uniformity in fuels found within and across landscapes (Hardy *et al.* 2008). Similar limitations are noted in the realm of ecology, where conventional methods of inventory are designed to classify abundance of dominant vegetation rather than individual organisms using most common species characterization (Thompson 2004).

Fire is a dynamic process, influenced by discontinuities and variability that are not fully captured in traditional fuels measurements. Commonly used direct measurements of fuels are taken from planar transects or point intercept coupled with dry-weighed biomass samples (Brown 1974; Brown 1981) These direct sample protocols are labor intensive and limited in scale and they are not efficient at estimating fine fuels such as grasses (Loudermilk *et al.* 2009). Estimation of bulk density of shrubs and grasses requires unrealistic assumptions that inherently oversimplify the fuel elements (Van Wagner 1968). Yet, fine-scale patterns of surface fuels are complex and relate to spatial measurements of fire intensity in low-intensity fire regimes (Loudermilk *et al.* 2012, 2014). Fine scale fire effects have also been commonly described in frequently burned pine conifer forests, where variability of fire intensity depends on the matrix and orientation of

flammable grasses, forbs, shrubs, and pine needles (Thaxton and Platt 2006; Mitchell *et al.* 2009). New fire behavior models combined with new fuels measurement techniques are now providing opportunities to better understand patterns of fuels and the effects of fine-scale fire behavior, and the research community is active in rethinking approaches to fuels inventory and developing alternative methods (Hiers *et al.* 2009).

A relatively new approach to characterize fuels is by application of active remote sensing in the form of Light Detection and Ranging (lidar), which potentially characterizes fuel beds continuously by collecting height and reflectance properties of fuel objects (Seielstad and Queen 2003; Hudak *et al.* 2015). Lidar remote sensing is limited in its ability to directly matching biophysical parameters with similar field measurements (Popescu *et al.*2002; Hopkinson *et al.* 2005; Riano *et al.* 2007; Streuker and Glenn 2006; Glenn *et al.* 2010). Platforms such as terrestrial laser scanners (TLS) collect enormous quantities of point data (mm to cm point spacing) for small areas (1m – 1ha), but are victim to issues of sampling variability. TLS point density degrades over distance and data collection must be executed from multiple angles to reduce the effects of occlusion as energy is intercepted by taller and larger objects that shadow the other parts of the scan (Hosoi and Omasa 2006; Rowell *et al.* 2016a). Moreover, studies are generally limited to extraction of biometrics of individual identifiable objects within larger fuelbeds, for example for shrubs in open arctic environments (Vierling *et al.* 2013; Greaves *et al.* 2014) and sagebrush steppe (Olsoy *et al.*2014). Attempts at characterizing mixed fuelbeds (e.g., nearly all fuelbeds at fine grain) with terrestrial laser scanning have shown the difficulties in unmixing objects or types within laser point clouds to characterize mass and heights per fuel type (Loudermilk *et al.* 2009; Rowell and Seielstad 2012; Rowell *et al.* 2016a)

To address limitations of TLS, one approach uses parametric plant models to simulate biomass distributions. A small number of studies are utilizing three-dimensional models of trees and plants to produce object-based simulations of ecosystems for use in a variety of applications, such as simulations to assess spectral properties of plants (Disney *et al.* 2009; Cawse-Nicholson *et al.* 2013; Woodgate *et al.* 2015) and modeling of airborne lidar data for individual tree inspection in forested environments (Disney *et al.* 2010, 2011). A related method for individual plant modeling is the application of Lindenmayer system (L-systems) fractal modeling for virtual construction of xeric shrubs for use in leaf-scale fire behavior simulations (Prince *et al.* 2014; Prince 2014). L-systems used in Prince *et al.* (2014) grows fractal plant features using assigned angles of rotation representative of the specific plant morphology. Prince *et al.* (2014) showed that bulk densities similar to those reported in the literature could be obtained from geometrically correct plant models of chamise, manzanita, and Utah juniper. In similar work, Parsons et al. (2011) used probability functions to distribute biomass throughout an individual tree canopies as a collection of simple shapes (cylinders and frustrums) using a pipe model approach. This approach has yielded highly detailed tree models that are applied in the FUEL3D model for improved understanding of fire dynamics within forest stands. FUEL3D uses allometric estimates of biomass based on inputs from the Forest Vegetation Simulator (FVS, United States Forest Service, http://www.fs.fed.us/fmsc/fvs/) that are distributed throughout individual trees as partitions of bole, branch, and needles. All of these studies focus on modeling the individual tree and shrub canopies. As of this study, there has been no similar examination of understory vegetation and surface fuels focused on construction of three dimensional assemblages of mixed fuel elements.

Here, we present methods for constructing spatially-explicit, highly-resolved, and realistic fuel beds using tools developed for 3D animation and modeling. Each fuel element/type (e.g. shrub, grass, needle, etc.) is discretized in the fuelbed, allowing for direct accounting of metrics such as height, volume, cover, surface area, density, and mass. We then examine the fuelbeds through comparison with *in situ* nadir imagery and field measurements, and explore the utility of these models as tools to better understand spatial variability in fuel properties and to improve remote sensing of fuel beds and fine-grained fire modeling. Finally, we compare simulated fuelbed height distributions with TLS-derived height distributions to assess correspondence of the two methods as a preamble to future incorporation of lidar ray-tracing for simulating TLS.

Our research centers on a main objective of developing realistic and quantifiable simulated surface fuelbeds in longleaf pine ecosystems. We approached this objective in three phases: first, we generated fuel simulations from parametric plant models using high resolution nadir photo imagery and detailed height measurements and parameterized them with biomass estimates for discrete fuel elements; second, we transposed the models to an independent validation site and compared biomass estimates to actual dry weights; and third we derived and contrasted height distributions from the simulations and TLS data.

4.3 Methods

4.3.1 Study Area

Two field campaigns were conducted to acquire data at Eglin Air Force Base (AFB), Florida, in October 2012 and February 2014. Eglin AFB (30°3212 N, 86°4344 W) is located in the panhandle of northwestern Florida, USA, which was originally a unit of the former

Choctawhatchee National Forest; Eglin is an important resource in the management of longleaf pine ecosystems with 180,000 ha of longleaf pine sandhills and flatwoods.

4.3.2 Field Observations

The October 2012 data were collected as part of the Prescribed Fire Combustion and Atmospheric Dynamics Research Experiment (RxCadre) funded by the Joint Fire Sciences Program (11-2-1-11). Fuels data were collected at twenty three 0.5 m^2 plots around small replicate prescribed fire sampling blocks (20 m x 20 m) nested within a larger burn unit. These small replicate blocks are referred to as highly instrumented plots (HIPs). Height metrics for each plot were collected (maximum and mean height for grass, forbs, shrubs, and litter). Each plot was clipped of all vegetation, sorted by fuel type, and samples were oven-dried at 70°C for 48 hours and then weighed (Ottmar *et al.* 2016b).

The February 2014 data were collected as part of a Department of Defense Strategic Environmental Research and Development Program (SERDP) funded project (#RC-2243). Vegetation and fuel characteristics were gathered in nine plots located in longleaf pine sandhills of Eglin AFB. Plots measured one by three meters in size and were gridded into cells measuring 10 cm by 10 cm, so that each of the nine plots contained 300 cells. For each cell, point intercept measurements of plant species and fuelbed height were collected. Fuel measurements included fuel and litter depths (cm), and presence or absence of fuels. As part of a separate experiment (O'Brien et al. 2016), longleaf cones were randomly distributed at densities of 0, 5, or 10 per m^2.

4.3.3 Workflow Description

Workflow is divided into three phases (Figure 18), 1) Model development and parameterization, 2) Replication and validation of simulations, and 3) TLS and simulation

comparison. Phase 1 outlines the development of plant models and construction of fuelbeds via interpretation of nadir and oblique photography and subsequent application of generalized fuel mass allocations. Phase 1 also outlines the development of these methods and application of generalized fuel mass allocations (see surface area and fuel mass). Phase 2 describes the replication of the technique at an independent site along with comparisons of simulated and measured biomass and height. Phase 3 examines the derivation and comparison of TLS-based and simulated height distributions.

4.3.4 Fuel Bed Simulations

Synthetic fuel beds (Figure 19) were generated through a series of steps starting with the Onyx Garden Suite (Onyx Computing Inc. 1992-2008, http://www.onyxtree.com) a parametric plant modeling system that allows users to adjust physical parameters of individual plant elements to create three-dimensional plant models. This model generator was used to produce individual plant elements representative of types observed in our field plots. Fuel elements for each plant model were selected based on primary life-form measurements collected in the field campaign including models of tall grass (senesced), moderate stature grass (senesced), low grass (senesced), tall shrubs, low shrubs (senesced), low shrubs (evergreen), longleaf pine litter, deciduous oak litter, other deciduous litter, and longleaf pine cones. Height dimensions of the models were parameterized based on average heights coincident with identifiable plants located in nadir photographs collected at each plot. The horizontal extent of plant elements and objects in the litter were determined from measurements in rectified plot photos in a Cartesian coordinate space, using the southwest corner of the plot as the origin.

Fuelbeds were constructed as assemblages of plants, litter, and cones using the freeware Blender 2.74 (www.blender.org). Blender is typically used as a platform to produce scenes and

objects for three-dimensional renderings for use in graphic design and tree-dimensional animation applications. Onyx-based plant and litter objects were imported into the Blender environment as wavefront open format file input (.obj). Identifiable objects such as tall grass, isolated moderate stature grass, shrubs, and cones, were positioned by their artesian coordinates as measured in the rectified high resolution nadir plot photography in the ArcGIS environment (ESRI, Redlands, California, USA). Each fuel element contains an anchor point representing the center of the object on the ground plane. This point was the location used to place each element. Distributions of other fuel elements such as clusters of deciduous litter, long-leaf litter, and congruous clumps of grass were placed within bounded areas as defined by presence/ absence of each fuel type specified by the field-collected point intercept data. Groupings of fuel elements were refined based on visual comparison with plot photography, as the point intercept data omits areas of data between sample points. The final scenes were exported to an x,y,z text format representing the fuel bed with all elements included (e.g.,herbaceous plants and grasses, needles, oak leaves, litter, and cones). Each x,y,z point represents a vertex from a mesh object of a fuel element and is attributed with specific fuel type (e.g., grass, needle, cone, etc.)

The SERDP data were used to develop and parametrize the models in Phase 1 as the spatial resolution of the nadir photo imagery and density of measured fuelbed heights were more highly resolved than in the data collected from the RxCadre experiment. The simulation techniques developed from the SERDP project were replicated for the RxCadre data. However, because these data were less intensively sampled for fuelbed height metrics (Figure 19), oblique imagery was used to place fuel elements in the simulation.

Figure 18. The diagram depicts the three phases of work conducted to produce fuel simulations (phase 1), replicate and validate biomass at an independent site (phase2), and compare simulated and TLS height distributions (phase 3).

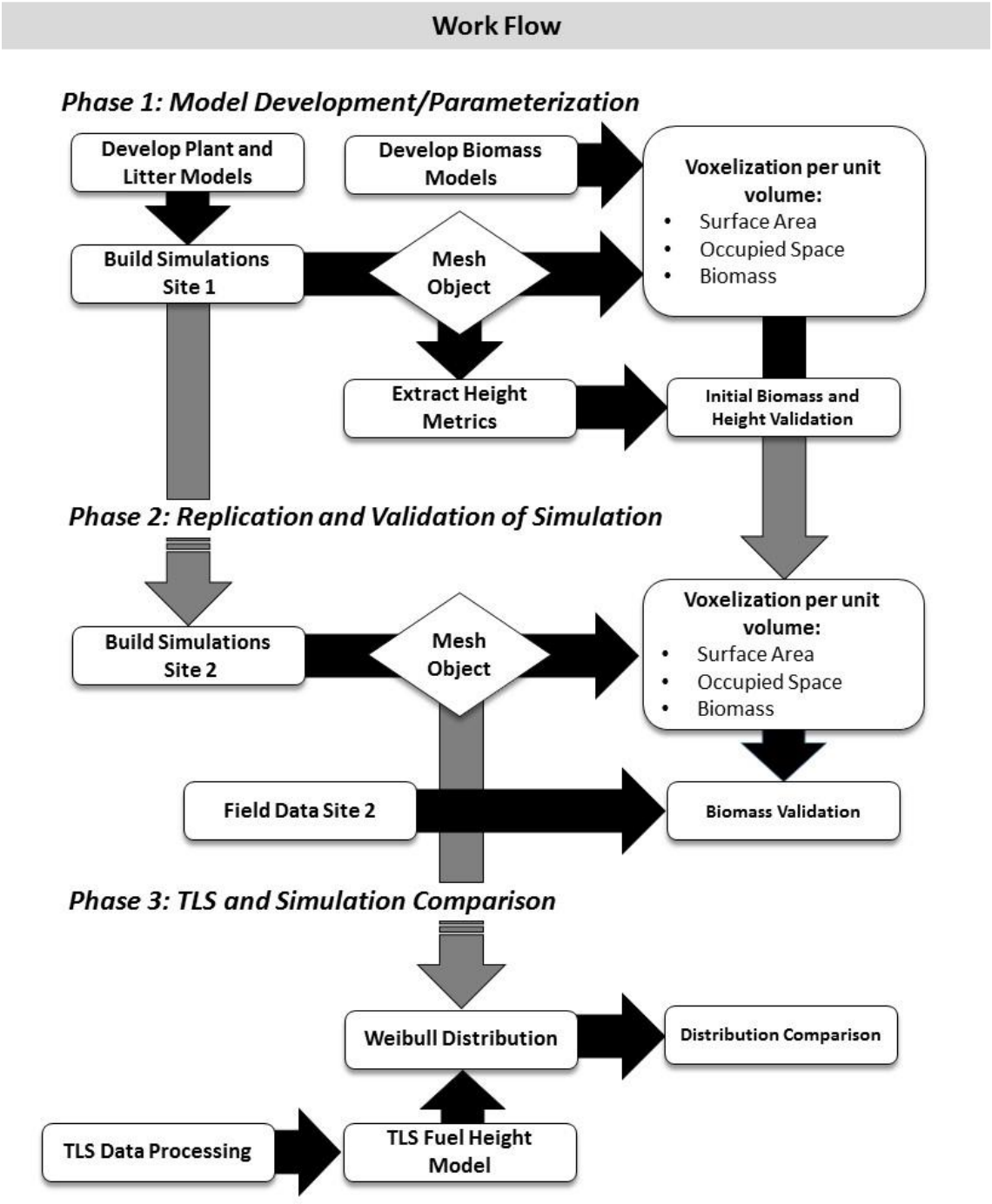

Figure 19. A comparison of synthetic fuelbeds for plot 1 (1A) with the nadir plot photo (1B) and plot 7 synthetic fuelbed (1C) with the nadir plot photo (1D). This comparison demonstrates that placement of objects is coincident between photo and the synthetic fuelbed and the objects used to populate that simulation behave like real plants with some generalization.

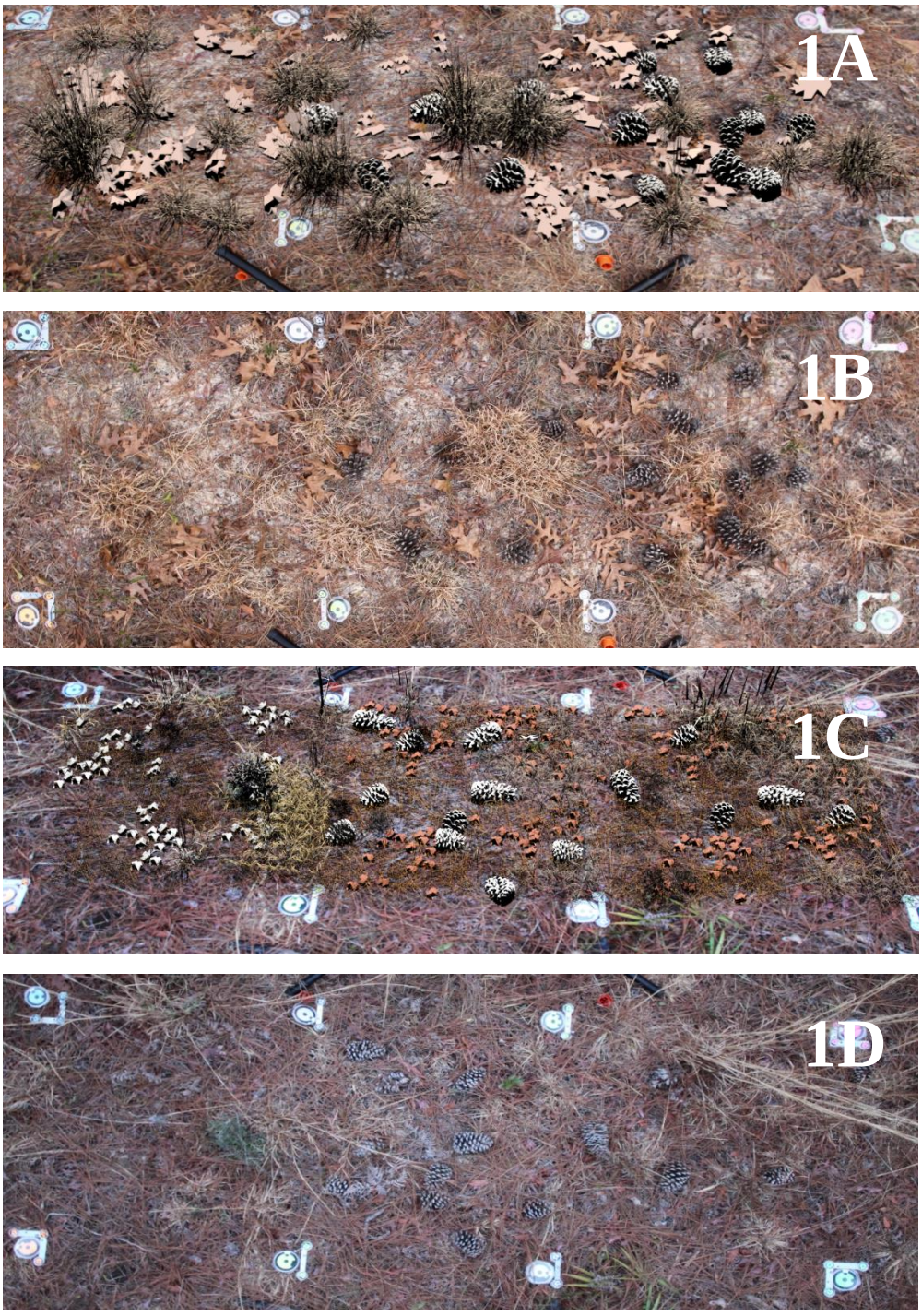

4.3.5 Voxelization

A voxelized approach was taken to reduce the dimensionality of the data and to exploit analysis techniques that rely on cell-based arrays. Each fuel bed was voxelized using the approach outlined in Hosoi and Omasa (2006). Voxels, 3D pixels that allow for volumetric representation of discontinuous surfaces using a regularly spaced three-dimensional grid were developed (Stoker 2009). A three-dimensional search cube was applied to the x,y,z files to summarize the number of fuel vertices found within each 1 cm^3. A benefit of voxel analysis is the ability to depict areas of missing and present data in geometric space. In the domain of fuelbed geometry, voxelization allows for the ability to examine connectivity in three-dimensions, which is paramount to understanding where fuel elements exist and how they are distributed in space. The 1 cm^3 voxel resolution was selected based on two criteria:

1.) Within the shrub grassland matrix 1cm^3 voxel cells allow for characterization of both clusters of grass clumps (grass blades are typically ≤ 1cm in width) and larger shrub components (e.g. leaves and branches > 1 cm in width).
2.) This grain size preserves gaps between clusters of fuel elements. Larger grains (e.g. > decimeter) begin to fill gaps and generalize the fuel bed in ways that limit further analysis.

4.3.6 Filled Volume

Previous work using terrestrial laser scans of grass-shrub fuel beds has shown that plant material concentrates in the lower part of the fuel bed in the form of densely clustered leaves and stems of grass bunches and plant litter and the upper part of the fuelbeds typically contain more dispersed stems and grass inflorescence (Rowell and Seielstad, 2012; Rowell *et al.* 2016a). Total occupied volume of each 1 m^2 subplot was calculated by summing the total number of occupied voxel cells present.

4.3.7 Surface Area and Fuel Mass

To realize the full value of modeled fuelbeds for examining fuels variability, it was necessary to relate the vertices that define each fuel elements to specific fuel properties. Vertices density was determined to be a poor representation of plant material, as some plants that have large amounts of biomass were represented by a relatively small numbers of vertices in the plant models. To overcome this, we calculated fuel surface area for each fuel type using the MESH_SURFACEAREA routine in IDL (Exelis VIS, Boulder, Colorado, USA) for each 1 cm^3 voxel cell in. The meshing algorithm used incorporates mesh normals to connect vertices, allowing calculation of the surface area for each resulting polygon. Total surface areas per 1 m^2 subplot is reported in Table 10. We then used the surface area calculations to weight mass per occupied volume in our simulated fuelbeds on a voxel by voxel basis. Additional information concerning fuel mass and fuel volume are needed to impute bulk density, particle density, and packing ratio.

For fuel mass, we examined the literature to find general data describing fine-grained biomass properties of representative grasses, longleaf pine litter and cones, and turkey oak leaves (Table 8). We use the shrub biomass properties for the forb biomass estimation as we were unable to find appropriate biomass estimates for this fuel type. Then we calculated an average mass of each fuel (derived from the literature) per mm^2. For example, for grass we took the average mass per unit area reported in the literature for the species little bluestem and used associated cover and height to generate a plant volume. From these dimensions we calculated a mass per area (mm^2) for each plant/litter model. For cones, we use average mass of a longleaf pine cone divided by average volume of cones in our dataset. These average density estimates were used to distribute biomass within each element in the simulated fuel beds in the following way. The purpose of this admittedly indirect method of biomass estimation was to account for the high variability in vertex

density within fuel elements that is not obviously related to density of biomass. The weighting assumes that surface area calculated from our meshes is directly related to mass.

Table 8. List of the studies used to produce the portioned biomass allocation used to predict the biomass for each voxel for little blue stem, turkey oak litter, longleaf pine litter, and longleaf cones. Biomass partitions are reduced to biomass for grams per mm^2.

Grasses

Fuel Type	Study	Study site	Treatment	Reference Biomass	Reference Units	Cover (%)	Height (cm)	Biomass (grams/mm^2)
Aristidia stricta Michx.	Brockway *et al*. 1998	Marion County, FL	Herbicide	15.5	Grams per m^2	57.8	*	0.00155

Cones

Fuel Type	Study	Study site	Treatment	Reference Biomass	Reference Units	Cover (%)	Length (cm)	Biomass (grams/mm^3)
Pinus palustris	Fonda and Varner 2004	Ocala, FL	-	59.1	Grams per cone	-	**	0.000591

Longleaf Pine Litter

Fuel Type	Study	Study site	Treatment	Reference Biomass	Reference Units	Cover (%)	Height (cm)	Biomass (grams/mm^2)
Pinus palustris	Fonda 2001	Ocala, FL	2x2 Factorial design	14.21	Grams per m^2	100	5	0.002321

Turkey Oak Litter

Fuel Type	Study	Study site	Treatment	Reference Biomass	Reference Units	Cover (%)	Height (cm)	Biomass (grams/mm^2)
Quercus Laevis	Kane *et al.* 2008	Jones Ecological Center	Lab experiment	15	Grams per 35 cm^2	100	6.2	0.000197

4.3.8 Calculating Height Metrics

Height metrics were extracted from the simulated fuelbeds on a 10 cm grid within each plot by applying a 10 cm equal spaced point array and sampling a 10 cm^2 area around each centroid. Height metrics were only compared within the SERDP data, the RxCadre data were collected as plot averages and not spatially explicit. Fuel depth from the simulated fuelbed represents all heights found in the area as opposed to the point intercept data collected in the field which documents only intercepted heights at a point. Although we could have used the same approach and only considered objects from the modeled fuelbed that fell on top of the field measured points, it is extremely unlikely that field measurements would precisely coincide with features of our plant models and we instead chose to include any point found within the search area so we could express height variability per fuel cell. By applying the point network from our point intercept data to the simulated fuel beds, we also developed a suite of height metrics, including maximum, 99^{th} percentile, mean, inflection height, standard deviation, median height, standard deviation height, kurtosis, and skewness. All heights within a $100cm^2$ area around each field sample point were used to calculate these metrics from the artificial fuelbeds at a grain of 10cm. These metrics were ultimately compared to coincident field observed heights.

4.3.9 Terrestrial Laser Scanning Collection and Processing

Laser scans were collected pre- and post-fire using an Optech ILRIS^{TM} 3_6D-HD laser scanner at a 10kHz sampling frequency. Data were collected for the L2 forested burn blocks (RxCadre) which contained two years of fuel accumulation and plant growth since the last prescribed fire. The TLS instrument was positioned at the four corners of the HIPs plot, positioned an average distance of 7 m from the edge of the plot on a telescoping tripod set at a height of 2.74 m. The laser was pointed downward with an average inclination of -30° and a focal range of 20

m resulting in an average scan density of 8.4 mm. Reflective posts were placed on the southeast corner of every 0.25 m^2 sample plot around each HIPS plot resulting in twelve tie points per HIPs.

Terrestrial laser scans were aligned using the Polyworks software suite (Innovmetric, Quebec, Canada) and further point cloud spatial refinements were completed using CloudCompare (CloudCompare 2014; www.cloudcompare.org), an open source point alignment software package. Individual scans were merged together into a single dataset and projected on a UTM coordinate system through coincident GPS data collected for all HIPs corner points. A more in depth processing explanation can be found in Rowell *et al.* (2016a). Point clouds were subset into individual sample plots (n=23) by locating the reflective post on each corner and defining a clip polygon feature in ArcGIS (Environmental Research Systems Institute, Redlands, California, USA). A fuel height model (FHM) was generated by subtracting the geoid height from a local minimum height producing normalized height above ground. TLS point clouds were imported into R (www.r-project.org) for statistical analysis.

4.3.10 Statistical Analysis

Analyses are presented in the three phases described above parts: Phase 1: Parameterization and development of simulated fuelbeds and biomass estimations using high resolution nadir imagery and field-based height data (n=100 data points per plot) for the SERDP site. Height comparison is conducted using Pearson correlation. Phase 2: Replication of model development and biomass estimation for the RxCadre site and comparison with *in situ* measurements of biomass. Comparisons are conducted using Pearson correlation, ANOVA, and RMSE. Phase 3:Fuelbed height distributions comparison between TLS-based and simulation-based using Weibull distribution functions to analyze shape (α) and scale (β) parameters using the fitdistrplus

package (Delignette-Muller and Dutang 2015) in R. The Weibull function is fit to the TLS and simulated fuel height model using the maximum likelihood estimate method.

4.4 Results

4.4.1 Phase 1: Parametrization and Simulation Development in the SERDP plots

The simulated fuel beds closely resembled the plot photos in appearance and geometry (Figure 14) and share characteristics with field measurements in terms of fuel depth and cover. In this study fuel depth and cover are the only directly comparable metrics between the field measured and the simulated fuelbed data as no other field data were collected.

4.4.2 Height Metrics

Comparisons of field and simulated fuel depth (Table 9) were well correlated with correlation coefficients ranging from 0.75 to 0.96. The tightest correspondence occurred in plot 6 ($r = 0.96$, p-value < 0.001). Plots with high densities of overhanging grass stems proved most variable when compared against the point intercept data with correlation coefficients ranging from 0.81 to 0.88. In all cases the tallest measurements from the field and simulated fuel heights related well, with less correspondence in the lower reaches of the fuel beds. Plots with generally low stature fuels and isolated taller grass fuels performed best. The largest residual standard error occurred in plot 3 where a lattice of overhanging grass stems crisscrossed the plot. The field point intercept data often miss these sparse objects, whereas careful attention was given to adding them in generation of the simulated fuelbeds.

Table 9. Simulated fuelbed heights correlate well with measured fuel depth, with most variability resulting from grass blades in the simulation crossing in the 10 cm^2 grid cell. Residual standard errors (RSE) were greatest in plot 3 which had a lattice of reproductive grass stems that were bent across the plot.

Plot	Correlation	*df*	p-value	Confidence Interval (95%)	RSE
1	0.94	298	< 0.001	0.92 - 0.95	5.76
2	0.81	298	< 0.001	0.81 - 0.87	8.98
3	0.84	298	< 0.001	0.80 - 0.87	14.36
4	0.75	298	< 0.001	0.69 - 0.79	4.88
5	0.86	298	< 0.001	0.82 - 0.88	3.70
6	0.96	298	< 0.001	0.94 - 0.96	2.21
7	0.88	298	< 0.001	0.85 – 0.90	5.76

4.4.5 Biomass Estimation

Estimates of per subplot biomass fell within expected ranges reported in the literature (Table 8) for grass, needles, cones, and deciduous litter, with three exceptions. Ranges for grass biomass were from 43.43 to 664.22 grams/m^2, needle litter ranged from 0.23 to 35.23 grams/m^2, and cone biomass ranged from 117.96 to 509.95 grams/m^2. Plots 3, 4, and 5 exhibited grass biomass estimates that exceeded expected norms. Occupied volume on these plots varied from consistent with other plots having similar fuel loads to nearly twice the average volume of all plots. Surface area for these same plots appears to be the primary driver of the larger biomass estimate as these plots average 150% more surface area to volume than plots that fell within expected biomass ranges. Volume and surface area per plot for each fuel type are reported in Table 8. Estimates of longleaf pine needle litter biomass performed within published ranges. These fuel layers potentially produce the most realistic estimates of mass as the strata is limited in depth (between 2 -5 cm) and has very clear physical boundaries, whereas the grass fuels require more interpretation regarding height and dispersion across the fuelbed. Bulk densities derived from the biomass and occupied volume averaged from 0.012 grams/cm^3 for grass to 0.077 grams/ cm^3 for cones. Longleaf pine litter had an average bulk density of 0.0007 cm^3.

Analysis of height distributions of biomass in the simulated fuelbeds shows that nearly 70% of grass biomass is located below 5.5 cm height, which is where the height biomass curves inflect upward (Figure 20). This inflection height corresponds with the transition from grass bunch to the sparser stems and inflorescence. Additionally, about 40% of the grass biomass occurs within 2 cm of the ground, occupying the litter layer more so than the aerial fuels within each fuel bed. All longleaf pine litter and deciduous oak litter biomass fell below the grass biomass inflection height

Table 10. Occupied voxel volume (OV), surface area (SA), biomass (B), and bulk density (BD) is reported for grass, needle litter, and cones for each plot's subplot.

		Grass				Needle				Cone			
Plot	**Sub-Plot**	**OV (cm^3)**	**SA (cm^2)**	**B (g/m^2)**	**BD (g/cm^3)**	**OV (cm^3)**	**SA (cm^2)**	**B (g/m^2)**	**BD (g/cm^3)**	**OV (cm^3)**	**SA (cm^2)**	**B (g/m^2)**	**BD (g/cm^3)**
1	1	11054	3663.21	56.78	0.005	17511	6932.18	16.09	0.0009	-	-	-	-
	2	11046	2801.95	43.43	0.004	18198	6487.15	15.05	0.0008	4697	63480.85	375.17	0.169
	3	21770	7263.36	112.58	0.005	18832	8735.35	20.27	0.0011	2285	28555.55	168.76	0.169
2	1	16684	4522.24	70.09	0.004	21933	15174.14	35.00	0.0016	4894	43556.27	257.42	0.169
	2	9360	2472.03	38.32	0.004	15174	10049.53	23.32	0.0015	-	-	-	-
	3	18439	5822.80	90.25	0.005	15174	15174.14	35.23	0.0023	6272	55960.62	330.73	0.189
3	1	51058	34956.00	541.82	0.011	4201	475.62	1.10	0.0003	4364	55138.75	325.87	0.133
	2	47682	38118.29	590.83	0.012	4729	505.45	1.17	0.0002	-	-	-	-
	3	24458	35151.61	544.85	0.022	12860	4376.90	10.16	0.0008	3290	40676.25	240.40	0.136
4	1	19909	19190.75	297.46	0.015	1015	92.87	0.22	0.0002	-	-	-	
	2	22176	22199.45	344.09	0.016	1053	69.52	0.16	0.0002	4808	64623.56	381.93	0.125
	3	27793	38783.47	601.14	0.022	3863	238.07	0.55	0.0001	2382	33877.55	200.22	0.118
5	1	28619	42834.00	663.93	0.023	4465	319.45	0.74	0.0002	6169	86286.14	509.95	0.120
	2	28577	42853.20	664.22	0.023	8166	2131.55	4.95	0.0006	3105	43023.9	254.27	0.122
	3	30865	44981.79	697.22	0.023	3286	98.52	0.23	0.0001	-	-	-	-
6	1	10500	6805.63	105.49	0.010	9246	2546.17	5.91	0.0006	-	-	-	-
	2	11273	8774.84	136.01	0.012	2457	43.64	0.10	0.00004	1060	19959.0	117.96	0.898
	3	11208	8599.48	133.29	0.119	2457	43.64	0.10	0.00001	5299	73975.02	437.19	0.121
7	1	17074	234.19	3.63	0.0002	144	0.85	0.002	0.00001	-	-	-	-
	2	23257	7023.64	108.87	0.005	201	1.18	0.46	0.00001	2946	7887.48	174.1	0.169
	3	9209	2555.81	39.62	0.004	194	1.02	0.45	0.00001	4857	14382	287.04	0.169

Figure 20. Mean biomass for 1 cm height bins for all plots in Phase 1 are shown (solid line) bounded by standard deviation (dashed line). The bulk of biomass is allocated at the lowest strata of the fuelbed.

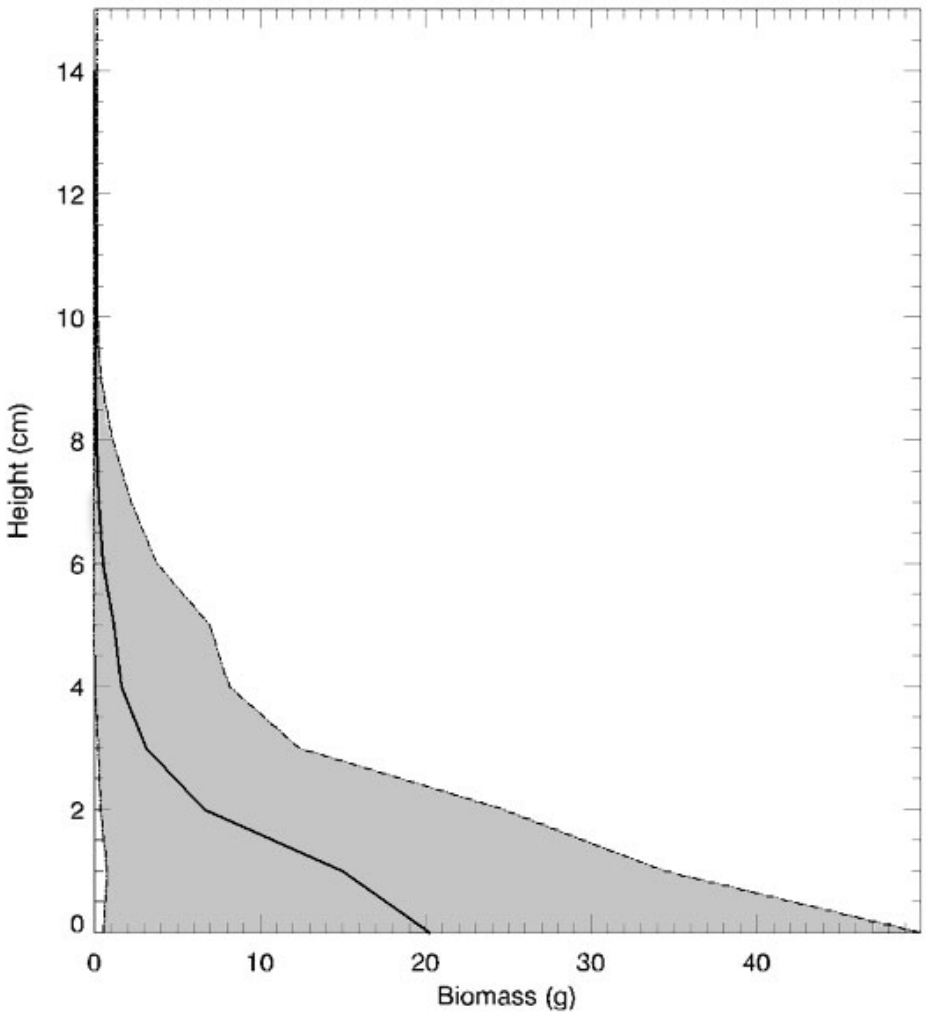

described above. Cone litter generally bisected the grass inflection height with fuel depth ranging from 5 to 8 cm.

4.4.4 Phase 2: Validation and Comparison in the RxCadre Plots

4.4.5 Biomass Validation

Biomass was estimated for the three dominant fuel types (needle litter, oak leaf litter, and perennial grasses) across the HIPs plots. The litter biomass estimates were combined into a single litter value, as the weighed biomass is described in a single litter term. Simulated litter biomass correlated well with oven-dried litter biomass (r=0.86, $P < 0.05$, RMSE = 15.8 g, Figure 21). ANOVA detailed no significant difference between mean simulated and actual litter biomass values (F = 1.05, $P < 0.93$, df =16, confidence level = 0.95). Litter averaged 80% (σ = 21%) of the total biomass for all clip plots combined from the weighed biomass data. Grass biomass represented a range of 2% to 17% of total biomass for eight clip plots and simulated biomass again correlated well with oven-dried biomass (r = 0.98, $P < 0.05$, RMSE=1.6g). Simulated forb biomass performed least well (r = 0.75, $P < 0.05$) revealing substantial variability in estimates when the species bracken fern models are present. There is difficulty in assessing if the error with these models is associated with the model or the field data classifications of emergent and non-emergent vegetation. In many of the plot photographs collected for the experiment, bracken ferns are desiccated and in some cases have perched litter on top. Therefore, these ferns may also be partitioned to the litter fuel class.

Figure 21. An equivalence scatter plot of the simulated litter and oven-dried litter biomass for each plot in the RxCADRE validation.

.

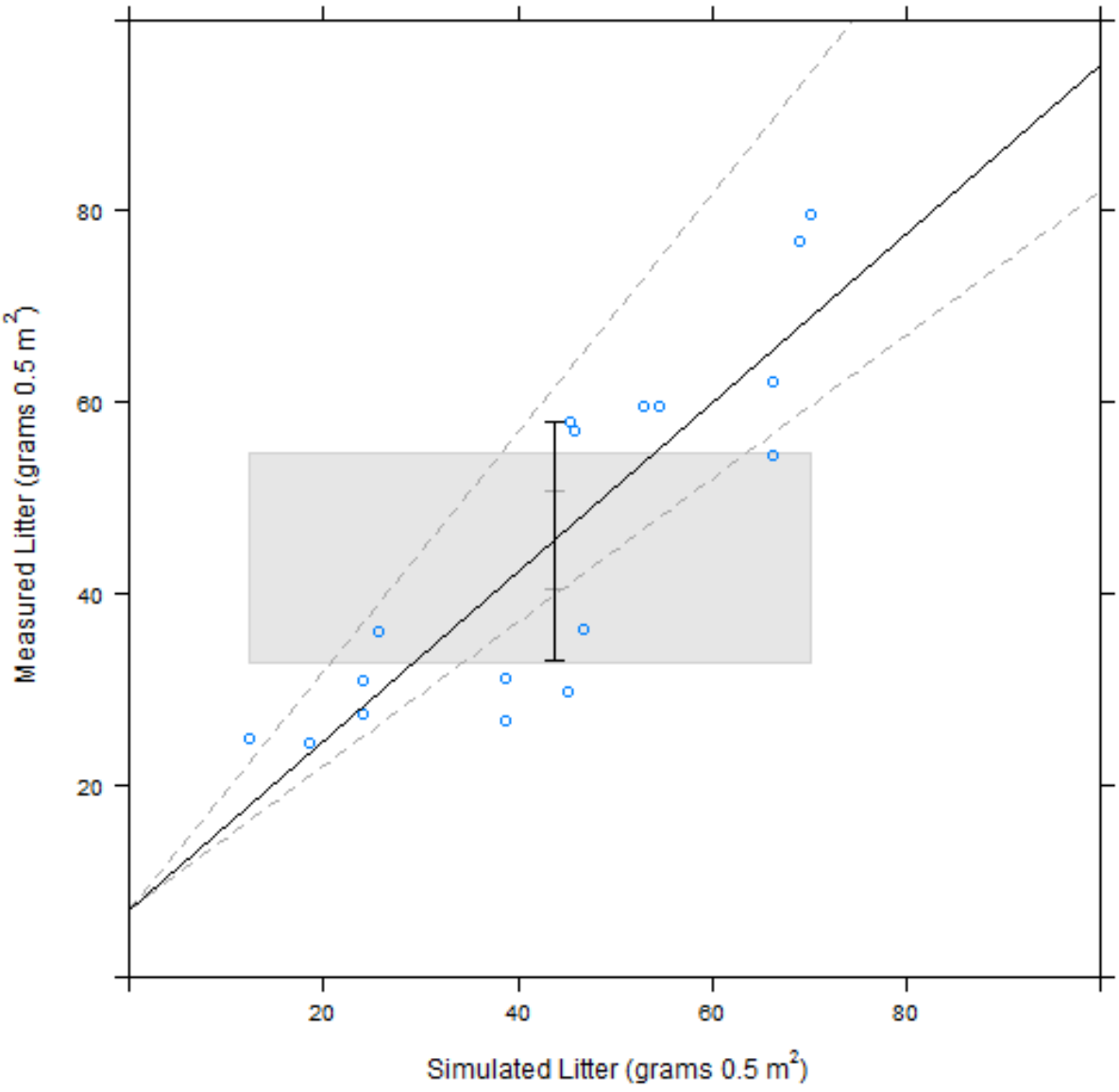

Figure 22. An equivalence plot between the Weibull α parameter derived from the TLS and simulation height distributions.

.

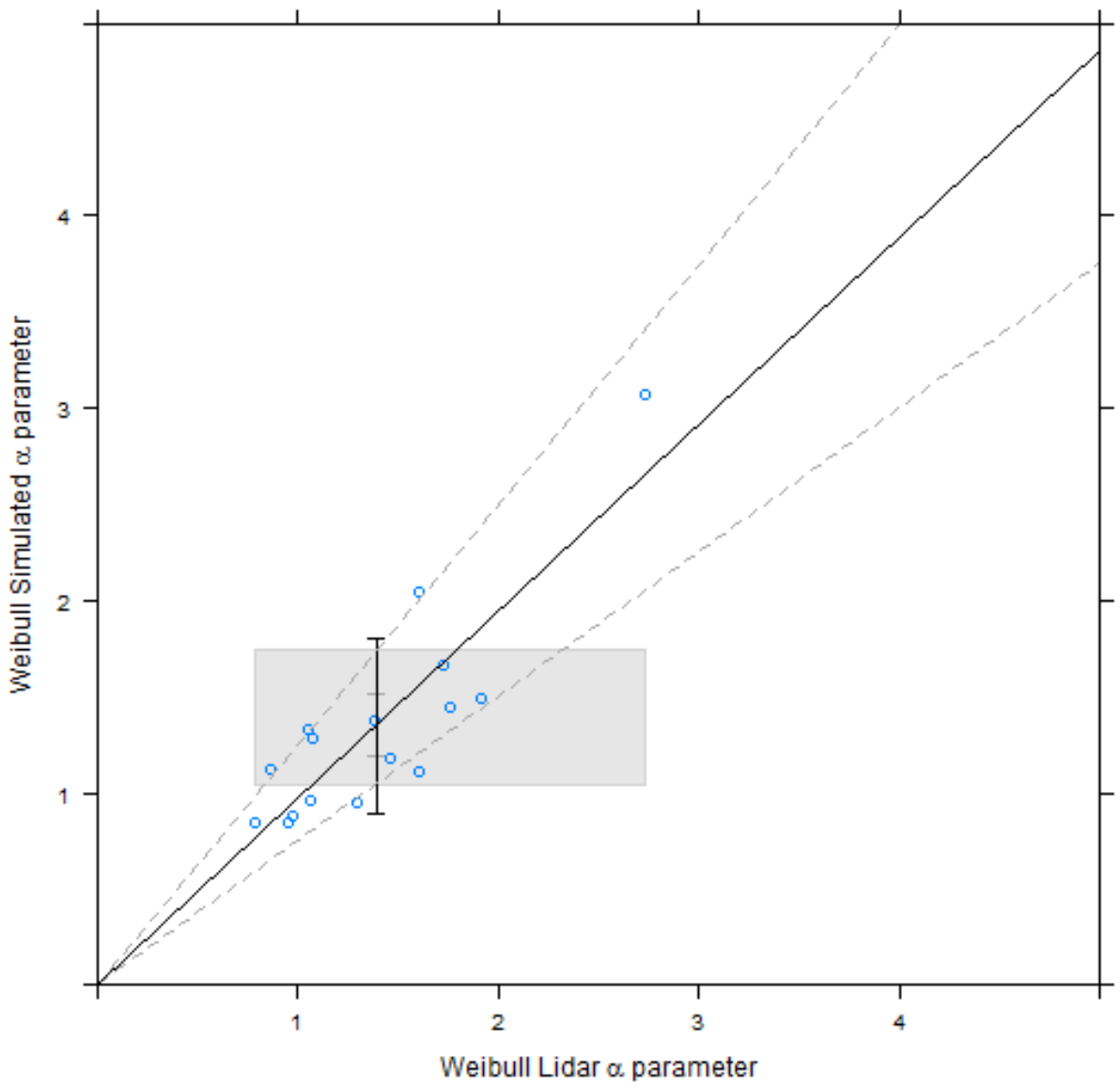

Figure 23. An equivalence plot between the Weibull β parameter derived from the TLS and simulation height distributions.

.

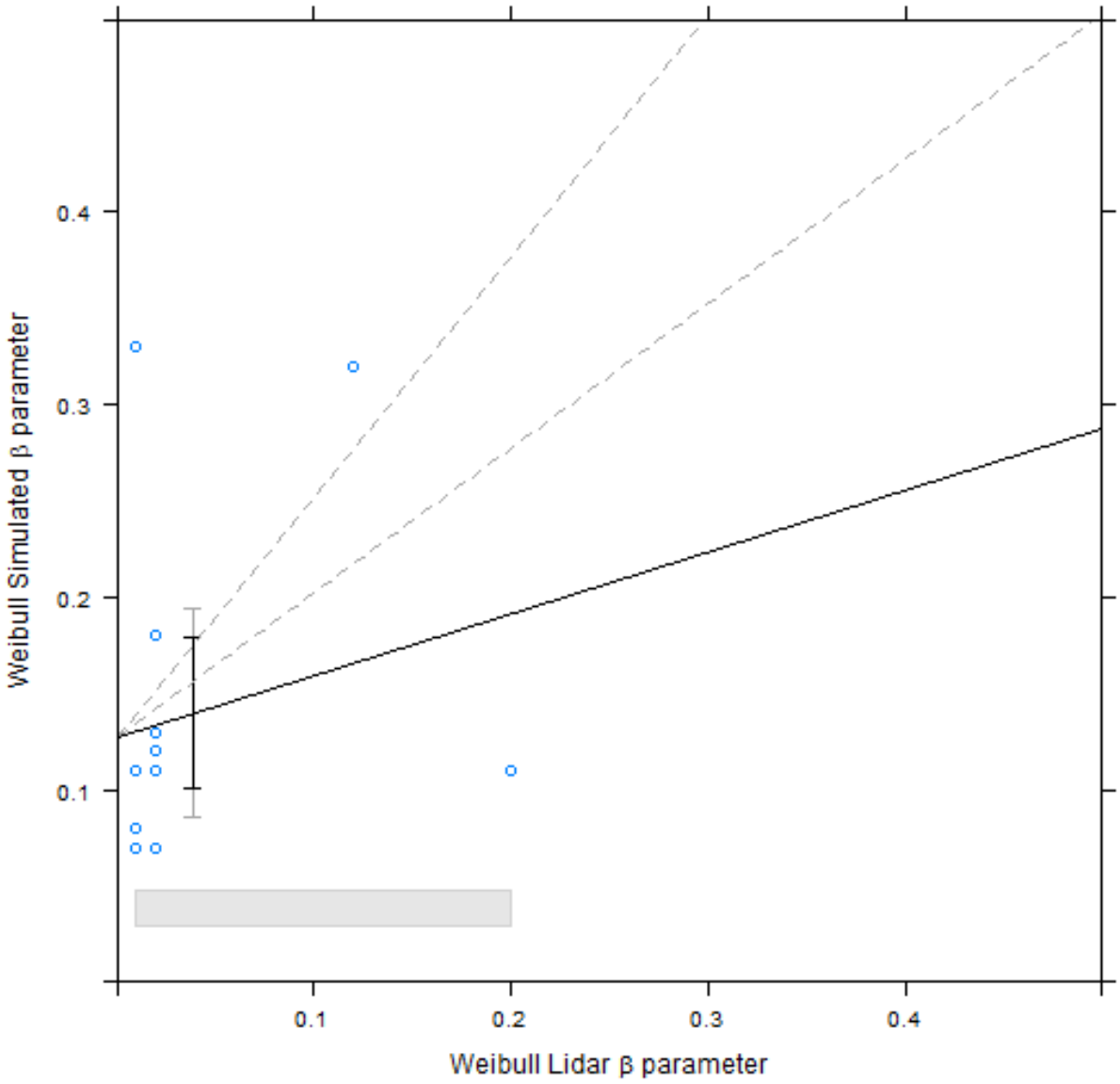

Figure 24. Weibull distributions for five example plots used in the RxCadre experiment demonstrate similarities between simulations and TLS-based height profiles.

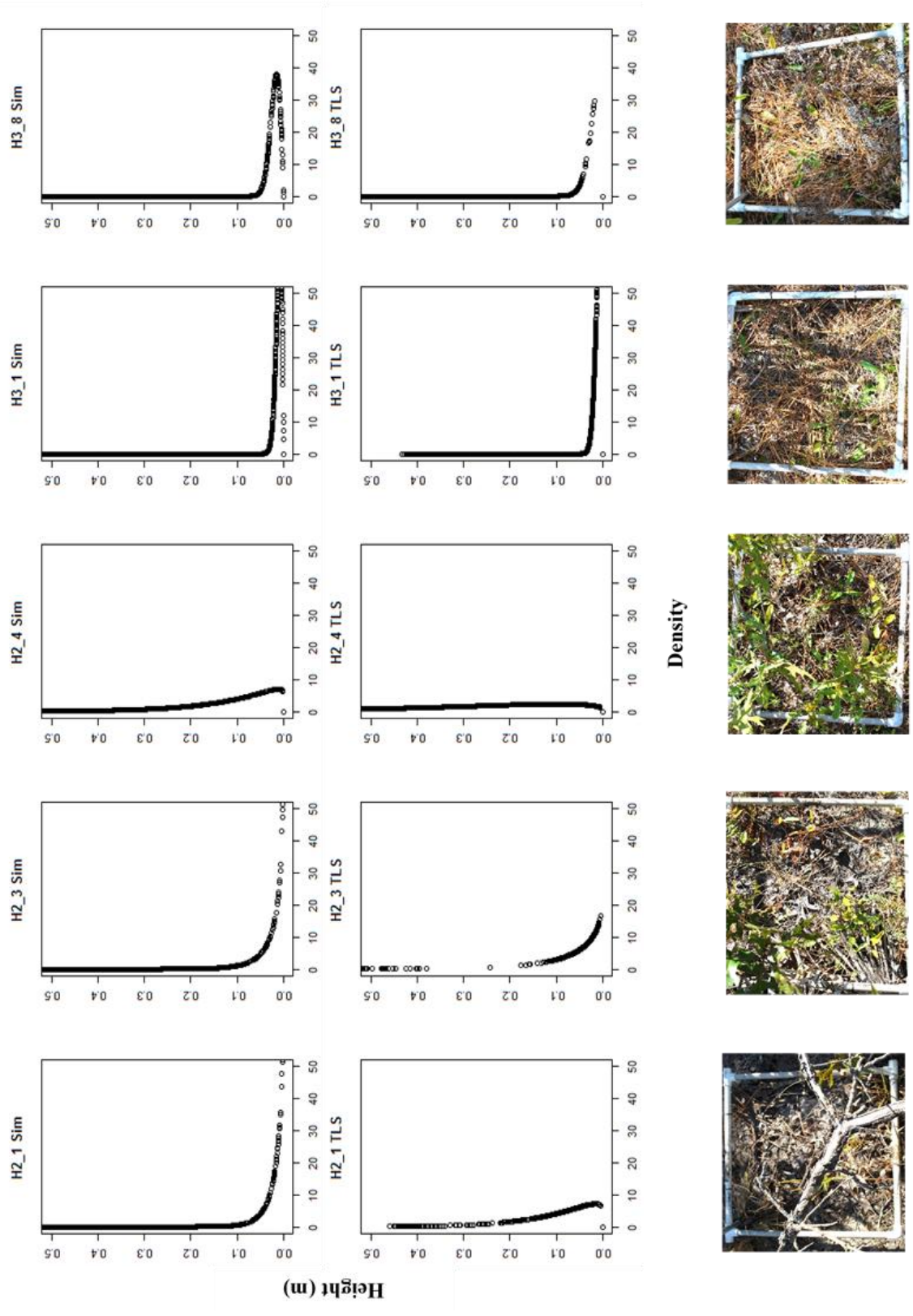

Figure 25. Biomass distributions for a mixed grass (A.), forb (B.), and litter (C.) plot demonstrating the vertical distribution of biomass per fuel type.

.

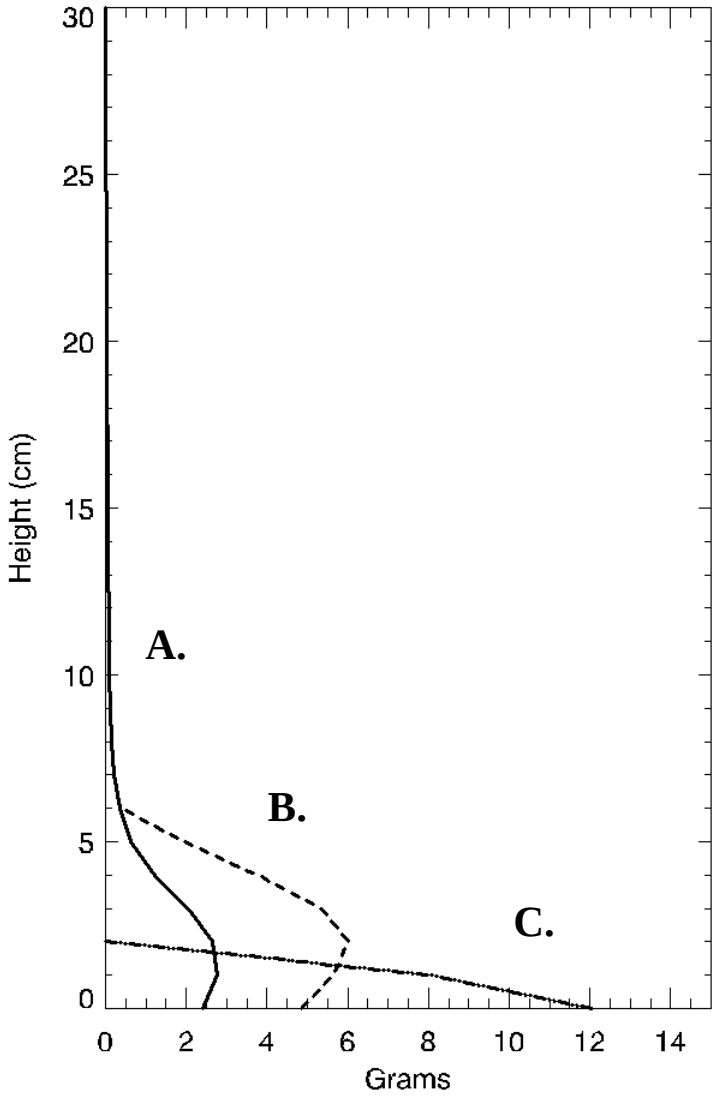

4.4.6 Phase 3: Weibull Distribution Comparison between Simulations and TLS

Weibull shape parameters (α) for the TLS-based point clouds and simulations compared well (r = 0.86, $P < 0.05$, Figure 22) indicating that the Weibull slopes are similar in both datasets. Weibull α parameters for the simulation data indicated a weak relationship with plots that are litter dominated (r = 0.65, $P < 0.05$), suggesting that low height objects in the litter bed influence the Weibull slope value. The scale parameters (β) performed poorly (r = 0.21, $P < 0.5$, Figure 23). Clearly there are disparities in data density between the TLS and simulation data with the simulation data density heavily weighted toward the litter bed ranging in height from 0 – 5 cm (Figure 24). Several plots (n=9) were partially obscured by adjacent or overhanging vegetation reducing the ability of the laser pulses to penetrate and accurately sample the litter layer of the plots

4.5 Discussion

This study provides a new approach for examining surface fuel variability at very fine scales (sub-meter). Simulated fuelbeds produce a high degree of visual realism (Figure 19) and share height and biomass attributes with field measurements. These fuel models and their metrics can be used to design fuelbeds that are consistent in measurement of structure and biomass. This consistency in fuel attributes is currently missing from inputs needed for physics-based fire behavior models. We view these fuelbed simulations as a bridge between field and remotely sensed data. Field sampling results in aggregation over large areas to infer average fuel loading (Ottmar *et al.*2016). As discussed previously, traditional inventory methods simplify the fuelbed at the cost of characterizing the full range of variability that exists. Furthermore, an attempt at describing surface fuel mass using airborne lidar was inadequate in the same study area (Hudak *et al.*2016). This may be attributable to the fine-scale heterogeneity of fuels associated with longleaf pine

ecosystems, where the need to identify and spatially describe fuel distributions in regards to fuel type and fuel structure (Loudermilk *et al.* 2012; O'Brien *et al.* 2016).

We have demonstrated that these simulations are highly correlated to field measured height and dry weight biomass. More importantly, these metrics can be allocated to specific fuel types (Figure 25), where other attempts using lidar have only looked at predicting overall fuel mass (Hudak *et al.*2016) or predicting fuel models (Seielstad and Queen 2003). O'Brien *et al.* (2016) suggest the allocation to fuel type is a better predictor of subsequent fire radiative energy then fuel mass alone. Active remote sensing platforms such as TLS collect rich data, but assessing the individual fuel elements with differing properties within complex fuelbeds is difficult and has yet to be executed satisfactorily (Rowell and Seielstad 2012). In frequent low-intensity fire regimes, this specific allocation of fuel mass as a function of type and structure has the potential to quantify variability in fire radiative energy that contributes directly to fire effects (O'Brien *et al.* 2016).

The key difficulty with mapping surface fuels using TLS is uncertainty regarding how the vertical distribution of the point cloud relates to complex matrices of fuels in the lowest strata of the fuelbed where the most influential fuels (e.g., pine litter, pine cones) are found (figure 25). The simulation approach we describe in this study performs best for characterizing these particular fuel types. Previously, Coops *et al.* (2007) interpreted Weibull distributions of airborne lidar and related the Weibull α and β parameters to characterize distributions of biomass within forested canopies in British Columbia, Canada. This study found correlations between Weibull parameters of lidar canopy height models and field measured height distributions, suggesting that airborne lidar data can be used to derive standard forest inventory information. For our research, it is clear that the amount of information we can glean from the surface fuels characterization of TLS-based height distributions is pivotal in characterizing fuel metrics. Within the RxCadre plots, TLS data

are underrepresenting the bulk of fuels occurring at the lowest heights of the fuelbed. This requires inference from vertical distributions of the upper reaches of the fuelbed to predict what the configuration of the lowest height strata of grass and litter are. The Weibull α parameters for both the TLS and simulated data suggest that we are describing the density of points and simulated objects distributed vertically.

The simulated Weibull distributions are based on the object vertices used to estimate surface area of the objects that are in turn used to predict biomass. From this, we infer that biomass is allocated similarly. Remington *et al.* (1992) demonstrated that the use of the three parameter Weibull characterizes grass biomass distributions based on grazing treatments in Colorado, USA. Our findings are similar to this study in that litter dominated plots are heavily weighted to lower heights with the highest concentrations of biomass.

Another important note is the effect of occlusion that results from laser pulses being intercepted by matter in the foreground or hanging over the plot of interest. Our analysis demonstrated that where this effect occurs, the ground surface sampling attenuates in regards to the actual number of objects present. Simulated fuel beds capture these elements and differences in the Weibull curves suggest that variability in TLS sampling may have a negative effect on predicting and distributing biomass in these systems. To overcome issues of occlusion, others have employed detailed and multi-angle TLS acquisition to produce high resolution scans that maximize laser pulse penetration into vegetation (Hosoi and Omasa, 2009). Previous studies have demonstrated that for identifiable individual shrubs in large area scans, TLS data can be used to estimate biomass across size gradients (Loudermilk *et al.* 2009; Olsoy *et al.* 2014; Greaves *et al.* 2015). The ability to discriminate specific inter-mixed fuel types and arrangements at the lowest reaches of the fuelbed is therefore difficult utilizing TLS data.

We demonstrate that the simulated fuelbed approach produces meaningful estimates of leaf litter, grass, and forb biomass that are interspersed across the fuel matrix (Figure 25). These findings suggest that our simulations provide an enhanced range of variability by tying precise height and fuel load metrics with field collected biomass. An advantage to this modeling technique is the absence of *a priori* knowledge of biomass to attribute across the fuelbed. Similarly, Parsons *et al.* (2006) attributes biomass to fractal tree models using biomass estimates derived by the Forest Vegetation Simulator (FVS), where allometrically derived biomass is allocated across the tree per voxel unit as a function of branch and needle fuel type. Vertical and horizontal distributions of fuelbeds are critical in the realm of understanding the role of fuels in fire behavior and post-combustion fire effects.

Our fuelbeds depicted higher concentrations of biomass near the bottom of the fuelbed (< 4cm) in grass fuels and showed a higher degree of variability in the lower reaches of the fuelbed than higher up. Similarly, the ratio of occupied versus unoccupied space in the fuelbed changes with height, with more open space in the upper reaches of the fuelbed and less available biomass. We are also able to describe the horizontal distribution of fuels and decompose this distribution by fuel type in a way that is not currently possible with field methods or remote sensing. An advantage to using this method is that estimates of biomass and bulk density are not prone to the same types of error that airborne or terrestrial lidar experience.

The description of fine scale fuelbed biomass and partition is important as fuels differentially combust based on changes in relative humidity and ambient temperature. Varner *et al.* (2015) demonstrates the differences in combustion, specifically that longleaf pine needle litter has an intense, brief, and high consumption burn period that makes this fuel type a primary carrier of fire in southeastern forests. Inversely, turkey oak litter has a long flaming and a protracted

smoldering period. Being able to distinguish between important fuel types and respective mass is important to understanding factors that influence heat flux and post-combustion fire effects (O'Brien *et al.*2016). Andersen *et al.* (2004) describe small deviations from assumptions of uniform distributions of fuels that propagate significant effects of canopy bulk density in forested ecosystems. The ability to describe these fuels in terms of available biomass, volume, and surface area by fuel type and across large areas is an exciting prospect for advancing wildland fire science.

4.5.1 Future work

We pose that limited field data does not need to inhibit finer grain characterization of these fuelbeds. In fact, a combination of general height characteristics, photography, and fuel load may suffice to produce accurate simulated estimates of a variety of fuel arrangements encountered in a landscape. Lidar data may act as a frame work to distribute these simulated estimates of fuels through probability models or distribution analysis (figure 6). However, characterizing large fuel beds (> 1 ha) using TLS is a difficult proposition. We suggest using Weibull relationships to link field data with TLS or airborne lidar vertical distributions with simulated fuelbeds as a way to populate a landscape. Specifically, integration of these data are crucial for creating consistent fuels data for validation of next generation fire behavior models, such as the Wildland Fire Dynamic Simulator (WFDS; Mell *et al.* 2009) and FIRETEC/higrad (Linn *et al.* 2006). Although the resolution of the simulated fuelbeds are computationally too expensive for integration into these fire behavior models, we suggest utilizing the TLS-based height distributions as a mechanism to extrapolate the amount and type of mass detailed in the simulations aggregated to coarser grain sizes. This technique may prove to be the most effective way to bridge the differences between field and lidar-based measurements.

From the perspective of lidar remote sensing, having a dataset parameterized to represent realistic 3D distributions of fuels and biomass will serve as a backdrop for simulating laser point clouds via ray tracing. Disney *et al.* (2009) showed results that indicated the importance of lidar instrument settings and energy/matter interactions within simulated tree canopy structure using the same parametric plant models in OnyxTree. This same study found that the ability to represent canopy architecture and elements discretely facilitated better understanding of how laser pulses penetrate tree crowns, with implications for predicting Leaf Area Index and related metrics (Disney *et al.* 2010). Palace *et al.* (2015) modeled canopy vegetation profiles and forest structure for comparison with similar airborne lidar metrics through simulated forest models in Costa Rican tropical forests. This study found that simulations using established allometries to produce simulated forests found that canopy height is not a significant predictor of biomass, but modeling forest profiles that estimate plant area fractions improved lidar-derived estimates of forest biomass.

The ability to produce realistic simulated laser point clouds is a significant proving mechanism for understanding how terrestrial laser scanners characterize fine fuels. Previous attempts at describing these fuels have been difficult due to occlusion and point sampling variability using terrestrial laser scanner data collected obliquely from a boom lift (Rowell *et al.* 2016a). Further work needs to be conducted to determine how well biomass estimated from the simulated fuelbed performs specifically integrating more intensely sampled fuelbeds. Automation of fuelbed construction is also imperative to reducing variability and subjectivity. We also foresee benefits for the integration of these findings with other high resolution simulation techniques, such as FUEL3D (Parsons, 2006), where we may begin to combine surface and canopy fuels for improved inputs used for physics-based fire behavior models.

4.6 Conclusions

In this paper, we presented results that demonstrate 3D fuelbed simulations can explain much of the variability of biomass allocation and height distributions that are difficult to estimate using TLS data. Though, the approach to building these simulations needs improvement in terms of automation and further validation, there is significant promise for using these methods to populate spatial datasets for use in CFD based fire behavior models. Assumptions of plant structure, biomass partition, and height estimation need to be refined to include a broader diversity of species found in the southeastern United States and similarly structure ecosystems worldwide. We intend to further investigate the integration of these surface fuelbed simulations with other canopy fuel modeling techniques (e.g. FUEL3D) and the ability to leverage remotely sensed data to extrapolate landscape-scale fuelbed models

Chapter 5 – Research Summary

The purpose of this research was to advance the application of active remote sensing techniques for generating robust and quantifiable estimates of surface fuels at multiple scales. The net contribution to fire science is methods, techniques, and spatially explicit and scalable data products which can be used for validating next generation CFD models and examining fire effects. Ultimately, the work of this dissertation along with subsequent advancements will enable better understanding of how fuels variability (and scale) modulate fire behavior and effects. This dissertation utilized TLS, ALS, and simulated data to: 1) demonstrate the ability to scan fuelbeds from a variety of angles and scales using TLS instruments and to validated estimates of fuel heights, 2) predict surface fuel load and fuel consumption at a variety of scales and fuel type configurations, and 3) employ three-dimensional surface fuelbed simulations to refine allocations of biomass and assess the potential limitations of TLS and observed data. The end result of this dissertation support the assertion that active remote sensing platforms can play a valuable role in wildland fuels science.

This work also expands on other studies (Olsoy et al. 2014; Greaves et al. 2014; and Cooper et al. 2017), to show that TLS is capable of producing robust estimates of individual and mixed fuel types. The results of this work also outline advantages of using TLS-estimated surface fuel load as a surrogate for observed data to increase sample size and improve estimates of surface fuel load over using observed data alone (Hudak et al. 2016). Finally, the use of three dimensional simulated fuelbeds improves our understanding of how fuelbed mass is distributed by type and spatial allocation. This result provides a bridge between field observation and active remote sensing-based fuels data that has previously not existed.

5.1 Ongoing Work

Field Sampling Methods

A key limitation regarding comparisons of TLS-derived and observed fuels is the issue that the two datasets are essentially completely different ways of sampling the fuelbed. The TLS data is more of a comprehensive representation of a population and depending on what data are collected in a field campaign, observed data are a generalization of the fuelbed. This mismatch is a constant problem in remote sensing. There are also uncertainties regarding the true occupancy of fuel volume within the actual fuelbed versus the way that TLS data represent the fuelbed as a voxel array. In this dissertation, I include a rationale for using a $10cm^3$ voxel dimension to bridge spaces effectively that may have been missed due to occlusion of the laser beam by fuel elements (e.g. shrubs).

Figure 26. The 3D voxel sampling cube is used to sample fuels at Pebble Hill Plantation in Thomasville, Georgia. This method collects observed data that is similar to the way TLS-derived voxels sample fuelbeds.

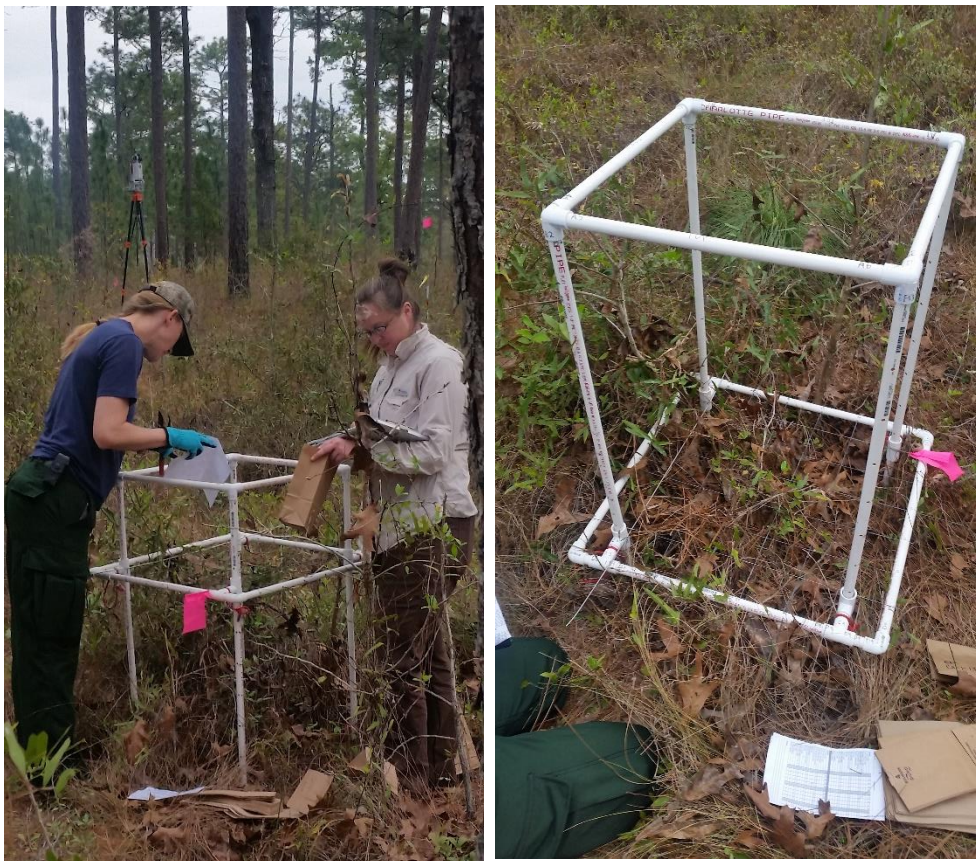

Consequently, I developed an alternative method of field sampling fuels that is designed to mimic the way TLS samples fuelbeds. The 3D voxel cube method (Figure 26) uses an adjustable height quadrat ($0.25m^2$) that raises or lowers in 10cm increments. The quadrat itself is subdivided into 25 ($10cm^2$) cells. This method allows for sampling the fuels as voxels and strata, where for each cell, representative fuel types and fuel mass (dry weight biomass), height is integrated into the measurement as a function of voxel cell sampled. This method will allow direct comparison of equivalent voxel measurements from TLS data, a plot based bulk density metric, distributions of biomass as a function of height, and inter-voxel variability through random sampling of voxel biomass for five voxels per strata.

Figure 27. Interpolated surfaces representing voxel occupancy from the 3D voxel cube sampling for a) forbs including vines and b) deciduous oak shrubs.

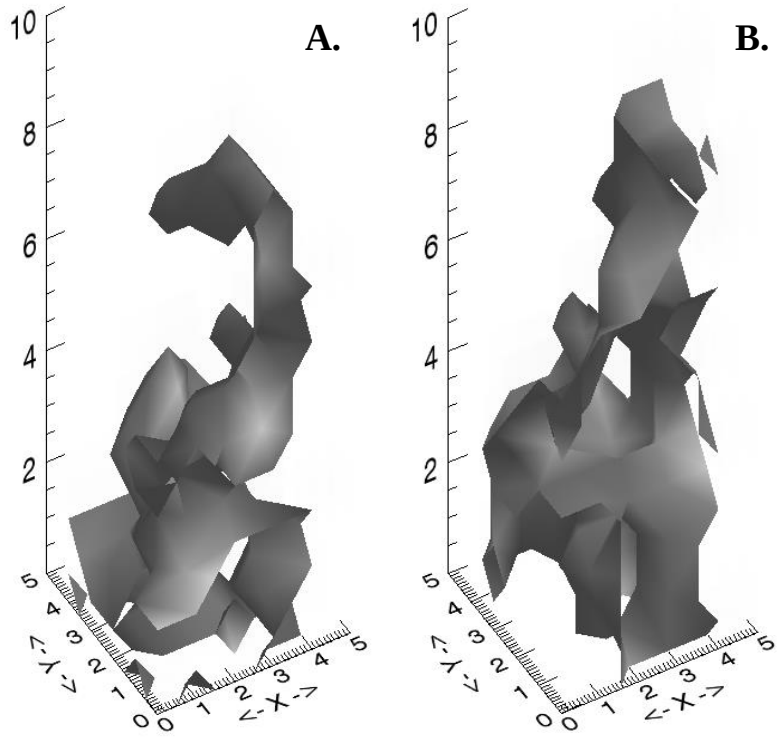

These data will allow for interpretations of distributions of fuel mass and bulk densities by fuel type (figure 27), which are spatially explicit and readily usable for both comparison with remotely sensed data and insertion into CFD models.

Drone based structure-from-motion

The advancement of UAS systems demonstrates strong potential for producing 3D datasets (Figure 28) that enhance the use of TLS-based fuel mass estimates. Experiments conducted in the southeastern United States have shown that cohesive point clouds can be generated using UAS systems. However, comparisons of the TLS and UAS point clouds have demonstrated that UAS systems produce points generally representative of the outer hull of fuel elements, whereas TLS data produce generally better representations of the structural components of the fuelbed. The advantage of UAS systems is their ability to capture relatively large areas of data (10-100 ha) as compared to TLS data that functionally is better at capturing data for 10-100m. A viable crosswalk is currently being developed to produce relationships between the TLS-derived fuel mass and the surface area derived from the hull sampling of the UAS data. I believe that UAS platforms are a natural fit as a scaling lane from TLS to coarser remotely sensed data to produce robust estimates of fuel mass. By validating TLS from plot data and then validating UAS data from TLS estimates of fuel mass, we increase the number of validation points that bolster fuel mass estimates. This assumption is based on the improvements described in chapter 3, where using the TLS estimates of fuel mass improved the estimates produced from ALS by nearly 30%.

Figure 28. UAS point clouds for the Pebble Hill Plantation are derived photogrammetrically and represent the outer hulls of fuel objects. These data can cover large areas and provide a scaling mechanism that allows for aggregation of TLS fuel mass to landscape scales.

5.1 Next Steps

The results of this dissertation provide a first step for integrating active remote sensing derivative products into a single encompassing fuels dataset for a broad array of applications. The results of this work can be merged with crown fuel characteristics from TLS (Ferrarase *et al*.2013) and individual stem products from ALS (Rowell *et al.* 2006; Rowell *et al*. 2009; Silva *et al*. 2016). By integrating these data into formats that are useable by STANDFIRE\CAPSIS (Parsons et al. 2016; Pimont *et al.* 2016), we are demonstrating significant advancements in development of fuels inputs to WFDS and FIRETEC\Higrad. These data also provide a one-of-a-kind validation dataset with which to investigate the validity of southeastern fuels\fire effects hypotheses posed by the wildland fuel cell concept and the ecology of fuels.

From the perspective of remote sensing, the three-dimensional simulations offer a unique potential to begin addressing issues of occlusion that are ubiquitous with TLS data acquisitions. Using ray tracing methods (Disney *et al.* 2009 and 2010; Yin *et al.* 2016) in combination with simulated fuel beds, I hope to better understand the energy-matter interactions that control how TLS and ALS characterize fuel properties, with expected improvements in fuel measurement and prediction.

References

Anderson HE (1982) Aids to determining fuel models for estimating fire behavior. USDA Forest Service, Intermountain Forest and Range Experiment Station, General Technical Report INT-122. (Ogden, Utah).

Andersen HE, McGaughey RJ, Reutebuch SE. (2005) Estimating forest canopy fuel parameters using LIDAR data. *Remote Sensing of Environment, 94, 441-449.* doi:10.1016/j.rse.2004.10.013

Andrews PL, Bevins CD, Seli, RC (2005) BehavePlus fire modeling system, version 4.0: User's Guide. Gen. Tech. Rep. RMRS-GTR-106 Revised. Ogden, UT: Department of Agriculture, Forest Service, Rocky Mountain Research Station. 132p.

Bartlette RA, Reardon J, Curcio GM (2005) Characterizing Moisture Regimes for Assessing Fuel Availability in North Carolina Vegetation Communities. JFSP Research Project Reports. 146.

Battaglia MA, Mitchell RJ, Mou PP, Pecot SD (2003) Light transmittance estimates in longleaf pine woodland. *Forest Science*: 49:752-762.

Beer T, Enting IG (1990) Fire spread and percolation modeling. *Mathematical and Computer Modeling.* 13(11):77-96. doi: https://doi.org/10.1016/0895-7177(90)90065-U

Burgan RE; Rothermel RC (1984) BEHAVE: fire behavior prediction and fuel modeling system— FUEL subsystem. USDA Forest Service, Intermountain Range and Experiment Station, General Technical Report INT-167. (Ogden, UT).

Brockway DG, Outcalt KW. (2000) Restoring longleaf pine wiregrass ecosystems: Hexazinone application enhances effects of prescribed fire. *Forest Ecology and Management.* 137, 121-138

Brown, JK (1974) Handbook for inventorying downed woody material. Gen. Tech. Rep. INT-16, USDA Forest Service, Intermountain Forest & Range Experiment Station, Odgen, UT. 24 p.

Brown, JK, Bevins CD (1986) Surface fuel loadings and predicted fire behavior for vegetation types in the northern Rocky Mountains. *Research note INT-358.* U.S. Forest Service, Missoula, Montana.

Cawse-Nicholson K., van Aardt J, Romanczyk P, Kelbe D, Krause K, Kampe, T. (2013). A study of energy attenuation due to forest canopy in small-footprint waveform lidar signals. In ASPRS Annual Conference.

Clark KL, Skowronski N, Hom J, Due Veneck M, Pan Y, Van Tuyl S, Cole J, Patterson M (2009) Decision support tools to improve the effectiveness of hazardous fuel reduction treatments in the New Jersey Pine Barrens. *International Journal of Wildland Fire. 18(3):268:277*

CloudCompare. 2014. CloudCompare: 3D point cloud and mesh processing software: open source project. http://www.cloudcompare.org.

Cooper SD, Roy DP, Schaaf CB, Paynter I (2017) Examination of the potential of terrestrial laser scanning and structure-from-motion photogrammetry for rapid nondestructive field measurement of grass biomass. *Remote Sensing.* 9(6):531-544. doi: 10.3390/rs9060531

Coops NC, Hilker T, Wulder MA, St-Onge B, Newham G, Siggins A, Trofymow JA. (2007) Estimating canopy structure of Douglas-fir forest stands from discrete-return LiDAR. *Trees.* 212:295-310. doi: 10.1007/s00468-006-0119-6

Dell JE, Richards LA, O'Brien JJ, Loudermilk EL, Hudak AT, Pokswinski SM, Bright BC, Hiers JK (2017) Overstory-derived surface fuels mediate plant species diversity in frequently burned longleaf pine forests. *Ecosphere*. 8(10):e01964. doi: 10.1002/ecs2.1964

Disney MI, Lewis PE, Bouvet M, Prieto-Blanco A, Hancock S. (2009) Quantifying Surface Reflectivity for Spaceborne Lidar via Two Independent Methods, *IEEE Transactions on Geoscience and Remote Sensing*, 47 ,9 , 3262 – 3271

Disney MI, Kalogirou V, Lewis P, Prieto-Blanco A, Hancock S, Pfeifer M. (2010) Simulating the impact of discrete-return lidar system and survey characteristics over young conifer and broadleaf forests. *Remote Sensing of Environment*, 114, 1546-1560. doi:10.1016/j.rse.2010.02.009

Disney MI, Lewis P, Gomez-Dans J, Roy D, Wooster MJ, Lajas D. (2011) 3D radiative transfer modelling of fire impacts on a two-layer savanna system. *Remote Sensing of Environment*, 115, 1866-1881.doi:10.1016/j.rse.2011.03.010

Dupont S, Brunet Y (2008) Edge flow and canopy structure: A large-eddy simulation study. *Boundary-Layer Meteorology.* 126(1):51-71. doi: https://doi.org/10.1007/s10546-007-9216-3

Dupont S, Brunet Y (2006) Simulation of turbulent flow in an urban forested park damaged by a windstorm. *Boundary-Layer Meteorology.* 120(1):133-161. doi: https://doi.org/10.1007/s10546-006-9049-5

Eitel JUH, Magney TS, Vierling LA, Brown, TT, Huggins DR (2014) LiDAR based biomass and crop nitrogen estimates for rapid, non-destructive assessment of wheat nitrogen status. Field Crop. Res. 159, 21–32.

Falk, DA, Miller CM, McKenzie D, Black A.E. (2007) Cross-scale analysis of fire regimes. *Ecosystems* 10:809-823.

Fernandes PM, Catchpole WR, Rego FC (2000) Shrubland fire behavior modelling with microplot data. *Canadian Journal Forest Research.* 30:889-899.

Finney MA (2004) FARSITE: fire area simulator- model development and evaluation. Research Paper RMRS-RP-4 Revised. Ogden, UT: U.S. Department of Agriculture, Forest Service, Rocky Mountain Research Station. (47 pages).

Finney MA (2002) Fire growth using minimum travel time methods. *Canadian Journal of Forest Research*. 32(8), 1420–1424.

Finney MA (2001) Design of regular landscape fuel treatment patterns for modifying fire growth and behavior. *Forest Science*, 47(2): 219-228.

Fonda, R.W. (2001). Burning characteristics of needles from eight pine species. *Forest Science*. 47:390-396.

Fonda, R., Varner, JM (2004). Burning characteristics of cones from eight pine species. *Northwest Science.*78: 322-333.

Garcia M, Danson FM, Riaño D, Chuvieco E, Ramirez FA, Bandugula V (2011) Terrestrial laser scanning to estimate plot-level forest canopy fuels. *International Journal of Applied Earth Observation and Geoinformation.* 13(4):636-645.

Glitzenstein JS, Platt WJ, Streng DR (1995), Effects of Fire Regime and Habitat on Tree Dynamics in North Florida Longleaf Pine Savannas. *Ecological Monographs*, 65: 441–476. doi:10.2307/2963498

Greaves HE, Vierling LA, Eitel JUH, Boelman NT, Magney TS, Prager CM, Griffin KL (2017) Applying terrestrial lidar for evaluation and calibration of airborne lidar-derived shrub biomass estimates in Arctic tundra. *Remote Sensing Letters*, 8:2, 175-184. doi: http://dx.doi.org/10.1080/2150704X.2016.1246770

Greaves HE, Vierling LA, Eitel J, Boelman NT, Magney TS, Prager CM, Griffin KL (2015) Estimating aboveground biomass and leaf area of low-stature Arctic shrubs with terrestrial LiDAR. *Remote Sensing of Environment* **164**, 26-35. doi: 10.1016/j.rse.2015.02.023

Glenn NF, Spaete LP, Sankey TT, Derryberry DR, Hardegree SP, Mitchell JJ (2010) Errors in LiDAR-derived shrub height and crown area on sloped terrain. *Journal of Arid Environments* **75**, 377-382. doi: 10.1016/jaridenv.2010.11.005

Glenn NF, Streuker DR, Chadwick DJ, Thackray GD, Dorsch SJ (2006) Analysis of LiDAR-derived topographic information for characterizing and differentiating lands

Hardy C, Heilman W, Weise D, Goodrick S, Ottmar R. (2008) Fire behavior advancement plan; A plan for addressing physical fire processes within the core fire science portfolio. Final report to the Joint Fire Sciences Program Board of Governors. http://www.firescience.gov/projects/08-S-01/project/08-S-01_final_report_08-s-01.pdf

Hendricks JJ, Wilson CA, Boring LR (2002) Foliar litter position and decomposition in a fire-maintained longleaf pine–wiregrass ecosystem. *Canadian Journal of Forest Research* 32, 928–941. doi:10.1139/X02-020

Hiers JK, O'Brien JJ, Mitchell RJ, Grego JM, Loudermilk EL (2009) The wildland fuel cell concept: an approach to characterize fine-scale variation in fuels and fire in frequently burned longleaf pine forests. *International Journal of Wildland Fire* **18**, 315–325. http://dx.doi.org/10.1071/WF08084

Hopkinson C, Chasmer LE, Sass G, Creed IF, Sitar M, Kalbfleisch W, Treitz P (2005) Vegetation class dependent errors in lidar ground elevation and canopy height estimates in a boreal wetland environment. *Canadian Journal of Remote Sensing*, **31:2**, 191-206.

Hosoi F, Omasa K (2008) Estimating vertical plant area density profile and growth parameters of a wheat canopy at different growth stages using three-dimensional portable lidar imaging. *ISPRS Journal of Photogrammetry and Remote Sensing* **64**, 151–158. doi: 10.1016/j.isprsjprs.2008.09.003

Hosoi F, Omasa K (2007) Factors contributing to accuracy in the estimation woody canopy leaf area density profile using 3D portable lidar imaging. *Journal of Experimental Botany* **58**, 3463–3473. doi: 10.1093/jxb/erm203

Hosoi F, Omasa K (2006) Voxel-based 3-D modeling of individual trees for estimating leaf area density using high-resolution portable scanning lidar. *IEEE Transactions on Geoscience and Remote Sensing* **44**, 3610–3618. doi: 10.1109/TGRS.2006.881743

Hudak AT, Dickinson MB, Bright BC, Kremens RL, Loudermilk EL, O'Brien JJ, Hornsby BS, Ottmar RD. (2016) Measurements related to fire radiative energy density and surface fuel consumption – RxCADRE 2011 and 2012. *International Journal of Wildland Fire*, 25, 25-37. doi:http://dx.doi.org/10.1071/WF14159

Gupta V, Reinke KJ, Jones SD, Wallace L, Holden L (2015) Assessing metrics for estimating fire induced change in the forest understorey using terrestrial laser scanning. *Remote Sensing*, 7(6):8180-8201. doi:10.3390/rs70608180

Jakubowski MK, Wenkai L, Qinghua G, Kelly M. (2013) Delineating Individual Trees from Lidar Data: A Comparison of Vector- and Raster-based Segmentation Approaches. *Remote Sensing.* 5(9): 4163-4186. doi:10.3390/rs5094163

Johnson, EA (1992) Fire and vegetation dynamics: Studies from the North American boreal forest. Cambrige: Cambrige University Press.

Johnson, EA, Miyanishi, K (2001) Forest fires: Behavior and ecological effects. San Diego; Academic.

Kane JM, Varner JM, Hiers J. (2008) The burning characteristics of southeastern oaks: Discriminating fire facilitators from fire impeders. *Forest Ecology and Management, 256, 12, 2039-2045.* doi:10.1016/j.foreco.2008.07.039

Keane RE (2013) Describing wildland surface fuel loading for fire management: a review of approaches, methods and systems. *International Journal of Wildland Fire* **22**, 51–62. doi: 10.1071/WF11139

Keane RE, Gray K, Bacciu V (2012) Spatial variability of wildland fuel characteristics in northern Rocky Mountain ecosystems. USDA Forest Service, Rocky Mountain Research Station, Research Paper RMRS-RP-98. (Fort Collins, CO).

Keane RE, Burgan R, van Wagtendonk J (2001) Mapping wildland fuels for fire management across multiple scales: Integrating remote sensing, GIS, and biophysical modeling. *International Journal of Wildland Fire* **10** , 301–319. http://dx.doi.org/10.1071/WF01028

Kim AM, Olsen RC, Béland M (2016) Simulated full-waveform lidar compared to Riegl Vz-400 terrestrial laser scans. Proceedings Volume 9832, Laser Radar Technology and Applications XXI; 98320T (2016); doi: 10.1117/12.2223929

Kirkman LK, Goebel PC, Palik BJ, West LT (2004) Predicting plant species diversity in a longleaf pine landscape. *Ecoscience*.11:1, 80-93.

Kirkman LK, Mitchell RJ, Helton RC, Drew MB (2001). Productivity and species reichness across an environmental gradient in a fire-dependent ecosystem. *American Journal of Botany.* 88:2119-2128.

Kuhn M (2017) A short introduction to the caret package.

Li A, Glenn NF, Olsoy PJ, Mitchell JJ, Shrestha R (2015) Aboveground Biomass Estimates of Sagebrush Using Terrestrial and Airborne LiDAR Data in a Dryland Ecosystem.Agricultural and Forest Meteorology 213: 138–147. doi:10.1016/j.agrformet.2015.06.005

Liang X, Litkey P, Hyyppa J, Kaartinen H, Vastaranta M, Holopainen M (2012) Automatic stem mapping using single-scan terrestrial laser scanning. *IEEE Trans. Geosci. Remote Sens, 50*,661–670.

Linn RR, Cunningham P (2005) Numerical simulations of grass fires using a coupled atmosphere–fire model: basic fire behavior and dependence on wind speed. *J. Geophys. Res., 110, D13107, doi:10.1029/2004JD005597.*

Linn RR, Reisner J, Colman J, Winterkamp J (2002) Studying Wildfire Using FIRETEC. *International Journal of Wildland Fire.* 11:1-14.

Loudermilk EL, Hiers JK, O'Brien JJ, Mitchell RJ, Singhania A, Fernandez JC, Cropper WP, Slatton KC (2009) Ground-based LIDAR: a novel approach to quantify fine-scale fuelbed

characteristics. *International Journal of Wildland Fire* **18**, 676–685. http://dx.doi.org/10.1071/WF07138

Loudermilk EL, O'Brien JJ., Mitchell RJ., Cropper WP., Hiers JK, Grunwald S, Grego J, Fernandez-Diaz JC. (2012) Linking complex forest fuel structure and fire behaviour at fine scales. *International Journal of Wildland Fire* **21**, 882–893. http://dx.doi.org/10.1071/WF10116

Loudermilk EL, Stanton A,. Scheller RM, Dilts TE, Weisberg PJ, Skinner C, Yang J. (2014) Effectiveness of fuel treatments for mitigating wildfire risk and sequestering forest carbon: A case study in the Lake Tahoe Basin, *Forest Ecology and Management*, 323, 1, 114-125, http://dx.doi.org/10.1016/j.foreco.2014.03.011

Loudermilk EL, Hiers JK, Pokswinski S, O'Brien JJ, Barnett A, Mitchell RJ (2016) The path back: oaks (*Quercus* spp.) facilitate longleaf pine (*Pinus palustris*) seedling establishment in xeric sites. *Ecosphere* 7*(*6*): e01361*. 10.1002/ecs2.1361

Martin DE, Dell JD (1978) Planning for prescribed burning in the inland northwest. Gen. Tech. Rep. PNW-GTR-076. Portland, OR: U.S. Department of Agriculture, Forest Service, Pacific Northwest Research Station: 1-67.

Maynard T, Princevac M, Wiese DR (2016) A study of the flow field surrounding interacting line fires. *Journal of Combustion*. 2016:6927482, 12 pages. http://dx.doi.org/10.1155/2016/6927482

McKenzie D., Miller C, Falk, DA (2011) *The landscape of ecology of fire*. Doerdrecht, the Netherlands; London, United Kingdom; Heidelberg, Germany; New York, USA: Springer+Media B.V. 312 p.312.

McGaughey RJ (2014) FUSION/LDV: Software for LIDAR data analysis and visualization, Version 3.42. USDA Forest Service, Pacific Northwest Research Station (Seattle, WA).

Mell W, Maranghides A, McDermott R, Manzello SL (2009). Numerical simulation and experiments of burning Douglas fir trees. *Combustion and Flame.* 156,:2023–2041.

Mell W, Jenkins MA, Gould J, Cheny P (2007) A physics based approach to modeling grassland fires. *International Journal of Wildand Fire* **16**, 1–22. doi: 10.1071/WF06002

Montes-Helu MC, Kolb T, Dore S, Sullivan B, Hart SC, Kock G, Hungate BA (2009). Persistent effects of fire-induced vegetation change on energy partitioning and evapotranspiration in ponderosa pine forests. *Agriculture and Forest Meterology.* 149:491-500.

Morvan D, Dupuy JL (2004) Modeling the propagation of a wildfire through a Mediterranean shrub using a multiphase formulation. *Combustion and Flame* **138**, 199–210. doi: 10/1016/j.combustflame.2004.05.001

Mitchell, RJ, Hiers JK, O'Brien J and Starr G. (2009) Ecological forestry in the southeast: Understanding the ecology of fuels. *Journal of Forestry*. 107(8) 391-397.

Mitchell RJ, Hiers JK, O'Brien JJ, Jack SB, Engstrom RT (2006) Silviculture that sustains: The nexus between silviculture, frequent prescribed fire, and conservation of biodiversity in longleaf pine forests of the southeastern United States. *Canadian Journal of Forest Research.* 36:2724-2736.

Mueller-Dombois D, Ellenburg H (1974) Aims and methods of vegetation ecology. Wiley and Sons, New York.

Mueller E, Mell W, Simeoni A (2014). Large eddy simulation of forest canopy flow for wildland fire modeling. *Canadian Journal of Forest Research*. 44. 1534-1544. doi:10.1139/cjfr-2014-0184

Mutch RW, Arno SF, Brown JK, Carlson CE, Ottmar RD, Peterson JL (1993) Forest health in the Blue Mountains: A management strategy for fire-adapted ecosystems. USDA Forest Service General Technical Report PNW-GTR-310. 14 pp.

Mutlu M, Popescu SC, Stipling C, Spencer T (2008) Mapping surface fuel models using lidar and multispectral data fusion for fire behavior. *Remote Sensing of Environment.* 112:274-285.

O'Brien JJ, Hiers, JK, Callaham MA, Mitchell, RJ, Jack S. (2008) Interactions among overstory structure, seedling life-history traits and fire in frequently burned neotropical pine forests. Ambio 37: 542-547.

O'Brien JJ, Loudermilk EL, Hornsby B, Hudak AT, Bright BC, Dickinson MB, Hiers JK, Teske C, Ottmar RD. (2016) High-resolution infrared thermography for capturing wildland fire behavior – RxCADRE 2012. *International Journal of Wildland Fire*, 25, 62-75. doi: http://dx.doi.org/10.1071/WF14165

O'Brien JJ, Loudermilk EL, Hornsby B, Polswinski S, Hudak A, Strother, Rowell E, Bright B (2016) Canopy derived fuels drive patterns of in-fire energy release and understory plant mortality in a longleaf pine (*Pinus palustris*) sandhill in Northwest FL, USA. *Canadian Journal of Remote Sensing.*

Olsoy P, Glenn N, Clark P, Derryberry D (2014) Aboveground total and green biomass of dryland shrub derived from terrestrial laser scanning. *ISPRS Journal of Photogrammetry and Remote Sensing*, **88**, 166-173. doi: 10.1016/j.isprsjprs.2013.12.006

Ottmar RD, Hiers JK, Butler, BW, Clements CB, Dickinson MB, Hudak AT, O'Brien JJ. Potter BE, Rowell EM, Strand TM Zaijowski (2016a) Measurments, datasets and preliminary results from the RxCADRE project- 2008, 2011, and 2012. *International Journal of Wildland Fire*, 25, 1-9. doi: http://dx.doi.org/10.1071/WF14161

Ottmar RD, Hudak AT, Prichard SJ, Wright CS, Restaino JC, Kennedy MC, Vihnanek RE (2016b) Pre-fire and post-fire surface fuel and cover measurements collected in the

southeastern United States for model evaluation and development. *International Journal of Wildland Fire*, 25, 10-24. doi: http://dx.doi.org/10.1071/WF15092

Ottmar RD, Sandberg DV, Riccardi CL, Prichard SJ (2007). An overview of the Fuel Characteristic Classification System – quantifying, classifying and creating fuelbeds for resource planning. *Canadian Journal of Forest Research*. 37:2383-2393.

Ottmar RD, Vihnanek RE, Mathey JW (2003). Stereo photo series for quantifying fuels. Volume Via: Sand hill, sand pine scrub, and hardwoods with white pine types in the southeast United States with supplemental sites for volume VI. PMS 838, National Wildfire Coordinating Group, Boise, ID. 78p.

Palace MW, Sullivan FB, Ducey MJ, Treuhaft RN, Herrick C, Shimbo JZ, Mota-E-Silva J. (2015) Estimating forest structure in a tropical forest using field measurments, a synthetic model and discrete return lidar data. *Remote Sensing of Environment*, 161, 1-11. doi: http://dx.doi.org/10.1016/j.rse.2015.01.020

Parsons, R.(2006) FUEL-3D: A spatially explicit fractal fuel distribution model. Fuels Management—How to Measure Success: Conference Proceedings. 28-30 March 2006; Portland, OR. Proceedings RMRS-P-41. Fort Collins,CO: U.S. Department of Agriculture, Forest Service, Rocky Mountain Research Station.

Parsons RA, Mell WE, McCauley P. (2011) Linking 3D spatial models of fuels and fire: Effect of spatial heterogeneity on fire behavior. *Ecological Modelling,* 222, 679-691.

Pecot SD, Horsley SB, Battaglia MA, Mitchell RJ (2005). The influence of canopy, sky condition, and solar angle on light quality in a longleaf pine woodland. *Canadian Journal of Forest Research.* 35:1356-1366.

Pfennigbauer, M (2010) Improving Quality of Laser Scanning Data Acquisition through Calibrated Amplitude and Pulse Deviation Measurement. Proceedings of SPIE 7684:6841F–76841F–10.

Pickett BM, Isackson C, Wunder R, Fletcher TH, Butler BW, Weise DR (2009) Flame interactions and burning characteristics of two live leaf samples. *International Journal of Wildland Fire* **18**, 865–874. doi: 10.1071/WF08143

Pimont F, Parsons R, Rigolot E. de Coligny F, Dupuy J, Dreyfus P, Linn RR (2016) Modeling fuels and fire effects in 3D: model description and applications. *Environmental Modelling and Software*. 80:225-244.

Pimont F, Dupuy J, Linn RL, Dupont S (2009) Validation of FIRETEC wind-flows over a canopy and a fuel-break. *International Journal of Wildland Fire*. 18. 775-790. 10.1071/WF07130

Popescu S, Zhao K (2008) A voxel-based lidar method for estimating crown base height for deciduous and pine trees, *Remote Sensing of Environment*, 112(3): 767-781.

Popescu SC, Wynne, RH, Nelson RF (2002) Estimating plot-level tree heights with LiDAR: local filtering with a canopy-height based variable window size. *Computers and Electronics in Agriculture* **37:1,** 71-95. doi: 10.1016/S0168-1699(02)00121-7

Prince, DR, Fletcher ME, Shen C, Fletcher TH. (2014) Application of L-systems to geometrical construction of chamise and juniper shrubs. *Ecological Modelling*, 273, 86-95. http://dx.doi.org/10.1016/j.ecolmodel.2013.11.001

Prince, DR. (2014) Measurement and Modeling of Fire Behavior in Leaves and Sparse Shrubs. Disertation , Bringham Young University, Provo, Utah, USA.

Remington KK, Bonham CD, Reich RM. (1992) Blue grama-buffalograss respondes to grazing: A Weibull distribution. *Journal of Range Management*, 45, 272-276.

Riaño D, Chuvieco E, Ustin SL, Salas J, Rodriguez-Pérez JR, Ribeiro LM, Viegas DX (2007) Estimation of shrub height for fuel type mapping combining airborne LiDAR and simultaneous color infrared ortho imaging. *International Journal of Wildland Fire* **16:3**, 341-348. doi: 10.1071/WF06003

Riaño D, Meier E, Allgöwer B, Chuvieco E, Ustin SL (2003) Modeling airborne laser scanning data for the spatial generation of critical forest parameters in fire behavior modeling. *Remote Sensing of Environment*. 86(2):177-186, https://doi.org/10.1016/S0034-4257(03)00098-1.

Robertson KM, Ostertag TE (2009) Biomass equations for hardwood resprouts in fire-maintained pinelands in the southeastern United States. South J appl For 33:121–128.

Robinson AP, Duursma RA, Marshall JD (2005) A regression-based equivalence test for model validation: shifting the burden of proof. *Tree Physiology*,25:903-913.

Rothermel RC (1972) A mathematical model for predicting fire spread in wildland fuels. Res. Pap. INT-115. Ogden, UT: U.S. Department of Agriculture, Intermountain Forest and Range Experiment Station. 40 p.

Rowell EM, Seielstad CA, Ottmar RD (2016a) Developing and validating fuel height models for the RxCADRE experiments. *International Journal of Wildland Fire* , 25, 38-47. doi: http://dx.doi.org/10.1071/WF14170

Rowell EM, Loudermilk EL, Seielstad C, O'Brien JJ (2016b) Using Simulated 3D Surface Fuelbeds and Terrestrial Laser Scan Data to Develop Inputs to Fire Behavior Models. *Canadian Journal of Remote Sensing.* 42(5):443-459. doi: 10.1080/07038992.2016.1220827

Rowell E, Seielstad C (2012) Characterizing grass, litter, and shrub fuels in longleaf pine forest pre-and post-fire using terrestrial LiDAR. SilviLaser 2012, 16-19 September, 2012, Vancouver, Canada. 1-8.

Rowell E, Seielstad C, Goodburn J, Queen L (2009) Estimating plot-scale biomass in a western North American mixed-conifer forest from lidar-derived tree stems. Paper presented at the Proceedings SilviLaser Conference at College Station, Texas, USA.

Rowell E, Seielstad C, Vierling L, Queen L, and Shepperd W (2006) Using Laser Altimetry-based Segmentation to Refine Automated Tree Identificantionin Managed -Forests of the Black Hills, South Dakota. *Photogrammetric Engineering and Remote Sensing*, 72(12): 1379-1388.

Rowell E (2005) Estimating Forest Biophysical Variables from Airborne Laser Altimetry in a Ponderosa Pine Forest, Masters thesis, South Dakota School of Mines and Technology, Rapid City, South Dakota, 99 p.

Sandberg, DV, Hardy CC, Weise DR, Rehm R, Linn RR. (2003). Core fire science caucus. Second International Wildland Fire Ecology and Fire Management Congress. Association for Fire Ecology, 16-20 November 2003.

Scott JH, Reinhardt ED (2001) Assessing crown fire potential by linking models of surface and crown fire behavior. Res. Pap. RMRS-RP-29. Fort Collins, CO: U.S. Department of Agriculture, Forest Service, Rocky Mountain Research Station. 59 p.

Seielstad C, Stonesifer C, Rowell E, Queen L (2011) Deriving fuel mass by size class in Douglas-fir (*Pseudotsuga menziesii*) using terrestrial laser scanning. *Remote Sensing* **3**, 1691–1709. doi: 10.3390/rs3081691

Seielstad CA, Queen LP. (2003) Using airborne laser altimetry to determine fuel models for estimating fire behavior. *Journal of Forestry*. 101(4): 10-15

Silva CA, Hudak AT, Vierling LA, Loudermilk EL, O'Brien JJ, Hiers JK, Jack SB, Gozalez-Benecke C, Lee H, Falkowski MJ, Khoravipour A (2016) Imputation of individual longleaf pine (*Pinus palustris* Mill.) tree attributes from field and LiDAR data. *Canadian Journal of Remote Sensing*, 42:554-573. doi: https://doi.org/10.1080/07038992.2016.1196582

Skowronski N, Clark KL, Hom J, Patterson M (2007) Remotely sensed measurements of forest structure and fuel loads in the Pinelands of New Jersey. *Remote Sensing of Environment*. 108(2):123-129.

Stoker J. (2009) Volumetric visualization of multiple return LIDAR data – using voxels. *Photogrammetric Engineering and Remote Sensing*, 75(2):109-112.

Strand T, Gullett B, Urbanski S, O'Niel S. Potter B, Aurell J, Holder A, Larkin N, Moore M, Rorig M (2016) Grassland and forest understorey biomass emissions from prescribed fires in the southeastern United States – RxCADRE 2012. *International Journal of Wildland Fire*, 25:102-113. doi: https://doi.org/10.1071/WF14166

Streuker D, Glenn N (2006) LiDAR measurements of sagebrush steppe vegetation heights. *Remote Sensing of Environment.* **102:1**, 135-145. doi: 10.1016/j.rse.2006.02.011

Swetnam TW, Baisan CH (1996) Historical fire regime patterns in the Southwestern United States since AD 1700. USDA Forest Service General Technical Report RMRS. GTR 286. 11-32.

Thaxton JM and Platt WJ. (2006) Small-scale variation alters fire intensity and shrub abundance in a pine savanna. *Ecology*, 87(5), 2006, 1331–1337.

Thompson, W. L. 2004. Sampling rare or elusive species: concepts, designs, and techniques for estimating population parameters. Island Press, Washington, D.C., USA.

Umphries, T.A. Characterizing Fuelbed Structure, Depth, and Mass in a Grassland Using Terrestrial Laser Scanning. Master's Thesis, University of Montana, Missoula, MT, USA, 2013.

Van der Zande D, Hoet W, Jonckheere I, Van Aardt J, Coppin P (2006) Influence of measurement set-up of ground-based LiDAR for derivation of tree structure. *Agricultural and Forest Meteorology* **141**, 147–160. doi: 10.1016/j.agrformet.2006.09.007

Van Wagner, CE. (1968) The line intersect method in forest fuel sampling. *Forest Science,* 14(1), 20-27.

Van Wagtendonk, JW (2006) Fire as a physical process. *In fire in California ecosystems, eds. N.G. Sugihara, J.W. van Wagtendonk, J. Fites-Kaufman, K.E. Shaffer, and A.D. Thode.* 38-57, Berkeley: University of California Press.

Varner JM, Kane JM, Banwell EM, Krye JK. (2015) Flammability of litter from southeastern trees: A preliminary assessment.. 2015. Proceedings of the 17th biennial southern silvicultural research conference. e–Gen. Tech. Rep. SRS–203. Asheville, NC: U.S. Department of Agriculture, Forest Service, Southern Research Station. 551 p.

Vierling, L., Xu, Y, Eitel, J, and Oldow, J (2013) Shrub characterization using terrestrial laser scanning and implications for airborne LiDAR assessment. *Canadian Journal of Remote Sensing* **38:6**, 709-722. doi: 10.5589/m12-057

Walker J, Peet RK (1984) Composition and species diversity of pine-wiregrass savannas of the Green Swamp, North Carolina. Vegetatio, 55: 163. https://doi.org/10.1007/BF00045019

Wahlenburg WG (1946) Longleaf pine, its use, ecology, regeneration, protection, growth, and management. Charles Lathrop Pack Forestry Foundation, United States Forest Service.

Woodgate W, Disney M, Armston JD, Jones SD, Suarez L, Hill MJ, Wilkes P, Soto-Berelov M, Haywood A, Mellor A, (2015) An improved theoretical model of canopy gap probability for Leaf Area Index estimation in woody ecosystems, *Forest Ecology and Management*, 358, 15, 303-320, http://dx.doi.org/10.1016/j.foreco.2015.09.030.

Yin T, Lauret N, Gastellu-Etchegorry J (2016) Simulation of satellite, airborne and terrestrial LiDAR with DART (II): ALS and TLS multi-pulse acquisitions, photon counting, and solar noise. *Remote Sensing of Environment*, 184:454-468. doi: /10.1016/j.rse.2016.07.009